Technische Universität München

Fakultät für Medizin

Development of a therapeutic vaccine against chronic Hepatitis B virus infection in a preclinical model system

-

Therapeutic vaccine against chronic HBV infection

Abdul Moeed

Vollständiger Abdruck der von der Fakultät für Medizin der Technischen Universität München zur Erlangung des akademischen Grades

eines Doktors der Naturwissenschaften (Dr. rer. nat.)

genehmigten Dissertation.

Vorsitzender:	Prof. Dr. Carsten Schmidt-Weber
Prüfende/-r der Dissertation:	1. Prof. Dr. Percy A. Knolle 2. Prof. Dr. Jörg Durner

Die Dissertation wurde am 14.05.2020 bei der Technischen Universität München eingereicht und durch die Fakultät für Medizin am 06.10.2020 angenommen.

Printed with the support of German Academic Exchange Service "DAAD"

…..to my parents

ACKNOWLEDGMENTS

First and foremost, my deepest gratitude goes to Prof. Dr. Percy Knolle, who has the attitude and substance of a genius. He convincingly inculcated me with a spirit of adventure regarding research through his invaluable guidance, intellectual acumen, and scientific discussions. I can say without the fear of contradiction that without his continuous feedback and appreciation this dissertation would not have been possible. I could not have imagined having a better advisor and mentor for my doctoral studies.

I am highly indebted to advisory member Prof. Dr. Jörg Durner for his guidance and support throughout my dissertation. His supportive input during our meetings has further refined my research. My sincere thanks to my mentor PD Dr. Nina Kallin for her insightful comments, encouragement, continuous guidance and mentoring throughout the tenure of doctoral candidacy.

I would like to express my sincere gratitude to the Director Institute of Virology TUM/Helmholtz center Munich Prof. Dr. Ulrike Protzer for providing me her lab space and technical resources that were necessary for my research work. My appreciation and sincere gratitude also extend to PD Dr. Anna Kosinska for her invaluable contribution to my dissertation. Anna's mutual contribution towards designing and conducting preclinical trials, data analysis, mentorship and her early insights launched the greater part of this dissertation. Besides, I highly appreciate the technical support by my colleague Abdallah Yassin in developing ex vivo system for T cell proliferation. I would also like to appreciate the sincere efforts of our laboratory technicians Silke, Sava and Anna for providing support and ensuring smooth functioning of the lab. Also, the histology work discussed in the dissertation would not have been possible without the support of Dr. Katja Steiger, Olga Seelbach, Marion Mielke and Anne Jacob.

Many thanks to Prof. Dr. Marc Pellegrini, Division head of Infectious Diseases and Immune Defense Walter and Eliza Hall Institute (WEHI) Melbourne, for inviting me to his lab as a visiting scholar and providing me technical support during my institutional stay. I would like to pay my special regards to PD Dr. Greg Ebert of WEHI for mentoring and broadening my knowledge concerning novel therapeutic approaches to exploit cell signaling pathways for elimination of chronic infections.

I am highly indebted to my fellow lab mates for their kind support, inspiration, interesting discussions and all exciting memories we have experienced together in the last four years. Also, my heartfelt thanks to “Chai team” that provided platform for interdisciplinary cooperation, cultural exchange, making new friends besides making Chai and putting up with my buffoonery.

I am extremely grateful and blessed of the fact that the journey of my doctoral degree ended up producing not only nice scientific data but also faithful friendships. I would like to pay my special regards to Suliman, Abdallah, Sainitin, Deepti, Sarah, Omnia, Shubankar, Julie, Tobi, Eric, Max, Zaheer, Tariq, and Mahmood for their unconditional support especially during the times of tribulation.

I would like to acknowledge with gratitude the support, love and prayers of my parents and siblings throughout my career development. Even their mere presence provided me the sense of security enabling me to purse my goals with more peace of mind, grit and persistence. Many thanks to my aunts for their token of appreciation, prayers and affection. Besides, I am grateful to my old chums Suliman, Haseeb, Mulla Ali, Salman, Munawar, Riaz, Umar, Umair, Mohsin, Waseem and Amin for being there when I needed them most.

Finally, I would like to thank Higher Education Commission Pakistan and German Academic Exchange Service for providing financial and technical support throughout my academic years. Any omission in this brief acknowledgment doesn’t mean lack of gratitude.

TABLE OF CONTENTS

TABLE OF CONTENTS

SUMMARY

There are approximately 260 million humans around the world suffering from chronic Hepatitis B infection. Although available antiviral therapies can limit HBV replication, but there is no immunotherapy for a functional cure of chronic HBV infection. HBV-specific CD8+ T cell responses determine the outcome of infection and there is weak and dysfunctional HBV-specific CD8+ T cell responses during persistent viral infection, while strong and polyclonal CD8+ T cell responses are associated with the resolution of HBV infection. Previously, a heterologous therapeutic vaccination strategy, consisting of HBV proteins as prime vaccination followed by a modified vaccinia ankara (MVA) viral vector encoding HBV antigens as boost were developed, which successfully overcame the immune tolerance observed during persistent HBV infection in a preclinical model employing HBV-transgenic mice model with low to medium levels of HBV antigen. However, this therapeutic vaccination failed to induce functional HBV-specific CD8+ T cell responses in the presence of high HBV antigen levels. Here we have shown that the combination of therapeutic vaccination and injection of a TLR9-ligand (CpG) increased the efficacy of vaccination to overcome HBV-specific immune tolerance even in high-viremic preclinical HBV infection models. CpG is known to induce intrahepatic myeloid cell aggregates also known as iMATEs though TLR9-signaling, that support CD8+ T cell activation, expansion and differentiation into effector cells. Our findings demonstrated that the combination of heterologous therapeutic vaccination followed by iMATE induction increased vaccine-induced HBcAg-specific CD8+ T cell responses, leading to enhanced immune control of HBV in preclinical models of persistent HBV infection. Furthermore, we also characterized ex vivo the contribution of different intrahepatic myeloid cell populations for CD8+ T cell expansion and found that CpG-triggered hepatic inflammatory myeloid cells enhanced the survival and proliferation of CD8+ T cells, while hepatic macrophages isolated from naïve murine liver, inhibited such expansion. This ex vivo system, where the phenotype and mechanisms determining the outcome of the myeloid cell – CD8+ T cell crosstalk can be studied in detail, will provide a suitable model system to identify the molecular mechanisms that help to overcome hepatic immune tolerance during chronic HBV infection.

1. INTRODUCTION

1.1 Preamble – Hepatitis B

Hepatitis B virus (HBV) is estimated to have infected one third of world's population. Recent studies revealed that HBV has significant contribution in increasing disease burden pertaining to hepatotropic viruses. There are approximately 260 million people across the globe persistently infected with this small DNA virus which has non-cytopathogenic effect on host, and it has enormous capacity to replicate without causing deleterious effects to the liver. it can also elicit immunopathology culminating to hepatic cirrhosis and hepatocellular carcinoma (HCC). These maladies are responsible for around 780,000 deaths annually (Stanaway, Flaxman et al. 2016). Although, there are potential treatment regimens for HBV like nucleoside/nucleotide analogues or pegylated interferon IFN-α therapy (Gish, Jia et al. 2012), but due to lack of sustained effect of these therapies, it requires long-term treatment resulting in probable complications in terms of resistance, toxicity and financial burden (Levrero, Testoni et al. 2016). Ideally, there should be persistent loss of viremia and HBs antigen after successful antiviral therapy, however, there is no complete functional cure of chronic HBV infection so far, as it is indeed difficult to eliminate the nuclear cccDNA (covalently closed circular DNA) from infected hepatocytes. In order to clear the chronic HBV infection, clearance of cccDNA and restoration of HBV-specific immune response is needed (Zeisel, Lucifora et al. 2015).

The outcome of chronic HBV infection depends on the contribution of virus specific CD8+ T cell responses in antiviral immunity (Chisari and Ferrari 1995; Bertoletti and Ferrari 2012; Schuch, Hoh et al. 2014; Gish, Given et al. 2015) that signify the importance of therapeutic vaccination as a potential alternative approach to induce HBV-specific immunity (Kosinska, Bauer et al. 2017). Over the last years, several studies were conducted to cure chronic HBV infection through therapeutic vaccination, but no promising outcome is achieved so far (Lim, Agcaoili et al. 2019). Whereas, heterologous prime-boost vaccine is still a remarkable choice to generate strong multi-functional virus specific T cell mediated immunity to break immune tolerance in chronic HBV infection (Backes, Jäger et al. 2016). Therapeutic vaccination aims to trigger both humoral and cell mediated immunity, and it might be further synergized through immunomodulation. For instance, TLR-9 ligand induced hepatic inflammation resulting

in cluster formation of inflammatory myeloid cells; these cell aggregates were named as iMATEs (intrahepatic myeloid cell aggregates support T cell expansion), which supported expansion of cytotoxic T lymphocytes (CTLs) resulting in clearance of HBV in preclinical HBV infection model (Huang, Wohlleber et al. 2013). Hence, a novel robust combinatorial antiviral therapy is needed, which could also be tailored with hepatic immune modulators to boost vaccine-induced HBV-specific T-cell immunogenicity, rendering safe and life-long immunity against chronic HBV infection.

1.2 Characteristics of adaptive immune response to HBV

1.2.1 T-cell mediated immunity in liver microenvironment

Due to the unique anatomic site, the liver is constantly exposed to the blood through systemic circulation, which is rich in nutrient and also harboring pathogenic degradation products that enter from gut (Jacob, Goldberg et al. 1977). Therefore, the hepatic immune system in normal physiological condition does not evoke immune response against pathogen-associated molecular patterns (PAMPs) to avoid liver damage following innate immune response. There are several regulatory mediators that promotes tolerance rather than immunogenic response such as PAMPs-induced secretion of transforming growth factor TGF-β by hepatic stellate cells or interleukin IL-10 from Kupffer cells. As a consequence, PAMPs are scavenged and eliminated from the circulation while maintaining the liver homeostasis. (Bissell, Wang et al. 1995; Knoll, Schlaak et al. 1995). These mediators also regulate the functions of antigen presenting cells (APCs) and T lymphocytes (Levings, Bacchetta et al. 2002). On the other hand, there are certain enzymes in microenvironment that limit the inflammation and T cell mediated immunity. For instance, the enzymatic activity of tryptophan 2,3-deoxygenase and indoleamine 2,3-deoxygenase convert their respective substrates into immune regulatory molecules (Ito, Hoshi et al. 2010). Moreover, the expression of arginase results in metabolism of arginine which is an essential amino acid for lymphocyte proliferation in hepatic microenvironment. As a consequence, it creates a tolerogenic microenvironment that limits the inflammation and T-cell mediated immunity in liver (Das, Hoare et al. 2008).

Hepatic T lymphocytes are remarkably heterogenous concerning their versatile phenotypic profiles, which also define their inflammatory or anti-inflammatory functions during liver disease. The activation of T cells ensues after crosstalk with liver

parenchymal cells while roaming through sinusoidal vasculature. This imminent activation of T cells is manifested by expression of activation markers like CD25 and CD69, which subsequently leads to the formation of CD45RO memory T cells (Volpes, van den Oord et al. 1991). The priming of T cells favors the immunological tolerance in normal physiological condition, but the balance of immunity in liver microenvironment shifts towards immunogenicity during the viral infection. Thereby, T cells could reactivate or re-stimulate through IL-12 and CD28 mediated signaling to exert antiviral immunity (Böttcher, Schanz et al. 2013). The activation of T lymphocyte under immunogenic microenvironment is also responsible for autoimmune hepatitis, but regulatory T cells (Tregs) and effector T cells are also upregulated in those patients who did not receive immunosuppressive therapy (Taubert, Hardtke-Wolenski et al. 2014). This demonstrates multi-dimensional and complex dysregulation in intrahepatic T cell repertoire in autoimmune disease (Ferri, Longhi et al. 2010). On the other hand, there are other nonclassical T cell populations such as γT and δT cell (Racanelli and Rehermann 2006). Despite, comprising of only small portion of overall hepatic T cells, these cells have significant contribution in regulating liver inflammation (Hammerich and Tacke 2014).

1.2.2 HBV-antigen specificity of CD8+ T cells

Lymphocytes have highly diverse antigen receptors that are produced by cascade of events of highly diverse somatic recombination (Cannon, Haire et al. 2004). Their sensitivity to discriminate even insignificant variations in antigen confers great degree of accuracy to target different viruses. However, the high precision of lymphocytes towards specific antigen during adaptive immune response may also result in immune escape by virus following minor mutations in the viral genome. Interestingly, occurrence of viral immune escape in T cell mediated immunity is quite rare in HBV as compared to HCV or HIV. So far, most of the studies that reported escape mutation by virus, focused on T cell responses to epitopes of HBV presented by globally common class I human leukocyte antigen (HLA) allele HLA-A*0201 (Bertoletti, Costanzo et al. 1994; Bertoletti, Sette et al. 1994). Nevertheless, T cell responses are not strong enough to exert selection pressure (Rehermann, Pasquinelli et al. 1995; Rehermann and Thimme 2019), but immune selection pressure by CD8+ T cells has also been suggested after investigating HLA genotype on DNA sequences of HBV through a

population-based approach in two studies (Desmond, Gaudieri et al. 2012; Kefalakes, Budeus et al. 2015).

It is difficult to determine the specificities of CD8+ T cells, as the information related to HBV epitopes is limited and the frequency of CD8+ T cell responses against HBV is very low (Bertoletti and Ferrari 2016). Nevertheless, it is observed that HLA-A2 restricted responses against the HBc antigen epitope (HBc 18-27) are associated with immune control and resolution of HBV infection (Maini, Boni et al. 1999; Kefalakes, Budeus et al. 2015). Furthermore, the quantity of HBV specific CD8+ T cells is very low in circulation in patients with chronic HBV infection. It is frequently below the baseline level of ex vivo detection by enzyme linked immune absorbent spot (ELISpot) quantification, intracellular cytokine staining or HLA peptide multimers (Boni, Fisicaro et al. 2007; Bertoletti and Ferrari 2016; Park, Wong et al. 2016). However, this technical constraint was resolved through enrichment of CD8+ T cells that bind to HLA-A2 HBV multimer, providing the opportunity to compare HBV-specific CD8+ T cells with respect to their specificities. After employing this approach, HBs antigen-specific T cell responses were observed only in a minority of patients with low level of chronic HBV infection i.e. HBe antigen was negative, while HBc antigen-specific responses were quite distinctive including differences in functional responses (Hoogeveen, Robidoux et al. 2019; Schuch, Alizei et al. 2019). Apart from that, immunological staining of infected human liver sections with antibodies against HLA-A*0201 restricted epitopes of HBc and HBs antigen also demonstrated spatio-temporal distribution of different specificities. It was noticed that the efficiency of presentation of HBc and HBs epitopes was different in hepatoma cell lines and primary human hepatocytes (Khakpoor, Ni et al. 2019). Therefore, these findings further increase degree of complexity by potentially preventing T cells of correct HBV specificity to encounter hepatocytes carrying respective antigen.

1.2.3 CD8+ T cell immune surveillance in acute HBV

Adaptive immune response is considered to play integral role in control and elimination of HBV infection (Chisari 2000). Indeed, several studies have shown that C8+ T cells contribute significantly in eliminating the virus during the progression of liver disease. Moreover, there is a strong relationship between the onset of multi-specific and polyclonal CD8+ T cell mediated immune response in liver and clearance infected

hepatocytes during acute infection of HBV and HCV in humans and chimpanzees (Cooper, Erickson et al. 1999; Maini, Boni et al. 1999; Lechner, Wong et al. 2000; Thimme, Oldach et al. 2001; Thimme, Bukh et al. 2002). It has been reported that the recurrence of circulatory CD8+ T cells is related to decreased viremia and the onset of hepatic infection, but functionality of virus specific CD8+ T cells was also impaired throughout the acute phase till the resolution of infection (Maini, Boni et al. 1999; Zhou, Cao et al. 2009; Goel and Boland 2012).

Virus-specific CD8+ T clear the infected hepatocytes through cytolytic, noncytolytic and noncanonical pathways. Cytolysis of infected cells is mediated through FAS/FASL, whereas noncytolytic clearance of virus is mediated by cytokines through inhibition of viral replication. Whereas, noncanonical effector function of CD8+ T cells and cytokine-mediated elimination do not require necessarily the killing of infected hepatocyte. Several studies have already established the mechanisms of CD8+ T cell mediated targeting of antigen in preclinical mice model system of viral Hepatitis. For instance, adoptively transferred HBV-specific CD8+ T cells triggered antiviral cytokines curtailing viral replication, consequently activating cytotoxic T lymphocytes (CTLs) that further subdued the viral replication (Guidotti, Ishikawa et al. 1996). Of note, it has also been shown that during the acute HBV infection in chimpanzees, most of HBV DNA was cleared before the peak of liver damage and T lymphocyte infiltration, suggesting the prominent contribution of non-cytolytic effector function involving IFN-y and TNF secretions. it was also noticed that the rate of HBcAg clearance was slower in infected cells and it was not associated with increase in sALT levels, cytolytic activity or number of regenerating hepatocytes. Hence, it was established that the noncytolytic activity is also crucial in the reduction of HBcAg during acute HBV infection (Guidotti, Rochford et al. 1999). Whereas, other studies also emphasized the support of cytolytic effector mechanism (Ando, Guidotti et al. 1994; Thimme, Wieland et al. 2003). Hence, both cytolytic and noncytolytic antiviral activities are indispensable to resolve acute HBV infection. Whereas, sometimes host immune cells prefer noncytolytic antiviral activity as survival strategy to avoid immunopathology through downregulation of antigen expression, but it also provides platform for viral immune escape, leading to the persistence of HBV antigen even for decades after resolution of acute HBV infection(Rehermann, Ferrari et al. 1996).

1.2.4 Differential role of CD8+ T cells immune in chronic HBV

Despite cytotoxic T cell mediated immune responses against acute hepatitis infection, the persistence of HBV is reported even after decades of recovery (Rehermann, Ferrari et al. 1996). Besides, virus specific CD8+ T cell frequencies are quite modest during acute resolving HBV infection, which decrease further in chronic HBV infection representing less than 0.2% of peripheral CD8+ T cells (Bertoletti and Ferrari 2016). Due to persistent viral infection, downregulation of antigen specific CD8+ T cell responses were observed, leading to the exhaustion and deletion of functional CD8+ T cells (Wedemeyer, He et al. 2002; Penna, Pilli et al. 2007). Thereby, HBV-specific CD8+ T cell responses were barely noticed in chronic HBV infection.(Ferrari, Penna et al. 1990; Bertoletti, Costanzo et al. 1994; Maini, Boni et al. 2000; Webster, Reignat et al. 2004; Boni, Fisicaro et al. 2007). The phase of infection and the degree of viral replication determine the overall profile of virus specific CD8+ T cells. Although, considerable peripheral multi-specific virus specific CD8+ T cell responses were detected ex vivo in the patients with low viral burden, but virus specific CD8+ T cell responses in patients with high levels of viral DNA (>10^7 copies/ml) were rarely noticed after ex vivo stimulation (Webster, Reignat et al. 2004). Along the line of previous findings, it was found that immune system constantly raided by viral and sub-viral particles eliciting CD8+ T cell responses repetitively, lead to an exhaustive state of virus specific CD8+ T cells (Mueller and Ahmed 2009; Utzschneider, Alfei et al. 2016). However, the mechanisms behind subsequent dysfunctional CD8+ T cell responses following large quantities of HBs and HBe antigens in circulation are not well understood so far.

1.2.5 Molecular mechanisms associated with dysfunctional HBV-specific CD8+ T cell responses

Recent findings concerning to the underlying molecular mechanisms responsible for inducing disruptive virus specific CD8+ T cell responses, provided us deep insight into understanding the dynamics of chronic HBV infection (Knolle and Thimme 2014; Wherry and Kurachi 2015; Ferrari, Boni et al. 2017). On the one hand, it is observed that upregulation of intracellular pro-apoptotic protein Bcl2 interacting mediator (Bim) resulted in deletion of virus specific CD8+ T cell in chronically infected patients (Lopes, Kellam et al. 2008). On the other hand, it was also revealed that there might be insufficient priming of virus specific CD8+ T cells by antigen presenting cells (APCs)

resulting in impaired activation and expansion of CD8+ T cells while encountering with antigen. Besides, several studies indicated that dysfunctional dendritic cells (DCs) in chronic HBV infection are responsible for reduced activation potential and impaired functional response by virus specific CD8+ T cells (Wang, Xing et al. 2001; Beckebaum, Cicinnati et al. 2002; van der Molen, Sprengers et al. 2004; DUAN, Zhuang et al. 2005). In accordance with these findings, phenotype of HBV-specific CD8+ T cells was predicted to resemble like naïve CD8+ T cells with increased expression of CD45RA, CD27, CD28 and CCR7 (Appay, van Lier et al. 2008).

Whereas, circulatory virus-specific CD8+ T cells in patients of chronic HBV infection also manifested impaired functional response failing to proliferate and produce antiviral cytokines like IFN-y (Boni, Fisicaro et al. 2007). The failure of effective CD8+ T cell response has been related to the high viral antigen levels. Although, the antigen is presented by APCs constantly on MHC molecules, but persistent circulation of viral particles comprising of soluble HBsAg and HBeAg resulted in dysfunctional HBV-specific CD8+ T cell responses. Particularly, HBeAg explicitly involved in transforming the phenotypic profile of functional HBV-specific CD8+ T cells during the course of HBV infection (Reignat, Webster et al. 2002). Interestingly, seroconversion of HBsAg restored CD8+ T cell responses and elicited strong adaptive immune response compared to only reduction in antiviral burden without HBsAg-seroconversion (Boni, Laccabue et al. 2012). Defective CD8+ T cell responses are usually followed by chain of events during chronic HBV infection, subsequently altering phenotypic profile of virus-specific CD8+ T cells with increased expression of inhibitory molecules like program death-1 (PD-1) (Boni, Fisicaro et al. 2007; Fisicaro, Valdatta et al. 2010), cytotoxic T lymphocyte antigen-4 (CTLA-4) (Schurich, Khanna et al. 2011), T-cell immunoglobulin mucin-3 (TIM-3) (Nebbia, Peppa et al. 2012; Wu, Shi et al. 2012) and CD244 (2B4) (Raziorrouh, Schraut et al. 2010). Consistent with the phenotype of exhausted CD8+ T cells, PD-L1 expression on hepatocytes has also been elevated, suggesting the induction of tolerogenic hepatic microenvironment (Mühlbauer, Fleck et al. 2006). Of note, it is also revealed that CD8+ T cell dysfunction was more profound in the liver as compared to blood circulation (Fisicaro, Valdatta et al. 2010; Knolle and Thimme 2014).

Interestingly, several in vitro studies also described that functionality of HBV-specific CD8+ T cells could be restored at least partially through blocking these inhibitory pathways (Boni, Fisicaro et al. 2007; Fisicaro, Valdatta et al. 2010; Raziorrouh, Schraut et al. 2010; Schurich, Khanna et al. 2011; Wu, Shi et al. 2012). Preclinical HBV models also established the potential relevance of PD-1 blockade through antibodies for PD-L1 with enhanced HBV-specific cytotoxic T cell responses following adoptive transfer of virus specific CD8+ T cells in HBV-transgenic mice. Subsequently, IFN-y producing CD8+ T cells were increased suggesting improved functionality of CD8+ T cells after PD-1 blockade (Maier, Isogawa et al. 2007). Consistent with these findings, PD-1/PD-L1 pathway blockade along with combinatorial therapy of DNA vaccination and entecavir therapy in vivo resulted in improved virus-specific CD8+ T cell responses, leading to the persistent control of chronic viral infection of liver (Liu, Zhang et al. 2014). Therefore, manipulation of these inhibitory pathways together with CD8+ T cell co-stimulation could circumvent tolerance during chronic liver infection.

It is also noted that CD4+ T helper cells could induce CD8+ T cell dysfunction as well (Yang, Althage et al. 2010). On the other hand, the contribution of immunosuppressive cytokines like TGF-ß and IL-10 (Dunn, Peppa et al. 2009; Peppa, Micco et al. 2010; Maini, Mauri et al. 2012) along with increase in T-regs population (Stoop, van der Molen et al. 2005; Xu, Fu et al. 2006; Yang, Liu et al. 2007) resulted in functional impairment of CD8+ T cell. Besides, it was also reported that the concentration of IL-10 in liver microenvironment played instrumental role in resolution or persistence of chronic viral infection in preclinical models (Brooks, Trifilo et al. 2006; Ejrnaes, Filippi et al. 2006). On the one hand, it helped to reduce the tissue inflammation while acting as a typical immunosuppressive cytokine (Sun, Madan et al. 2009), on the other hand, it also circumvented acute liver damage and rescued T cells from imminent cell death through autocrine release of IL-10 by virus-specific CD8+ T cells (Fioravanti, Di Lucia et al. 2017). Apart from that, impaired CD8+ T cell responses were also associated with elevated hepatic arginase level (Chisari 1978; Sandalova, Laccabue et al. 2012), which metabolizes arginine followed by downregulation of CD3 ζ-chain leading to reduced activation with impaired CD8+ T cell function (Das, Hoare et al. 2008).

Increase in arginase level was also attributed to the accumulation of granulocytic myeloid derived suppressor cells (MDSCs) in liver during the chronic HBV infection

(Pallett, Gill et al. 2015). While hepatic activated-natural killer (NK) cells were also responsible for deletion of virus-specific CD8+ T cells that were vulnerable to apoptosis (Peppa, Gill et al. 2013; Boni, Lampertico et al. 2015) by the expression of stress ligand harbored by CD4+ T cells, which binds to NKG2D receptor on NK cells eliciting cytotoxic responses during HBV infection (Huang, Easom et al. 2017). Besides, hepatic NK cells also caused depletion of virus-specific CD8+ T cells that express TRAIL-R2 death receptor selectively (Peppa, Gill et al. 2013) by upregulating apoptosis-inducing ligand TRAIL during HBV infection (Dunn, Brunetto et al. 2007; Stegmann, Robertson et al. 2016). Several other studies also established the pivotal role of NK cells in regulation of virus-specific T cells during the progression of viral infection in different preclinical models (Lang, Lang et al. 2012; Waggoner, Cornberg et al. 2012).

As an effective immune response requires enhanced metabolic capacity and bioenergetics, it is noted that HBV-specific CD8+ T cells were unable to switch on to more robust pathway of oxidative phosphorylation to supplement glycolytic metabolism (Schurich, Pallett et al. 2016). It has been observed that mitochondrial dysfunction was associated with limited metabolic capacity of HBV-specific T cells. whereas, reduced expression of electron transport chain (ETC) proteins and impaired polarization of mitochondria were related to high levels of reactive oxygen species (ROS) in virus specific CD8+ T cells (Fisicaro, Barili et al. 2017). Along the line, several studies on preclinical tumor and viral models also showed relevance of defective mitochondrial biogenesis in exhaustive state of T cells, while epigenetic modifications were also reported in exhausted PD-1^{hi} T cells (Bengsch, Johnson et al. 2016; Scharping, Menk et al. 2016). These findings demonstrated several underlying mechanisms that contribute towards impaired adaptive immune response during chronic hepatitis B infection and combinatorial therapy manipulating these pathways may restore HBV-specific cell mediated immunity.

1.3 Therapeutic vaccination – potential cure of chronic HBV

The aim of therapeutic vaccination in chronic liver infection is to prime virus specific T cell responses, boost already primed T cells or both in such a way that the adaptive immunity shifts tolerogenic phase to robust immunogenic response. There were several therapeutic strategies employed in this regard, but regardless of demonstrating

favorable results in preclinical research (Elvidge 2015; Kosinska, Bauer et al. 2017), none has generated adequate antiviral immune response in patients of chronic HBV infection . In order to boost adaptive immune responses during chronic infection, the contribution of effective innate immunity is imperative to control and prevent HBV infection (Chen, Chen et al. 2017; Paul, Dickstein et al. 2017). Since, functional cure of HBV is manifested by induction of anti-HBs antibodies, therefore, while developing therapeutic vaccine it should be kept into consideration. Several studies revealed that protein-based prime effectively produced neutralizing antibodies (Backes, Jäger et al. 2016; Kosinska, Bauer et al. 2017). Inclusion of viral vectors in therapeutic vaccination strategy also proved to be immunogenic (Kosinska, Bauer et al. 2017). For instance, adenoviral vectors and modified vaccinia ankara (MVA) viral vector generated effective T cell responses in preclinical model system of persistent HBV infection (Martin, Dubois et al. 2015; Backes, Jäger et al. 2016). A common drawback of adenoviral vectors is already existing immunity; however, this limitation could be resolved using chimpanzee adenoviral vector, which is replication deficient virus and already administered as recombinant adenovirus-based vaccine in humans for HCV infection (Barnes, Folgori et al. 2012). Furthermore, T cell mediated immune responses were also further enhanced in healthy volunteers through boosting with MVA carrying antigens, but the outcome in diseased individuals with HCV infection was not so remarkable (Kelly, Swadling et al. 2016; Swadling, Halliday et al. 2016). Nevertheless, the readout of antigen-specific T cell responses against recombinant MVA virus encoded with antigens still gave us insight to develop similar recombinant vectors for HBV (Swadling, Capone et al. 2014). Therapeutic vaccine consisting in recombinant adenoviral vector generated only immunogenic recombinant-vector-specific T cells, which demonstrated no cross-reactivity with the infecting HCV virus (Kelly, Swadling et al. 2016; Swadling, Halliday et al. 2016). Therefore, heterologous prime-boost vaccination strategy with different antigens could be employed, so that new antigen-specific T cells could be primed (Bourgine, Dion et al. 2012; Backes, Jäger et al. 2016). The effectiveness of this approach still relies on the cross-reaction of vaccine-induced T cells with infecting virus.

While formulating vaccine constituents, selection of HBV-antigens and route of delivery should also be taken into consideration. Ideally, therapeutic vaccine against chronic HBV should cover relevant genotypes and immunogens. Although, it is previously

mentioned that HBV escape mutations are relatively less than HCV and HIV, but HBV could replicate using reverse transcriptase (RT) that is inherently error prone. Nevertheless, escape mutations have been observed in CHB patients (Bertoletti, Costanzo et al. 1994) and it has been suggested through interpretation of scientific data that the frequency of these T-cell escape mutations has been underrated (Desmond, Gaudieri et al. 2012; Kefalakes, Budeus et al. 2015). To overcome the occurrence of escape mutations, polyclonal and multi-specific T cell responses are needed. This could be achieved through optimizing already existing heterologous therapeutic vaccination (Backes, Jäger et al. 2016). besides, the knowledge regarding protective hierarchy of CD8+ T cells and HBV epitopes is limited (Bertoletti and Ferrari 2016); therefore, it is quite convincing approach to develop a therapeutic vaccine that includes all crucial viral proteins; HBV polymerase, HBV core and envelop proteins. While HBV envelope protein is critical in order to induce antibodies, and polymerase is also important because it has been described that polymerase specific T cells were well-preserved during chronic infection, due to perhaps reduced levels of antigen presentation (Kefalakes, Budeus et al. 2015; Bertoletti and Ferrari 2016; Park, Wong et al. 2016).

Most of the studies conducted in past regarding HBV epitopes were restricted to HLA-A2 (Lumley, Noble et al. 2016), therefore, we need to further characterize the repertoire of HBV epitopes, so that correlation between outcome of vaccine and specificities of CD4+ and CD8+ T cell responses could be studied in detail. As an alternative approach, rather than selecting immunogens in advance, personalized antigen reservoir from diseased individual could be used for autovaccination. Under this paradigm, it was observed that in vivo maturation of monocytes supported the expansion of T cells through cross-presentation of autologous HBsAg (Gehring, Haniffa et al. 2013). Along with the development of therapeutic vaccination strategies, several routes of vaccine delivery were also studied in detail including subcutaneous, intranasal and intramuscular with further modifications like electroporation to enhance the delivery and efficacy of DNA vaccines (Liu, Ascenzi et al. 2011). For instance, administration of malarial prophylactic vaccines intravenously increased the hepatic uptake and supported the proliferation of resident memory T cells (Ishizuka, Lyke et al. 2016). These outcomes raise the possibility of administering therapeutic vaccination parenterally for chronic HBV.

1.4 Strategies to enhance therapeutic vaccine responses

Due to significant development in unraveling the underlying regulatory mechanisms of immune response directed towards the HBV infection, several direct and indirect approached can be adopted to further enhance the efficacy of therapeutic vaccine against chronic HBV infection.

1.4.1 Boosting T cells responses through checkpoint modulations

The blockade of checkpoint inhibitors has been proved to be effective in cancer immunotherapy. Similarly, targeting PD-1 on T cells to enhance efficacy of vaccine against chronic HBV has shown tremendous potential as immunotherapeutic. During the trials for proof of concept, it has already demonstrated the capacity to enhance the vaccine against woodchuck hepatitis virus and lymphocytic choriomeningitis virus (Ha, Mueller et al. 2008; Liu, Zhang et al. 2014). in spite of the fact that, PD-1 pathway is responsible for tolerogenic hepatic microenvironment (Iwai, Terawaki et al. 2003; Isogawa, Furuichi et al. 2005; Fisicaro, Valdatta et al. 2010), in vivo PD-1 blockade did not induce inhibitory hepatic toxicity in patients of chronic HBV and HCC (El-Khoueiry, Sangro et al. 2017; Gane, Verdon et al. 2019). Therefore, combinatorial therapy involving PD-1 blockade is still considered as one of the favorites in immunotherapy. Other approach to enhance the efficacy of therapeutic vaccination is to combine one or more checkpoint inhibitors or on the other hand, use the combination of checkpoint inhibitors with co-stimulators; in vitro synergistic effect of PD-1 and TIM-3 or PD-1 and CTLA-4 has been observed on HBV-specific T cells (Schurich, Khanna et al. 2011; Nebbia, Peppa et al. 2012) and clinical trials has already been conducted using these approaches in diseased individuals with HCC (Iñarrairaegui, Melero et al. 2018) and other cancers. However, these interventions might induce immune-related toxicity in patients with uncomplicated chronic liver infections. Besides, it is also noted that human B cells and HBsAg-specific immune cell populations also have upregulated PD-1 expression (Burton, Pallett et al. 2018; Salimzadeh, Le Bert et al. 2018), thereby opening the window of opportunity to reinforce innate immune response through checkpoint modulation as previously described in macaques infected with simian immunodeficiency virus (Titanji, Velu et al. 2010). Furthermore, the antiviral activity of PD-1 expressing B cells was also reported to interlink with each other transcriptionally, as these cells also harbored high levels of T-bet (Burton, Pallett et al. 2018); which is

crucial for isotype commutation and antiviral activity in mice (Rubtsova, Rubtsov et al. 2013; Barnett, Staupe et al. 2016; Knox, Buggert et al. 2017).

Recent data also suggested a multifaceted role of PD-1 in homeostasis (Utzschneider, Legat et al. 2013; Wieland, Kemming et al. 2017; Bengsch, Ohtani et al. 2018), as PD-1 strongly expressed on activated T cells as well as on tissue resident T cells that also induced functional T cells responses via TCR (Kumar, Ma et al. 2017; Pallett, Davies et al. 2017). Furthermore, it has been observed that deleting PD-1 genetically increased the capacity of T cells to clear HBV-expressing hepatoma cells in highly expressing PD-L1 microenvironment (Otano, Escors et al. 2018), however, it has also induced unwarranted proliferation of T cells, leading to senesce of murine and human CD8+ T cells terminally (Odorizzi, Pauken et al. 2015; Otano, Escors et al. 2018). These outcomes were consistent with the fact that immune inhibitors like PD-1 supported T cells to maintain immune responses against constant stimulation of antigens, which enabled them to the control the infection (Wieland, Kemming et al. 2017; Utzschneider, Delpoux et al. 2018). Besides, it has been noted that knockdown of PD-1 genetically on human T cells triggered the compensatory expression of other checkpoints alternatively such as CTLA-4 and TIM-3 (Otano, Escors et al. 2018), in the meanwhile, exerting some degree of control on HBV-specific T cells in vitro (Schurich, Khanna et al. 2011; Nebbia, Peppa et al. 2012). The heterogenous and complex nature of checkpoint inhibition mechanism suggested that, there should be customized selection of molecules, emphasizing to utilize biomarkers to predict the outcome. On the other hand, these findings demonstrated the constraints in repetitive anti-PD-1 therapy during persistent stimulation of immune cells by antigens in chronic infection.

1.4.2 TLR agonists – as potential immunotherapeutic agents

Toll-like receptors (TLRs) are present on sentinel immune cells, and play crucial role in activation of innate immunity through detecting Pathogen-associated molecular pattern molecules (PAMPs); PAMPs consist of unique microbial molecules such as bacterial or viral DNA (Heymann and Tacke 2016). Several preclinical studies provided insight concerning mode of actions of different TLR-agonists, but in-depth analysis is still needed to define the role of TLR-agonists in complex hepatic microenvironment during chronic HBV. besides, other novel approaches should be explored to identify

potential combinatorial therapeutic vaccination strategies involving TLR-agonist, so that T cell mediated immune response could be further enhanced through two different mechanisms simultaneously.

Therapeutic approach involving TLR-agonists provided us an opportunity to modulate adaptive immunity indirectly without targeting T cells or B cells. The oral administration of TLR-7 agonist GS-9620 in chronic HBV patients has been shown to enhance the priming of DCs, which is followed by improved proliferation of functional HBV-specific T cells (Boni, Vecchi et al. 2018). However, TLR-7 agonist also induced expansion of NK cells upon treatment, but it did not result in deletion of HBV-specific T cells through NK cell-mediated cell death (Davidson, Maini et al. 2015). In this case, the survival of virus-specific T cell might be attributed to the expression of IFN triggering genes (Janssen, Brunetto et al. 2018) induced by TLR-7 signaling, as already described in murine LCMV infection model (Davidson, Maini et al. 2015). Notwithstanding, it failed to reduce HBsAg in vivo as sole agent for chronic HBV treatment in a double-blind phase II trial (Janssen, Brunetto et al. 2018). Hence, we need to further refine the knowledge regarding mode of action of TLR-7 agonist and investigate other combinatorial approaches such as combining TLR-7 with a potential therapeutic vaccine. Similarly, Phase II trials has been conducted with TLR-8 agonist GS-9688 in chronic HBV patients. it was also reported to support the expansion of HBV-specific T cells through induction of IL-12 signaling (Schurich, Pallett et al. 2013; Kurktschiev, Raziorrouh et al. 2014). Another immunostimulant consisted of inactive parapoxviral particle, which induced inflammation through TLR-9 signaling, has already been tested in phase I clinical trial in CHB patients (von Buttlar, Siegemund et al. 2014). The rationale behind targeting TLR-9 signaling pathway in chronic HBV infection was based on preclinical data that demonstrated the role of TLR-9 ligand in improving control of infection in combination with DNA vaccine than vaccine alone. It was demonstrated that intrahepatic myeloid cells formed cocoon like clusters upon TLR-9 signaling, providing shelter to hepatic CD8+ T cells from hepatic regulatory cues and supported their local expansion (Huang, Wohlleber et al. 2013). Apart from that, B cells could also express TLRs, providing direct target-based therapeutic approach through respective agonists. Therefore, we need to also enhance our understanding to exploit TLR-agonists directed towards B cells in the context of CHB treatment.

1.4.3 Other potential immune boosting strategies for therapeutic vaccination

Sometimes extensive epigenetic modifications cause limitations in therapeutic approaches directed towards blockade of T-cell signaling pathways. For instance, extensive epigenetic modifications were identified upon phenotypic and transcriptional profile of CD8+ T cell subsets PD-1^{hi} Eomes ^{hi} T-bet^{low}, which couldn't be altered through PD-1 blockade. As a consequence, it restrained the capacity of these CD8+ T cells to properly respond to anti-PD antibodies (Pauken, Sammons et al. 2016). After identifying exhaustion specific enhancer modules as new targets for genome-editing, it might be possible to enhance antiviral activity of T cells by altering epigenetic landscape (Sen, Kaminski et al. 2016). Among the different factors of T cell dysfunction, it is relatively easier to target mitochondrial defects in exhausted PD-1^{hi} T cells (Schurich, Pallett et al. 2016; Fisicaro, Barili et al. 2017). Along the line, it is reported that in vitro supplementation of mitochondrial antioxidants mitoquinone or MitoTEMPO that served as ROS scavenger, expanded functional HBV-specific CD8+ T cells (Fisicaro, Barili et al. 2017). Mitoquinone administration to HCV patients was also reported as safe and hepatoprotective (Gane, Weilert et al. 2010), which could serve as a potential adjuvant in therapeutic vaccine for chronic HBV. besides, it was also revealed that IL-12 increased mitochondrial polarization of HBV-specific CD8+ T cells, which enabled them to trigger oxidative phosphorylation to supplement glycolytic metabolism (Schurich, Pallett et al. 2016). these findings were in accordance with the previously reported contribution of IL-12 towards restoration of functional HBV-specific CD8+ T cells (Schurich, Pallett et al. 2013; Kurktschiev, Raziorrouh et al. 2014). As previously mentioned, arginase-1 producing granulocytic MDSCs catabolized L-arginine, which represents another metabolic checkpoint of potential significance in HBV infection. It has been shown in preclinical model system that supplementing T cells with L-arginine triggers metabolic changes leading to improved survival and memory formation (Geiger, Rieckmann et al. 2016).

While innate immune system can also negatively impact T-cell mediated immunity during chronic HBV infection, it creates the possibility of enhancing adaptive immune response through selectively blocking inhibitory innate immune responses in combination with therapeutic vaccination. For instance, NK cells have the capacity to delete HBV-specific T cells; thereby reducing scope of T cells to combat with antigens during chronic liver infection (Peppa, Gill et al. 2013; Huang, Easom et al. 2017). The

mechanism behind deletion of T cells was associated with the expression of death receptor TRAIL-R2 on HBV-specific T cells. Blockade of the TRAIL pathway through small molecules should harness the deletion of vaccine-induced HBV-specific T cells, resulting in enhanced T-cell responses. In addition to that, it may also curb the death of TRAIL-R2 expressing hepatocytes by TRAIL+ NK cells, subsequently reducing the liver damage and hepatic flares (Dunn, Brunetto et al. 2007). However, TRAIL blockade could also lead to liver fibrosis, but other regulatory TRAIL receptors such as TRAIL-R3/4 restrain the apoptosis of hepatic stellate cells thereby supporting the resolution of liver fibrosis (Singh, Otano et al. 2017).

Therapeutic interventions to boost endogenous HBV-specific T cell responses were highlighted so far, while genetically engineered chimeric antigen receptor (CAR) T cells are another front-runner in immunotherapy to boost immunogenicity in HBV-related HCC (Bertoletti and Rivino 2014). This approach circumvents the inadequate functional response of endogenous T cells, but CAR-T cells are also still vulnerable to the immunosuppressive hepatic microenvironment. Hence, the regulatory pathways discussed above could also be exploited while optimizing CAR-T cell therapy. Therefore, manipulation of different mechanisms involved in innate immunity besides therapeutic vaccine could also prove to be effective in enhancing immunogenicity of HBV-specific T cell responses during chronic HBV infection.

1.5 Research questions, aims and objectives

Aim of the research project is to improve the efficacy of therapeutic vaccination against chronic HBV infection. For that, we employed a well-established prime-boost vaccination strategy where initial protein vaccination is followed by application of a Modified Vaccinia Virus Ankara encoding HBV antigens. This protocol has been successfully developed over the last years by Prof. Protzer in the Institute of Virology and is at present the most promising therapeutic vaccine candidate against chronic Hepatitis B Virus infection. Therapeutic vaccination trials in HBV transgenic animals yielded promising results but HBV-specific T cell immunity faded away indicating that additional measures to increase the numbers of virus-specific CD8+ T cells are required to achieve control over chronic HBV infection (Backes, Jäger et al. 2016). The central hypothesis of my research project is that induction of iMATEs allow for massive expansion of HBV-specific CD8+ T cells that then can control HBV infection in

hepatocytes. The factors that determined the massive expansion of CD8+T cells within iMATEs are as follows: previous activation of CD8+ T cells in lymphoid tissues including strong co-stimulatory signaling; relocation of CD8+ T cells from lymphoid tissues to the liver; co-stimulation dependent (CD28/OX40/IL-15R signaling) activation of CD8+ T cells within iMATEs causing massive T cell proliferation (Huang, Wohlleber et al. 2013).

Firstly, we synchronized iMATEs induction with heterologous prime-boost vaccination in wild-type mice. Then, we defined the role of MVA being a potent viral vector in hepatic recruitment of inflammatory myeloid cells and CD8+ T cell expansion as compared to CpG. Next, we determined the efficacy of therapeutic vaccine with synchronized iMATEs induction in HBV1.3 transgenic mice and AAV-HBV mice model of chronic HBV infection. Thereafter, we investigated the proliferation potential of hepatic immune cell populations following CpG application in HBV1.3 transgenic mice and AAV-HBV mice. After these preclinical studies, we established ex vivo system of CD8+ T cell proliferation to characterize myeloid cell contribution towards CD8+ T cell expansion. This ex vivo system, where the phenotype and mechanisms determining the outcome of the myeloid cell – CD8+ T cell crosstalk can be studied in detail, providing us with the opportunity to identify the underlying mechanisms and overcome hepatic immune tolerance during chronic HBV infection.

2. MATERIALS AND METHODS

2.1 Materials

2.1.1 Instruments

ArchitectTM platform (Abbott Laboratories, Wiesbaden, Germany)
Reflotron Plus system (Roche Diagnostics, Risch, Switzerland)
CytoflexS flow cytometer (Beckman Coulter GmbH, Palo Alto, USA)
SA3800 spectral cell analyzer (SONY Biotechnology, Champaign, USA)
SP6800 spectral cell analyzer (SONY Biotechnology, Champaign, USA)
SH800S cell sorter (SONY Biotechnology, Champaign, USA)
autoMACS pro separator (Miltenyi Biotec)
Table centrifuge Heraeus Fresco 17 centrifuge (Thermo Fisher Scientific, USA)
Benchtop ThermoScientific Megafuge 8 (Thermo Fisher Scientific, Waltham, USA)
Heraeus Multifuge X3R centrifuge (Thermo Fisher Scientific, Waltham, USA)
Ultracentrifuge Optima LE 8014 (Beckman Coulter GmbH, Palo Alto, USA)
SONOPULS Ultrasonic Homogenizers UW2070 (BANDELIN electronic GmbH)
Axio Imager 2 research microscope (S2) (Zeiss, Oberkochen, Germany)
Axio Vert A1 research microscope (S1) (Zeiss, Oberkochen, Germany)
Embedding system EG1150 H (Leica Biosystems, Nussloch, Germany)
Paraffin embedding system cool unit TBS88 (Medite GmbH, Burgdorf, Germany)
Paraffin stretching table (Medite GmbH, Burgdorf, Germany)
Tissue infiltration machine ASP300 S (Leica Biosystems, Nussloch, Germany)
Rotary microtome (HM355S, ThermoFisher Scientific, Waltham, USA)
Counting chamber (Neubauer) 0.1mm 0.0025 mm^2 (Marienfeld, Germany)
Analytical balance Sartorius CP224S-OCE, CD2201 (Sartorius, Göttingen, Germany)
Corning LSE vortex Mixer (Thermo Fisher Scientific, Waltham, USA)
Masterflex perfusion pump (Novodirekt, Kehl am Rhein, Germany)
Incubator Heracell 150i (Thermo Fisher Scientific, Waltham, USA) Thermal shaker MaxQ4000 (Thermo Fisher Scientific, Waltham, USA)
Laboratory water bath TW8 (Julabo, Seelbach, Germany)
Laboratory scale LSM2000 PCE (Deutschland GmbH, Meschede, Germany)
pH Meter pH7110 (Inolab, Weilheim, Germany)
Biological safety cabinet ThermoScientific Safe 2020 (Thermo Fisher Scientific, USA)

2.1.2 Consumables

Blood collection tubes microvette 500 (LH-Gel Sarstedt, Nümbrecht)

Lancets Supra blood lancets (megro, Wesel)

Capilette for Reflotron, heparinized, 32 µL (Selzer Labortechnik, Germany)

Reflotron test strips GOT (AST) (Roche Diagnostics, Risch, Switzerland)

ARCHITECT HBeAg (Abbott Laboratories, Sligo, Irland)

ARCHITECT HBsAg (Abbott Laboratories, Sligo, Irland)

HSW Norm-Ject TBC syringes 1 ml - U100 (Servoprax, Wesel, Germany)

Omnican 100 insulin syringe (1 ml/100 I.U.) (B. Braun, Melsungen, Germany)

Cannulas Sterican (B. Braun, Melsungen, Germany)

- 0.9 x 40 mm 20 gauge
- 0.8 x 40 mm 21 gauge
- 0.45 x 25 mm 26 gauge
- 0.40 x 20 mm 27 gauge

Scalpel (Feather, Osaka, Japan)

Cellstar tubes sterile with conical bottom (Greiner Bio-one, Solingen, Germany)

- 15 ml
- 50 ml

Eppis micro-reaction tubes (Eppendorf, Hamburg, Germany)

- 0.5 ml
- 1.5 ml
- 2.0 ml

Falcon 40 µm cell strainer (Corning life sciences, USA)

Sterile filter Aerodisc 0.2 µm (Pall, Cornwall, UK)

Titer-tube micro test tubes (Bio Rad, Hercules, USA)

Flow cytometry tube (Sarstedt, Nümbrecht, Germany)

- 5 ml, 75 x 12 mm

Cytofix/Cytoperm kit BD Biosciences

Fix/Perm with Foxp3 kit BD Biosciences

CellTrace CFSE cell proliferation kit for flow cytometry (Invitrogen, Carlsbad, CA)

CountBright absolute counting beads (Invitrogen, Carlsbad, CA)

CD8a (Ly-2) microBeads, mouse (Miltenyi Biotec)

Glass tubes for high-strength centrifuge (Kimble Chase, Rockwood, TN / USA)

- 15 ml

- 30 ml

Histology cassettes (Thermo Fisher Scientific, Waltham, USA)

Cell culture flasks with filter screw cap (COTECH Vertriebs GmbH, Berlin, Germany)

- 25 cm^2
- 75 cm^2
- 150 cm^2

Cellstar cell culture plates (Greiner Bio-one, Solingen, Germany)

- 96-well plate
- V-shaped bottom

Cellstar cell culture plates, natural, sterile (Greiner Bio-one, Solingen, Germany)

- 96-well plate, flat bottom
- 48-well plate, flat bottom
- 24-well plate, flat bottom
- 6-well plate, flat bottom

Petri-dishes (Greiner Bio-one, Solingen, Germany)

Pasteur pipettes glass made, sterile (neolab, Heidelberg, Germany)

Pipette tips (Greiner Bio-one, Solingen, Germany)

- 10 µl
- 100 µl
- 1000 µl

Pipettes (Greiner Bio-one, Solingen, Germany)

- 5 ml
- 10 ml
- 25 ml

UZ tubes Ultra Clear (Beckmann Coulter, Palo Alto, USA)

- 14 x 89 mm
- 25 x 89 mm

Disposable plastic bag, 200 x 300 mm (Sarstedt, Nümbrecht, Germany)

2.1.3 Chemicals and reagents

DMEM, GIBCO Life Technologies, Carlsbad, USA

GBSS, PAN Biotech, Aidenbach, Germany

HBSS, Sigma Aldrich, St. Louis, USA

PBS Dulbecco (w/o Ca^{2+}, w/o Mg^{2+}), Biochrom AG, Berlin, Germany

RPMI Glutamax GIBCO, Life Technologies, Carlsbad, USA
Williams Medium E, PAN-Biotech, Aidenbach, Germany
FCS (fetal calf serum), PAN-Biotech, Aidenbach, Germany
BSA (bovine serum albumin), AppliChem, Darmstadt, Germany
Tris ($C_4H_{11}NO_3$) AppliChem, Darmstadt, Germany
EDTA, AppliChem, Darmstadt, Germany
Trypsin, PAN Biotech, Aidenbach, Deutschland
Sodium Azide, AppliChem, Darmstadt, Germany
Pyruvat, Sigma-Aldrich, St. Louis, MO/USA
Beta-Mercaptoethanol (C_2H_6OS), Sigma Aldrich, St. Louis, USA
Glutamine (L-), (200 mM), GIBCO Life technologies, Carlsbad, USA
Penicillin (10000 U/ml) / streptomycin (10mg/ml) GIBCO, Life Technologies, USA
Isolfluran Forene, AbbVie, Ludwigshafen, Germany
Brefeldin A solution (1000x), Thermo Fisher Scientific, Waltham, USA
Collagenase, Type II & IV, Thermo Fisher Scientific, Waltham, USA
Percoll, GE Healthcare, Biosciences-AB, Uppsala, Sweden
Sucrose ($C_{12}H_{22}O_{11}$), AppliChem, Darmstadt, Germany
Dimethyl sulfoxide (DMSO, C_2H_6OS), AppliChem, Darmstadt, Germany
Paraformaldehyde (PFA, H (-OCH_2) n-OH), AppliChem, Darmstadt, Germany
Cheluminate-HRP PicoDetect, AppliChem, Darmstadt, Germany
Bromophenol blue, Sigma Aldrich, St. Louis, USA
Butanol ($C_4H_{10}O$), AppliChem, Darmstadt, Germany
Ethanol, absolute ($C_2H_4O_2$), AppliChem, Darmstadt, Germany
Hydrochloric acid (HCl), Roth, Karlsruhe, Germany
Sodium hydroxide (NaOH), Roth, Karlsruhe, Germany
Calcium chloride ($CaCl_2$ x $2H_2O$), Merck, Darmstadt, Germany
H_2O, PCR-grade, Roche, Basel, Switzerland

2.1.4 Buffers and Culture Media

PBS (Fa. Biochrom) pH7,4

- 80 g/l NaCl
- 0.2 g/l KCl
- 1.44 g/l $NaHPO_4$ x $2H_2O$

100% Percoll stock solution

- 90 ml Percoll
- 10 ml 10X PBS (Sigma Aldrich)

80% Percoll solution

- 80 ml 100% Percoll stock solution
- 20 ml PBS

40% Percoll solution

- 40 ml 100% Percoll stock solution
- 60 ml PBS

25% Percoll solution

- 25 ml 100% Percoll stock solution
- 75 ml PBS

36% sucrose solution

- 36 g sucrose powder
- 64 ml H_2O

T cell medium

- RPMI Glutamax (500 ml)
- 10% (v/v) FCS
- 5 ml L-glutamine (200 mM)
- 5 ml penicillin streptomycin 10000 U/mL
- 500 µL (1:1000) Beta-mercaptoethanol

FACS Buffer

- 1X PBS
- 1% FCS
- 0.01% sodium azide

MACS Buffer

- 1X PBS
- 0.5% FCS
- 2 mM EDTA

2.1.5 CD8+ T cell activation cocktail

anti-CD3e functionally purified monoclonal antibody (clone 145-2C11) (eBioscience)

anti-CD28 functionally purified monoclonal antibody (clone 37.51) (eBioscience)

Interleukin-2 (Proleukin S) 1 x 10^6 IU/ml (Novartis)

or

Dynabead Mouse T-Activator CD3/CD28 (Thermo Fisher Scientific, Waltham, USA)
Interleukin-2 (Proleukin S) 1 x 10^6 IU/ml (Novartis)

2.1.6 MHC class I/SIINFEKL multimer

H-2Kb restricted HBcore peptide (core93-100 MGLKFRQL) (Prof. Busch, Institute of Microbiology)
H-2Kb restricted ovalbumin derived peptide (OVAS8L SIINFEKL) (Prof. Busch, Institute of Microbiology)
Strep-Tactin PE (IBA lifesciences)

2.1.7 FACS antibodies (murine)

CD4 (BV785) (clone L3T4) (BD Biosciences)
CD8a (PE/PE-Cy7/BV510/eF450) (clone 53-6.7) (BioLegend, San Diego, USA)
CD8 (PE) (clone 56.6-7) (BD Biosciences, Heidelberg, Germany)
Fixable Viability Dye (eF780/eF450) (eBioscience, Frankfurt, Germany)
Ki67 (FITC) (clone SolA15) (eBioscience).
CD11b (PE-Cy5) (clone HK1.4, M1/70) (BioLegend, San Diego, USA)
MHC-II (PE) (clone M5/114.15.2) (BioLegend, San Diego, USA)
Ly6C (PE-Dazzle 594/APC/AF674) (clone HK1.3) (eBioscience)
Ly6G (Gr-1) (APC/FITC) (clone RB6-8C5) BioLegend, San Diego, USA
CD80 (PE) (clone 16-10A1) (eBioscience)
CD86 (PECy7) (clone GL1) (eBioscience)
CD44 (BV711) (clone IM7) (BioLegend, San Diego, USA)
CD25 (eF450, PerCp-Cy5.5) (clone PC61.5) (BioLegend, San Diego, USA)
CD69 (PE-Cy7) (clone H1.2F3) (BioLegend, San Diego, USA)
PD-1 (CD279) (PerCp-eF710) (clone J105) (Thermo Fisher Scientific, USA)
CD90.1 (APC) (clone HIS51) (BioLegend, San Diego, USA)
CD19 (PE-eF610) (clone 1D3) (BioLegend, San Diego, USA)
IFN-γ (BV711, FITC) (clone XMG1.2) (eBioscience)
Human granzyme B (PE) (clone GRB04) (Invitrogen, Carlsbad, CA)

2.1.8 Immunohistochemistry antibodies

anti-HBcAg antibody (1:50 dilution) (Diagnostic Biosystems, Pleasanton, CA)
anti-Ki67 antibody (clone SP6, Abcam ab16667)

2.1.9 Recombinant virus for chronic HBV infection

AAV-HBV1.2 vector carrying 1.2-fold overlength HBV genome of genotype D (Kindly provided by Prof. Protzer, Institute of Virology, TUM)

2.1.10 Therapeutic vaccination material

Bis-(3'-5')-cyclic dimeric adenosine monophosphate (c-di-AMP) (InvivoGen)
HBcore protein as prime (APP Latvijas Biomedicinas, Riga, Latvia)
Recombinant MVA-HBcore (Kindly provided by Prof. Protzer and amplified in IMI)
CpG oligodeoxynucleotides (or CpG ODN 1668) (InvivoGen, San Diego, CA)
Non-CpG ODN (InvivoGen, San Diego, CA)

2.1.11 Software application

Aperio ImageScope by Leica Biosystems
EndNoteX9 Literature management by Thompson Reuters
FlowJo 10.6.1 by BD
Pestle and Spice v6 by NIH
GraphPad Prism v7 Statistics and Graphing by Graphpad Inc.
Illustrator CS5 Graphic designing by Adobe
Inkscape 0.92.4 drawing tool
Microsoft office 360

2.2 Methods

2.2.1 Amplification of Modified Vaccinia Ankara (MVA) virus

Modified Vaccinia Ankara (MVA) Virus is a potent viral vector that has significant contribution in developing therapeutic vaccine. It can encode more than one antigen to produce multivalent vaccine. MVA virus is biosafety level (BSL)-1 viral vector which has the adjuvant capacity to induce both humoral and cellular responses (Altenburg, Kreijtz et al. 2014). Amplification of MVA virus was performed to use it further for preclinical therapeutic vaccination trials against chronic Hepatitis B infection. The protocol of MVA virus amplification is as under;

2.2.2 Pre-amplification of MVA in DF-1 cell line

Modified Vaccinia Ankara (MVA) virus was amplified in UMNSAH/DF-1 cell line. DF-1 is a spontaneously immortalized chicken cell line which is derived from 10-day old East Lansing Line eggs. Primary chicken embryonic fibroblasts were dissociated and passaged in the culture (30-60% culture confluence) until they started to senesce. fibroblasts were grown for greater than 30 passages after identification of foci of non-senescent cells (Foster and Foster 1997). Firstly, DF-1 cells were cultured for 2 days in T175 cell culture flask with Dulbecco's Modified Eagle's Medium (DMEM) containing 4 mM L-glutamine, 4500 mg/l glucose, 1 mM sodium pyruvate, 1500 mg/l sodium bicarbonate, 10% FCS and 1% Penicillin-Streptomycin. After achieving 80-90% confluency, cell monolayer was infected inoculating with 3 ml viral suspension (MOI 0.1 PFU/cell) in DMEM and incubated for 2 hours at 37°C. Cell culture flask was gently rocked after 20 minutes of time interval. After incubation, DF1 cells were resuspended with 17 ml DMEM and incubated further for 2-3 days at 37°C. Next, cells were

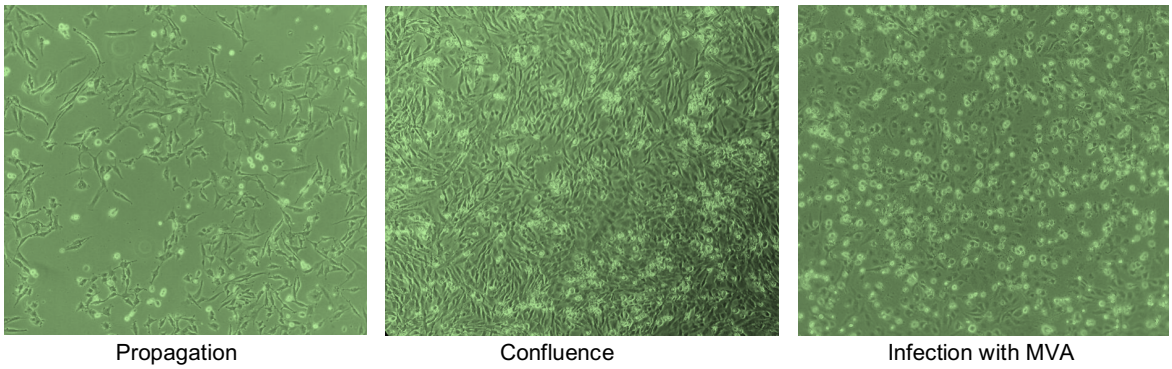

Figure 1. *Amplification of MVA in DF-1 cell line*

harvested including supernatant in 50 ml falcon tube using cell scraper after clear cytopathic effect (CPE) with 90-100% infection rate (Fig. 1) and stored at -80°C.

2.2.3 Infection of DF-1 cells with MVA

DF-1 cells were prepared in twenty T175 flasks and incubated for 24-48 hours at 37°C till 100% confluency was achieved. Then supernatants from cell culture flasks containing DF-1 cells were discarded. In the meanwhile, MVA-infected cell suspension was thawed at 37°C that was collected in previous step and further added 40ml of DMEM. Then we added 3ml of MVA-infected cell suspension to each cell culture flasks containing DF-1 cells incubated for 2 hours at 37°C. Cell culture flasks were gently shaken after 20 minutes of time interval. After incubation, cells were resuspended with 17 ml DMEM and incubated further for 2-3 days at 37°C.

2.2.4 Harvest infected DF-1 cells

DF-1 cells were harvested using cell scraper after 80-90% infection rate. Later the cells were added to six 50ml falcon tubes and centrifuged at 3500 x g (acceleration: 9, Deceleration: 9) for 5 minutes at 4°C temperature. We discarded the supernatant and harvested MVA-infected cells from pellets. Finally, we combined and resuspended the pellets in 30 ml 10 mM Tris (pH 9.0) and stored them at -80°C.

2.2.5 Virus purification

We performed three freeze thaw cycles (-80°C freezer/37°C water bath) with harvested MVA-infected cells. Later, we performed sonication with 100% amplitude through ultrasound homogenizer (3X for 30 seconds) under the safety cabinet. Cell suspension was kept on ice for at least 5 minutes after each sonication so that viral degradation by heat generated throughout the whole process could be avoided. After that cell suspension containing MVA virus was centrifuged at 3500 x g (acceleration: 9, Deceleration: 9) / 4°C for 5 minutes and collected the supernatant containing MVA virus in new 50 ml falcon. We repeat the sonication and centrifugation steps two more times after resuspending the pellet of previous falcon tube in 25 ml 10 mM Tris (pH 9.0) and discarded pellets in the end. Finally, we have three 50 ml falcon tubes containing MVA virus in 80 ml 10 mM Tris (pH 9.0). Then MVA virus was further purified through two steps of ultracentrifugation (sucrose gradient).

2.2.6 Sucrose gradient centrifugation

In order to purify MVA virus, sucrose density gradient centrifugation was performed using Ultracentrifuge Optima LE 8014 (Beckman Coulter GmbH, Palo Alto, USA). The process of centrifugation segregates particles of different densities through sucrose gradient. Firstly, SW32 buckets of ultracentrifuge were disinfected with 80% alcohol. Then 36% of sterile sucrose gradient was prepared by dissolving 36 g of sucrose powder in 64 ml H_2O and filtered through sterile filter Aerodisc 0.2 µm. After that 25 ml 36% sucrose was added in each of the 6 UZ tubes Ultra Clear 25 x 89 mm and carefully overlaid 13 ml MVA supernatant on top of the 36% sucrose solution layer. Then Ultra Clear tubes were placed in SW32 beakers and covers were fastened. Centrifuge tubes were tared precisely by adding 10 mM Tris (pH 9.0) (10 µl = 0.01 g). After placing the beakers in ultracentrifuge machine, they were centrifuged for 90 minutes at 13500 rpm, 4°C with max acceleration and max deceleration. After the centrifugation was finished, tubes were taken out using tweezer and supernatants were discarded. The pellets containing MVA were dried and resuspended in the final volume of 12 ml 10 mM Tris (pH9.0). Then MVA suspension could be stored at -80°C or processed further on the same day with second sucrose gradient centrifugation.

In order to perform second sucrose gradient, SW41 beakers were rinsed with 80% alcohol and let them dry completely. Then 10 ml 36% sucrose was pipetted out in each of the 6 UZ tubes Ultra Clear 14 x 89 mm and carefully overlaid 2 ml MVA suspension on top of the 36% sucrose layer. Then Ultra Clear tubes were placed in SW32 beakers and fastened the covers. Centrifuge tubes were tared precisely by adding 10 mM Tris (pH 9.0) (10 µl = 0.01 g) then centrifuged after placing them in SW41 beakers for 90 minutes at 13500 rpm, 4°C with max acceleration and max deceleration. Then UltraClear tubes were taken out with tweezers and supernatant was discarded. The pellets were dried and resuspended in a final volume of 300 µl 10 mM Tris (pH9.0) (increase volume up to 1 ml to avoid losing large parts of the pellets).

2.2.7 Virus titration

DF-1 cells were prepared in T75 cell culture flask 2 day before using them for titration. Then after discarding cell culture medium, cells were washed 2X with PBS. After that 2 ml trypsin was added to detach the cells and incubated them for 5 minutes at 37°C / 5% CO_2. After that cell suspension was shifted to 15 ml falcon tube and resuspended

with 8 ml DMEM with 2% FCS. Then 1 ml of DF-1 cell suspension was taken in a separate 15 ml falcon tube further diluted with 9 ml DMEM with 2% FCS. Thereafter, flat-bottom 96-well plate was taken and 100 µl of DF-1 cells were added per well and placed in incubator for 24-48 hours at 37°C / 5% CO2 before the titration. Once confluency of 60-80% was achieved then purified MVA virus was taken out of -80°C freezer and thawed on ice. Next, serial dilution was prepared in 1.5 ml eppis (micro-reaction tubes) from 10^{-2} to 10^{-13} with DMEM containing 2% FCS according to the illustration (Fig. 2). Besides, two independent dilution series were prepared as an internal control.

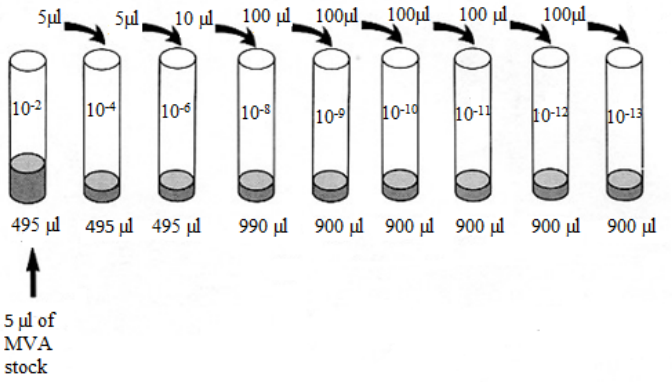

Figure 2. *Serial dilutions of MVA stock solution*

After preparing serial dilutions of MVA virus, 100 µl of each dilution was added (dilutions 10^{-8} to 10^{-13}) per well to flat-bottom 96-well plate that already contained 60-80% confluent DF-1 cells. In addition, only 100 µl DMEM (+/+ with 2% FCS) was also added as negative control to one column of wells and incubated for 7 days at 37°C/ 5% CO2 (Fig. 3). After incubation period was over, infection rate was observed in each dilution and counted the infected wells from the minimum MVA-infected dilution to the

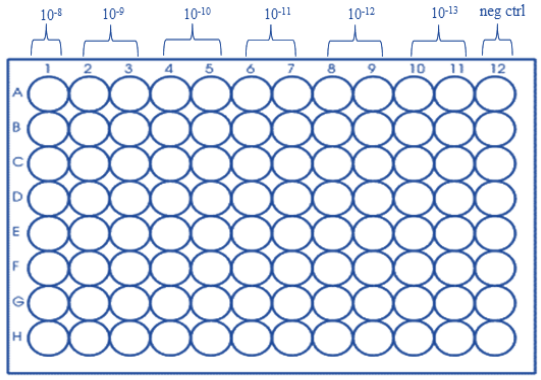

Figure 3. *DF-1 cell infection with serial dilutions of MVA*

next higher dilution. Finally, titer was calculated through determination of end-point dilution that would infect 50% of the inoculated wells (Kremer, Volz et al. 2012).

$$TCID_{50} / \log_{10} 50\% \text{ end-point dilution} = x - d/2 + (d\Sigma\, r/n)$$

Where,

x = highest dilution in which all wells are positive

d = log 10 of the dilution factor (d=1 10-fold dilution)

r = Number of positive wells per dilution

n = Total number of wells per dilution

2.2.8 Preclinical model system of chronic HBV infection

We conducted trials on HBV-transgenic mice (strain HBV1.3.32) on C57BL/6 background (Haplotype H-2b/b) containing 1.3 overlength HBV (genotype D, serotype ayw) genome. These mice (14-16 weeks old) were bred at the AVM Animal Facility, Helmholtz Center Munich. Wildtype C57BL/6 mice (haplotype H-2b/b) and B6-albino mice were purchased from Charles River Laboratories, Schulzfeld, Germany. In order to generate persistent infection of HBV in wildtype mice, we administered intravenous injection of 1×10^{10} genome equivalents (geq) of the AAV-HBV1.2 vector having 1.2-fold overlength HBV genome of genotype D (Dion, Bourgine et al. 2013). All animals were provided pathogen-free (SPF) condition as per institutional guidelines at the Animal Facility, University Hospital rechts der Isar, Technical University of Munich, or the Helmholtz Center Munich. Blood samples from animals were taken one day prior to the treatment and different experimental groups were in accordance with comparable levels of HBe and HBs antigens. All experiments were conducted during the light phase in the mice facility.

2.2.9 Heterologous prime boost vaccination with CpG application

We administered therapeutic vaccination as previously described by Backes et. al. (2016). Firstly, mice were vaccinated intramuscularly using insulin syringe with particulate HBcore protein prime followed by boost with recombinant Modified Vaccinia Ankara virus (MVA) vector carrying HBc antigen. HBcore protein was injected twice at two-week interval under isoflurane anesthesia intramuscularly (i.m.) into the quadriceps muscles of both hind limbs of mice. Protein prime comprised of 10 µg HBcAg expressed in E. coli (APP Latvijas Biomedicinas, Riga, Latvia) adjuvanted with 10 µg cyclic di-adenylate monophosphate (c-di-AMP) (InvivoGen, San Diego, CA).

Whereas, mice received 1×10^7 particles of recombinant MVA expressing HBcAg intramuscularly (i.m.) after two weeks of second protein immunization. We injected 20µg CpG/TLR9-L oligonucleotide (ODN 1668, InvivoGen, San Diego, CA) intravenously, while 20 µg non-CpG ODN (InvivoGen, San Diego, CA) injection was used as control.

2.2.10 Alanine aminotransferase (ALT) measurement

The blood samples were collected from mice in blood collecting tubes to measure the serum level of the liver enzyme alanine aminotransferase (ALT) by Reflotron Plus System (Roche Diagnostics, Risch, Switzerland). The blood was drawn from the facial vein using the Freckle technique. For this purpose, the mice are fixed manually and the vena facialis punctured with a 4 mm lancet and about 1-2 drops of blood were collected in small blood collecting tube. After the blood has been drawn, the sampling point on cheek of mice was compressed to stop the bleeding. Next, samples were centrifuged using benchtop centrifuge machine at 10000 x g for 5 minutes to separate blood plasma from the blood cells. Thereafter, the blood serum was diluted (1:4) in PBS and sALT levels were measured using Reflotron test strips GOT (AST) in Reflotron Plus System. The final readings were adjusted according to the dilution factor. The rest of the serum samples were stored at -20°C for further measurements of plasma HBs and HBe antigens. The minimum period between blood sample collections was 4 to 7 days. All necessary measures were taken in order to ensure minimal suffering of the animals.

2.2.11 Measurement of plasma HBsAg and HBeAg values

In order to measure HBsAg and HBeAg levels in serum, the blood samples were taken at different time-points during the animal trials. The blood plasma was diluted further (1: 30-50) in PBS and samples were dispatched for analysis to the laboratory diagnostics of the Institute of Virology at the Klinikum rechts der Isar. HBsAg and HBeAg levels were measured using ARCHITECT HBeAg/HBsAg kits in ArchitectTM platform in accordance with manufacturer’s guidelines. The final readings were adjusted according to the dilution factor. Thereafter, the data was processed using analytical tools for further analysis.

2.2.12 Purification of murine hepatic non-parenchymal cells

In order to isolate liver associated lymphocytes, mice were killed by cervical dislocation under isoflurane anesthesia. Liver sample was isolated and placed in 50 ml falcon tube containing 20 ml PBS at 4 °C. Next, liver sample was perfused with pre-heated 3 ml of 0.05 % collagenase solution (100 µl 50 mg/ml collagenase type IV in 10ml calcium-deprived buffer) using perfusion pump or 20cc syringe with 27G needle via the hepatic artery for a few seconds until it became completely pale. After that, each liver sample was transferred to large petri-dish and sliced into small pieces using curved scissors and after resuspending with 4 ml of 0.04% collagenase solution (80 µl of 50 mg/ml collagenase type IV in 10ml GBSS (PAN Biotech, Aidenbach, Deutschland) incubated for digestion at 37°C on shaking water bath. After digestion, the liver sample was meshed through a metal sieve 250 µm using plunger of sterile syringe and centrifuged at 50 x g (acceleration: 9, deceleration: 9) / 4°C for 2 minutes, after resuspending with 50 ml GBSS (PAN Biotech, Aidenbach, Deutschland). The supernatant was transferred to the new 50 ml falcon tubes and centrifuged at 800 x g (acceleration: 9, deceleration: 9) / 4°C for 10 minutes. Sample was rinsed and centrifuged again by repeating previous step by Phosphate Buffer Saline PBS Dulbecco (w/o Ca2+, w/o Mg2+) (Biochrom AG, Berlin, Deutschland). Cell pellet was collected and resuspended with 10 ml HBSS (Sigma Aldrich, St. Louis, USA). In the meanwhile, Percoll (GE Healthcare, Biosciences-AB, Uppsala, Sweden) gradient was prepared by adding 20 ml of 25% Percoll and underlying 15 ml of 80% Percoll using syringe with long needle. Next, liver cell suspension with HBSS was overlaid on the top of gradient carefully and centrifuged at 1349 x g (acceleration: 7, deceleration: 1) / 4°C for 30 minutes. After centrifugation, single cell suspension was collected between upper and lower layer of Percoll gradient in new 50 ml falcon tubes. After resuspending in 50 ml PBS solution cell suspension was centrifuged two times at 600 x g (acceleration: 9, deceleration: 9), 4°C for 5 minutes. Finally, the cell suspension was resuspended in 500 µl - 1000 µl of MACS buffer (1X PBS, 0.5% FCS and 2 mM EDTA) for further analysis.

2.2.13 Purification of hepatic lymphocytes

For the isolation of lymphocytes from the liver, mice were killed by cervical dislocation under isoflurane anesthesia. Liver sample was isolated and placed in 50 ml falcon tube containing 20 ml PBS at 4°C. Next, liver sample was perfused with PBS via the hepatic artery for a few seconds until it became completely pale. The liver was then meshed

with a plunger through a metal sieve and rinsed with 50 ml PBS in 50 ml falcon tube. The suspension was then centrifuged at 600 x g (acceleration: 9, deceleration: 9) / 20°C for 5 minutes and the supernatant was discarded. Each pellet of liver was resuspended in 8 ml GBSS with type II collagenase (1: 400) and incubated for 10 minutes at 37°C in a shaking water bath. Later, it was filled with PBS to stop the digestion and then cells were centrifuged at 600 x g (acceleration: 9, deceleration: 9) for 5 minutes. For the subsequent Percoll gradient (1400 x g / 20 min / acceleration 7 / deceleration 1/ 4°C), the cell pellet was suspended in 3 ml 40% Percoll solution and layered with 3 ml 80% Percoll solution in a 15 ml falcon tube. After the gradient was finished, the layer containing lymphocytes was collected and the cell suspension was washed twice with PBS 600 x g (acceleration: 9, deceleration: 9) for 5 minutes. Finally, the cells were resuspended in 500 µl to 1 ml MACS buffer for further analysis.

2.2.14 Purification of murine splenocytes

Single cell suspension of splenocytes was prepared as described by Stross and colleagues (Stross, Günther et al. 2012). The mouse was sacrificed by cervical dislocation under isoflurane anesthesia and the spleen was collected. The spleen was meshed through a metal sieve with a plunger and rinsed with PBS. The suspension was centrifuged at 600 x g (acceleration: 9, deceleration: 9) / 4°C for 5 minutes and the supernatant was discarded. In order to lyse the red blood cells, cell suspension of spleen was treated with 2 ml of ACK (Ammonium-Chloride-Potassium) lysing buffer and incubated for 2 min. The lysis was stopped by adding PBS and the suspension was again passed through a filter for separation. The cell suspension was then centrifuged at 600 x g (acceleration: 9, deceleration: 9) / 4°C for 5 minutes and resuspended in 3-5 ml MACS buffer for further analysis.

2.2.15 Purification of CD8+ T cells with CD8a Microbeads

After isolating spleen from mouse, single cell suspension of splenocytes was prepared according to the protocol discussed above (see 2.2.14). Thereafter, splenocytes were counted using counting chamber and then centrifuged at 600 x g (acceleration: 9, deceleration: 9) / 4°C for 5 minutes to collect cell pellet after discarding supernatant. The cell pellet was resuspended accordingly in 45 µl MACS Buffer and 5 µl murine CD8a (Ly-2) MicroBeads (Miltenyi Biotec) per 10^7 cells and incubated for 15 minutes at 4°C. Later, the cell suspension was rinsed with 20-30 ml MACS buffer and centrifuged at 600 x g (acceleration: 9, deceleration: 9) / 4°C for 5 minutes. Next, cell

suspension was resuspended in 500 µl MACS Buffer per 10^8 cells (or at least 500 µl) and placed in autoMACS Pro Separator (Miltenyi Biotec) to sort CD8+ T cells. After purifying CD8+ T cells, sorted-CD8+ T cells were counted using Neubauer counting chamber and resuspended in T cell medium (RPMI Medium 1640 (1X) + GlutaMAX-I 10% FCS, 1% L-glutamine, 1% Penicillin/streptomycin, 0.1% beta Merceptoethanol) for further analysis.

2.2.16 CFSE labelling of CD8+ T cells

CFSE (5(6)-Carboxyfluorescein diacetate N-hydroxysuccinimidyl ester) was used to determine CD8+ T cell proliferation. It is cell permeable dye that binds to intracellular proteins and yields the fluorescent carboxyflourescein molecule after intracellular esterases cleave the actetate group which has a peak excitation of 495 nm and peak emission of 521 nm. Hence, CFSE labelled CD8+ T cells can be detected through flow cytometry. While CD8+ T cell division could also be determined by sequential halving of CFSE flouresence intensity. In order to perform CFSE staining, single cell suspension of freshly isolated splenic CD8+ T cells (see 2.2.14-15) was washed and centrifuged 2X at 600 x g (acceleration: 9, deceleration: 9) / 4°C for 5 minutes with PBS and resuspended in 5 ml PBS. In the meanwhile, CFSE staining solution was prepared by adding 1µl of dye in 5 ml PBS. Next, both solutions were mixed together making 1 mM final concentration of CFSE and incubated for 20 minutes at 37ºC. After incubation, cell suspension was washed washed and centrifuged 2X at 600 x g (acceleration: 9, deceleration: 9) / 4°C for 5 minutes with T cell medium (RPMI Medium 1640 (1X) + GlutaMAX-I 10% FCS, 1% L-glutamine, 1% Penicillin/streptomycin, 0.1% beta Merceptoethanol) and resuspended in 2-3 ml for further analysis.

2.2.17 Ex vivo CD8+ T cell stimulation for cell proliferation assay

After CD8+ T cell isolation and labelling with CFSE (see 2.2.14-15), single cell suspension was counted using counting chamber under microscope and resuspended in falcon tube T cell medium (RPMI Medium 1640 (1X) + GlutaMAX-I 10% FCS, 1% L-glutamine, 1% Penicillin/streptomycin, 0.1% beta Merceptoethanol). Next, CD8+ T cells were stimulated with Dynabead Mouse T-Activator CD3/CD28 (CD8+ T cells: Beads; 1:1, 1:2, 1:4) and Interleukin-2 and kept in falcon tube for 30-60 minutes at 37°C. Then CD8+ T cell suspension containing Dynabeads and IL-2 added in sterile U-bottom 96-well plate with resuspension volume of 100 µl per well. Additionally, FACS-sorted myeloid cell suspension (see 2.2.22). was added to already activated-

CD8+ T cells (CD8+ T cells: Myeloid cells, 1:1) with resuspension volume of 100 µl per well. The samples were incubated for 72 hours to perform flow-cytometric analysis at different time-points.

2.2.18 Ex vivo CD8+ T cell stimulation for adoptive transfer

After purification of CD8+ T cells from murine spleen (see 2.2.14-15), cell suspension was resuspended in T cell medium (RPMI Medium 1640 (1X) + GlutaMAX-I 10% FCS, 1% L-glutamine, 1% Penicillin/streptomycin, 0.1% beta Merceptoethanol) to achieve $5x10^5$ CD8+ T cells/ml. In the meanwhile, sterile flat-bottom 12-well plate was coated with 10 µg/ml of each functionally purified aCD3 and a CD28 antibodies for 2 hours at 37°C. After incubation period, the supernatant was discarded, and plate was washed with 1 ml PBS. Then 3 ml of CD8+ T cell suspension containing 1.5 x 10^6 CD8+ T cells and 5 ng/ml mIL-2 were added in each well of 12-well plate and incubated at 37°C for 72 hours. After the incubation period was over, expanded CD8+ T cells were harvested in falcon tube and cell suspension was centrifuged at 600 x g (acceleration: 9, deceleration: 9) / 4°C for 5 minutes. Next, CD8+ T cells were counted using counting chamber under the microscope. Finally, the desired quantity of CD8+ T cells was resuspended in PBS and used further for adopted transfer.

2.2.19 Adoptive transfer of CD90.1+ CD8+ T cells

At first, murine CD90.1+ CD8+ T cells were purified from splenocytes and expanded ex vivo by adopting the protocol discussed above (see 2.2.18). After harvesting the activated CD90.1+ CD8+ T cells after 72 hours of ex vivo stimulation, cell suspension was washed with PBS and centrifuged at 600 x g (acceleration: 9, deceleration: 9) / 4°C for 5 minutes. Then cells were resuspended in PBS and counted using counting chamber under microscope. Next, $5x10^5$ cells (diluted in 100 µl PBS) were injected into animal intravenously via tail vein using 30G x 1/2 " needle with insulin syringe. Mice were kept for 72 hours till they were sacrificed. Liver and spleen were isolated and single cell suspensions were prepared to analyze the expansion of adoptively transferred CD8+ T cells using flow cytometry.

2.2.20 Immunohistochemistry

To analyze the livers using immunohistochemistry, the livers were briefly perfused with PBS via the portal vein and isolated from the animal. Tissue samples were sliced using scalpel from the large liver lobe and the pyramid lobe and placed in properly labelled

tissue cassettes. After that, cassettes were kept in 4% Paraformaldehyde (PFA) to fix the liver tissue for 48 hours at 4°C. The tissue samples were then dispatched to working group of Dr. Katja Steiger (Institute of Pathology, Klinikum rechts der Isar, Technical University of Munich) for further processing. After dehydration and embedding in paraffin, liver sections were made with a thickness of 2 µm using rotary microtome (HM355S, ThermoFisher Scientific, Waltham, USA) which were used further for hematoxylin-eosin staining (HE) and other immunohistology staining. A Bond Max system (Leica, Wetzlar, Germany, all reagents from Leica) was used to perform Immunohistochemistry with rabbit anti-HBcAg primary antibody (Diagnostic Biosystems, Pleasanton, CA; 1:50 dilution) or primary antibodies against Ki67 (clone SP6, Abcam ab16667) and horseradish peroxide coupled secondary antibody. After staining, slides were scanned with SCN 400 slide scanner (Leica Biosystems) and HBcore positive hepatocytes were defined based on distribution and intensity of the signal in random 10 view fields of 220L x 255W μm^2 (40x magnification) quantified per mm^2. After taking the values of HBcore positive hepatocytes, the data was further analyzed using statistical software.

2.2.21 Flow Cytometry (FACS)

In order to perform phenotypic characterization, single cell suspensions isolated from murine liver and spleen were transferred to a V-bottom 96-well plate. Flow cytometric data was obtained on Sony Biotechnology Spectral Analyzer SP6800, SA3800 (flow rate 5/acquisition time 1 min/resuspension volume 100 µl) and CytoflexS (Beckmann Coulter) flow cytometer. Whereas, sorting of myeloid cell populations was performed using Sony Biotechnology SH800 cell sorter. Later, the data was analyzed with FlowJo software. Besides, t-SNE was performed using flowJo to visualize high-dimensional data of activated CD8+ T cell population to define different cell populations with variable expression levels of activation markers CD25, CD44, CD69 and exhaustion marker PD1 over the entire period of observation. Furthermore, analysis of multiple marker expression on different CD8+ T cell populations was performed using “FlowJo’s Boolean make and/or gate function” and “Pestle & Spice v6 software”.

2.2.22 FACS Sorting of myeloid cells

Myeloid cells were sorted using Sony Biotechnology SH800 cell sorter. First, single cell suspension of hepatic non-parenchymal cells was prepared according to the protocol discussed above (see 2.2.12). The cell suspension in 15 ml falcon tube was pelleted

at 600 x g (acceleration: 9, deceleration: 9) / 4°C for 5 minutes and then resuspended in 500 µL FACS buffer containing cell surface antibodies (dilution 1: 200). Cell suspension was Incubated for 30 minutes at 4°C in the dark. Next, the cell suspension was washed and centrifuged twice with 5 ml FACS buffer at 600 x g (acceleration: 9, deceleration: 9) / 4°C for 5 minutes and resuspended in the final volume of 1 ml FACS buffer for FACS sorting. For unmixing, a single staining of the corresponding antibody was performed that is comparable to compensation with conventional flow cytometers. After the cell sorting, myeloid cells were counted using counting chamber under light microscope and resuspended accordingly in T cell medium or FACS buffer for further analysis.

2.2.23 Identification of HBcore specific CD8+ T cells using multimers

MHC class I/SIINFEKL multimer staining was performed before surface staining to detect HBc-Ag specific CD8+ T cells by flow cytometry. MHCI multimers conjugated with ovalbumin-derived peptide (OVAS8L SIINFEKL) or H-2Kb restricted HBcore peptide (core93-100 MGLKFRQL) were kindly provided by Professor Dirk Busch (Institute of Microbiology, TUM). For each sample, 0.4 µg of streptamer was used with 0.4 µg Strep-Tactin-PE (IBA-lifesciences) in 30 µl of FACS buffer and incubated on ice for 30 minutes. Further staining of surface markers was performed after a wash step with FACS buffer.

2.2.24 Cell surface staining for flow cytometry

The cell suspension in the V-bottom 96-well plate was pelleted at 600 x g (acceleration: 9, deceleration: 9) / 4°C for 2 minutes and then resuspended in 50 µL FACS buffer containing antibodies (dilution 1: 200). Cell suspension was Incubated for 30 minutes at 4°C in the dark. Later, the cell suspension was washed and centrifuged twice with 100 µl FACS buffer at 600 x g (acceleration: 9, deceleration: 9) / 4°C for 2 minutes and resuspended in the final volume of 100 µL FACS buffer for flow cytometric analysis. For unmixing, a single staining of the corresponding antibody was performed that is comparable to compensation with conventional flow cytometers. In addition, the fluorescence minus one control (FMO) of each fluorochrome were prepared to ensure reliable interpretation of flow cytometric data.

2.2.25 Intracellular staining of cytokines

The staining of intracellular cytoplasmic proteins was performed following the cell surface staining. After the surface staining, cell suspension was washed and centrifuged twice with 100 µl FACS buffer at 600 x g (acceleration: 9, deceleration: 9) / 4°C for 2 minutes. Then the cells are fixed in 100 µL fixation buffer for 30 minutes at room temperature. Thereafter, cells were washed and centrifuged twice with 100 µL 1X permeabilization buffer (freshly prepared with PBS from 10X permeabilization buffer) at 600 x g (acceleration: 9, deceleration: 9) / 4°C for 2 minutes and then intracellular staining was performed. For this purpose, the cells were resuspended in 50 µl 1X permeabilization buffer containing antibodies (dilution 1: 200) and incubated for 30 minutes / 4°C. The cell suspension was washed and centrifuged twice at 600 x g (acceleration: 9, deceleration: 9) / 4°C for 2 minutes with 100 µl 1X permeabilization buffer and finally resuspended in 100 µl FACS buffer for further flow cytometric analysis.

2.2.26 Statistics

Statistical analysis was performed using GraphPad Prism 7 (GraphPad Inc., CA). Statistical differences between different treatment groups and controls were analyzed using 2-way ANOVA with Tukey's multiple comparison correction, Kruskal Wallis test with Dunn's multiple comparison correction, Mann Whitney test and unpaired or paired t test. P-values less than 0.05 were considered as significant.

3. RESULTS

3.1 Synchronization of iMATEs induction with heterologous prime-boost vaccination in wild-type mice

In the beginning, we investigated optimal time-point for intravenous CpG application following therapeutic vaccination to increase efficacy of vaccine in C57BL/6 wild-type mice. We administered CpG at different time intervals following therapeutic vaccination. Later, we analysed CD8+ T cell responses in liver and spleen after 3 days of CpG application in immunized mice (see illustration 1). CpG induced iMATEs in liver

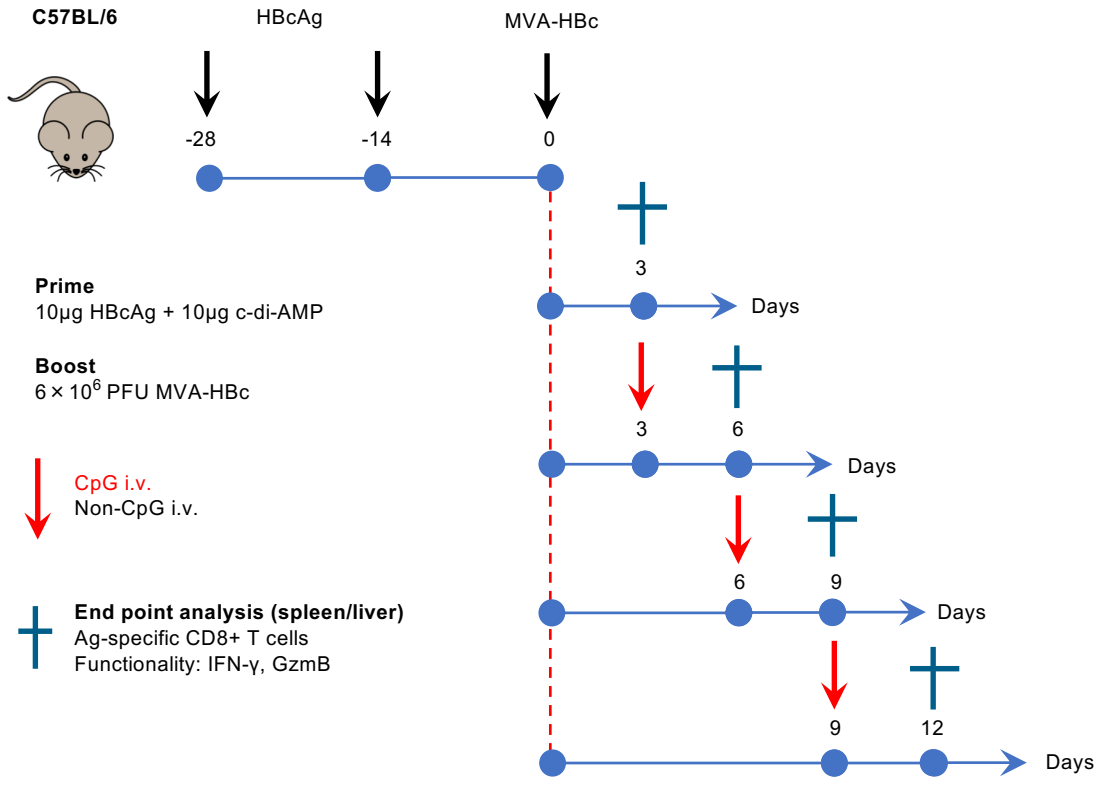

Illustration 1. *Schematic representation of optimization of iMATEs induction*

after intravenous injection in already vaccinated wild-type mice (Fig. 1b). We observed that CpG injection at earlier time-point i.e. after 3 days of heterologous therapeutic vaccination resulted in significant expansion of vaccine-induced HBc Ag-specific CD8+ T cells in liver (Fig. 1a). Meanwhile we also found significant increase in IFN-γ and GzmB expressing hepatic CD8+ T cells upon ex vivo stimulation with HBcore peptides (Fig. 1a). However, we didn't observe significant expansion of functional CD8+ T cells in spleen. CpG application at day 6 and 9 after therapeutic vaccination also didn't support local expansion of vaccine-induced HBc Ag-specific CD8+ T cells in liver.

These findings suggested that CpG supported further expansion of HBc Ag-specific CD8+ T cells in liver after priming of HBc Ag-specific CD8+ T cells through therapeutic vaccination. Whereas, earlier time point of CpG-injection following therapeutic vaccination further augmented hepatic CD8+ T cell expansion and effector function through iMATEs induction (Fig. 1b).

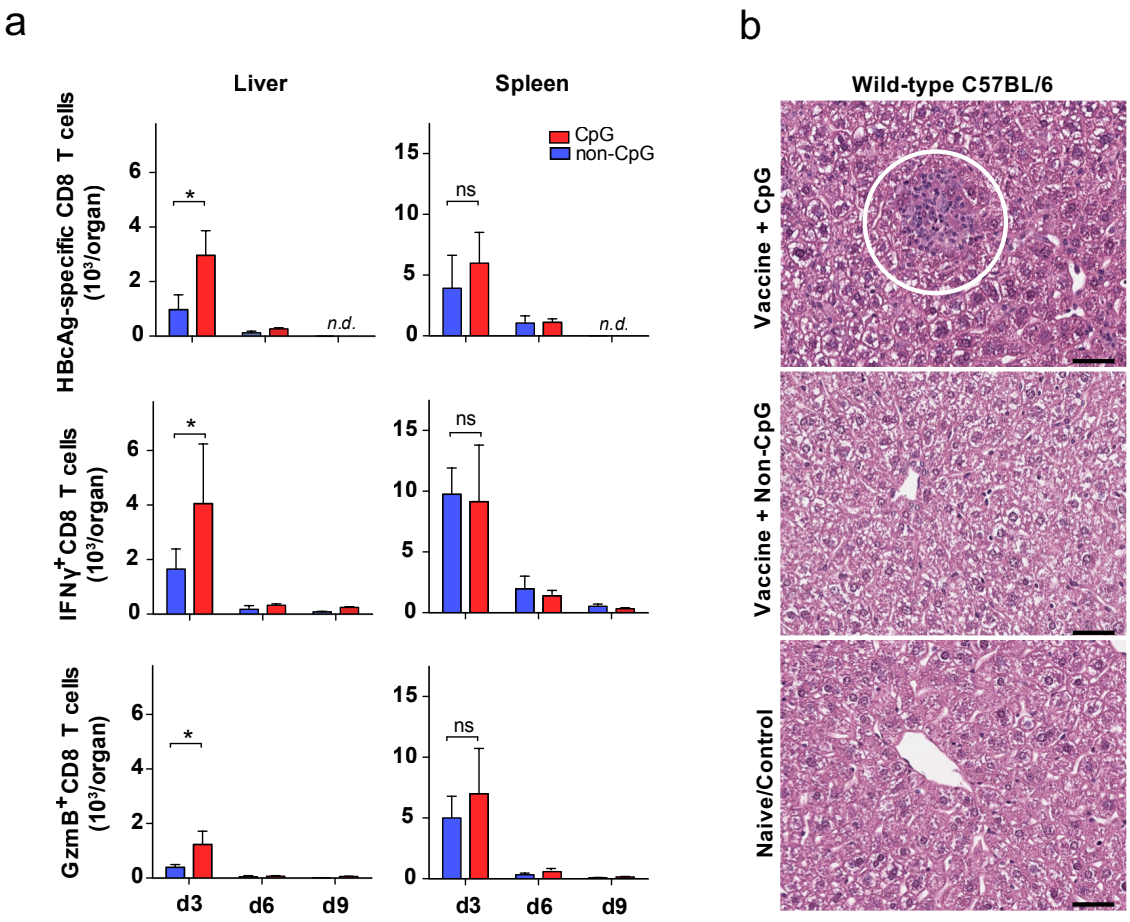

Figure 1. *Synchronisation of iMATEs induction with prime-boost vaccination in wildtype C57BL/6 mice. (a) Quantification of HBc Ag-specific CD8+ T cells and effector function of CD8+ T cells at day 3 after CpG or non-CpG control oligonucleotides injection in vaccinated mice. CpG or non-CpG was injected at day 3, day 6 and day 9 following MVA-HBc boost administration. IFN-γ and GzmB responses were measured after ex vivo stimulation with HBcore peptides. (b) H&E staining of liver slices detecting iMATEs at day 3 after CpG application (scale bar: 50um). Bars represent mean of n=3 mice + SEM. Statistical analysis was performed using paired t test. Bars indicate mean value of n=3 mice per group + SEM. Asterisks indicate statistically significant differences. * P-value <0.05, ns abbreviated as not significant.*

3.2 Role of Modified Vaccinia Ankara (MVA) virus vector in iMATEs induction

After synchronizing CpG with therapeutic vaccination strategy, we were interested to explore the role of MVA virus in expansion of CD8+ T cells and the recruitment of inflammatory myeloid cells in liver as compare to CpG. Hence, we administered MVA virus and CpG through parenteral routes and adoptively transferred $5x10^5$ CD90.1+ CD8+ T cells in B6-albino mice. We counted CD8+ T cells and Ly6C+ CD11b+ MHCII+ inflammatory monocytes in liver and spleen after 3 days of MVA and CpG injections. Besides, Liver tissues were also analysed to identify iMATEs within liver compartments (see illustration 2).

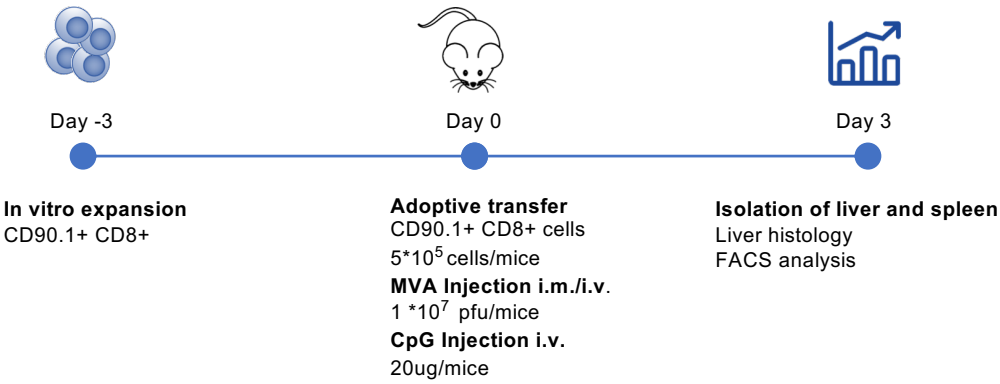

Illustration 2. *Study design of in vivo expansion of adoptively transferred CD8+ T cells*

We didn't detect clustering of mononuclear cell populations like iMATEs in liver after parenteral administration of MVA virus (Fig. 2b). Furthermore, intramuscular injection of MVA virus has insignificant impact on increase in CD8+ T cells and myeloid cells in liver and spleen. However, intravenous injection of MVA virus induced 3-fold more expansion of adoptively transferred CD8+ T cells in spleen than CpG. While CpG has not only highly significant effect on hepatic CD8+ T cell proliferation but also on increase in Ly6C+ CD11b+ MHC+ myeloid cell in liver (Fig. 2a).

From these findings we inferred that CpG favoured immunogenic hepatic microenvironment through Toll-like receptor 9 signalling, inducing local increase of CD8+ T cells and inflammatory myeloid cell populations in liver. While MVA virus being a potent viral vector evoked CD8+ T cell responses in secondary lymphoid organs such as spleen.

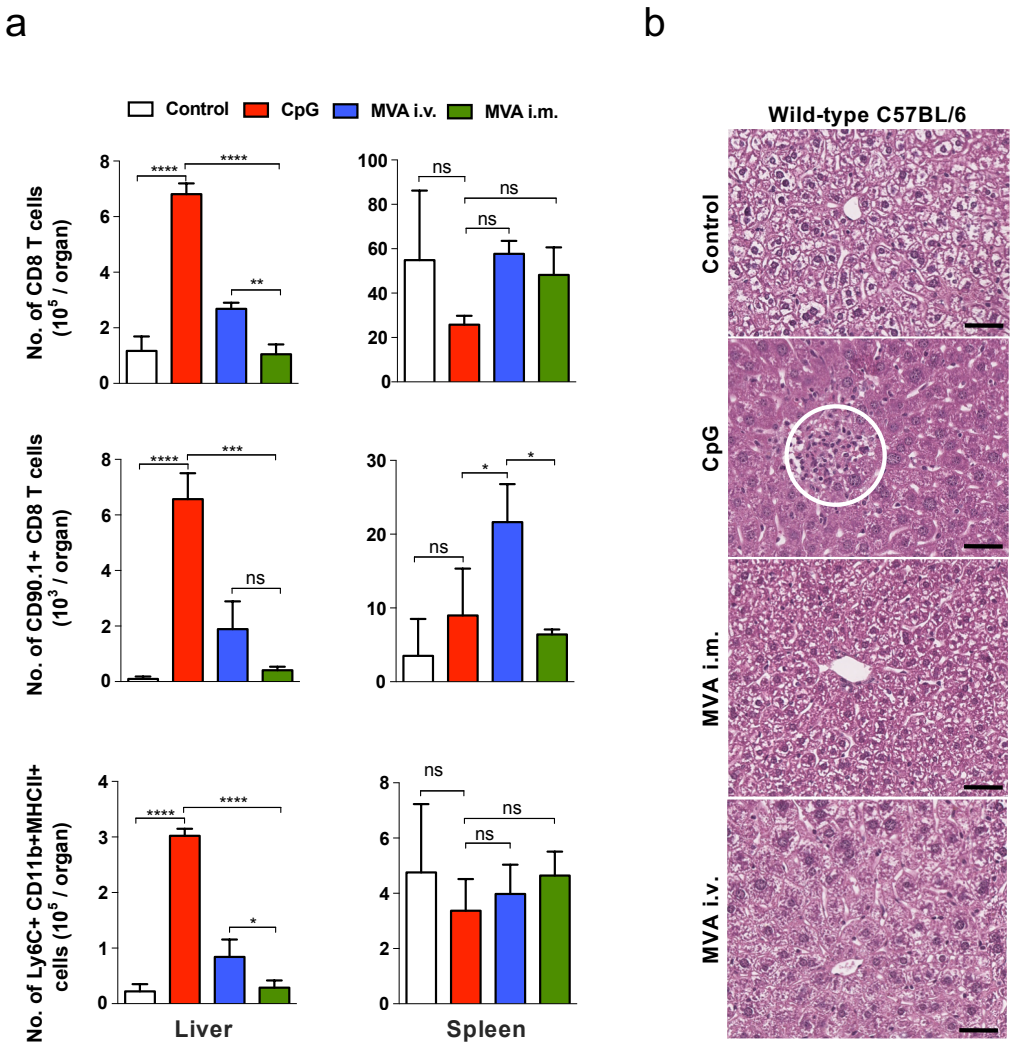

Figure 2. *Expansion of CD8+ T cells and Ly6C+ CD11b+ MHCII+ monocytes under the influence of Modified Vaccinia Ankara Virus (MVA) and CpG in liver and spleen. (a) Quantification of indigenous CD8+ T cells, adoptively transferred CD8+ T cells and Ly6C+ CD11b+ MHCII+ monocytes in liver and spleen respectively. (b) H&E staining of liver slices detecting iMATEs at day 3 after CpG and MVA administration (scale bar: 50um). Statistical analysis was performed using one-way ANOVA with Tukey's multiple comparisons test. Bars indicate mean value of n=3 mice per group + SD. Asterisks indicate statistically significant differences. * P-value <0.05, ns abbreviated as not significant.*

3.3 Synergistic effect of therapeutic vaccination (TherVacB) with iMATEs induction in HBV-transgenic mice

In previous experiments, we determined the optimal time-point to induce iMATEs after therapeutic vaccination against chronic HBV (TherVacB). Thereafter, we defined the role of MVA virus and CpG concerning immune responses in different anatomical sites. Here we evaluated virus-specific CD8+ T cell responses orchestrated by synchronized combinatorial therapy in HBV-transgenic mice with persistent infection (see illustration 3). Thymic tolerance due to clonal deletion makes the HBV transgenic mouse model the most demanding model for a therapeutic vaccine. We administered TherVacB in

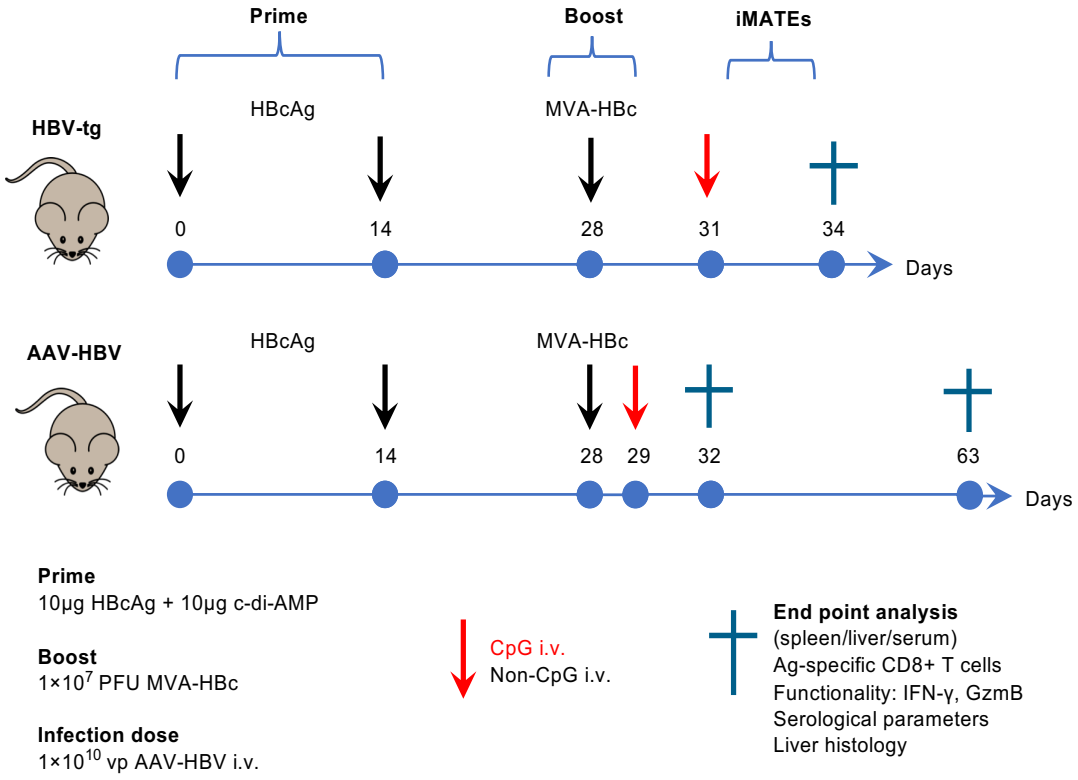

Illustration 3. *Schematic representation of synergy of TherVac B with iMATEs induction*

combination with CpG in HBV-transgenic mice with intermediate to high antigenemia (HBs Antigen 50-450IU/ml). we analysed the samples after 3 days of CpG application in immunized mice. CpG induced iMATEs regardless of TherVacB administration in HBV-transgenic mice (Fig. 3a). As functional HBc Ag-specific CD8+ T cells determine the outcome of infection, we analysed hepatic and splenic HBc Ag-specific CD8+ T cells using HBcore-multimer staining (Fig. 3b). We observed significant increase in

hepatic CD8+ T cells including HBc Ag-specific CD8+ T cells in mice treated with CpG besides TherVacB, whereas there is no considerable effect detected in spleen (Fig.

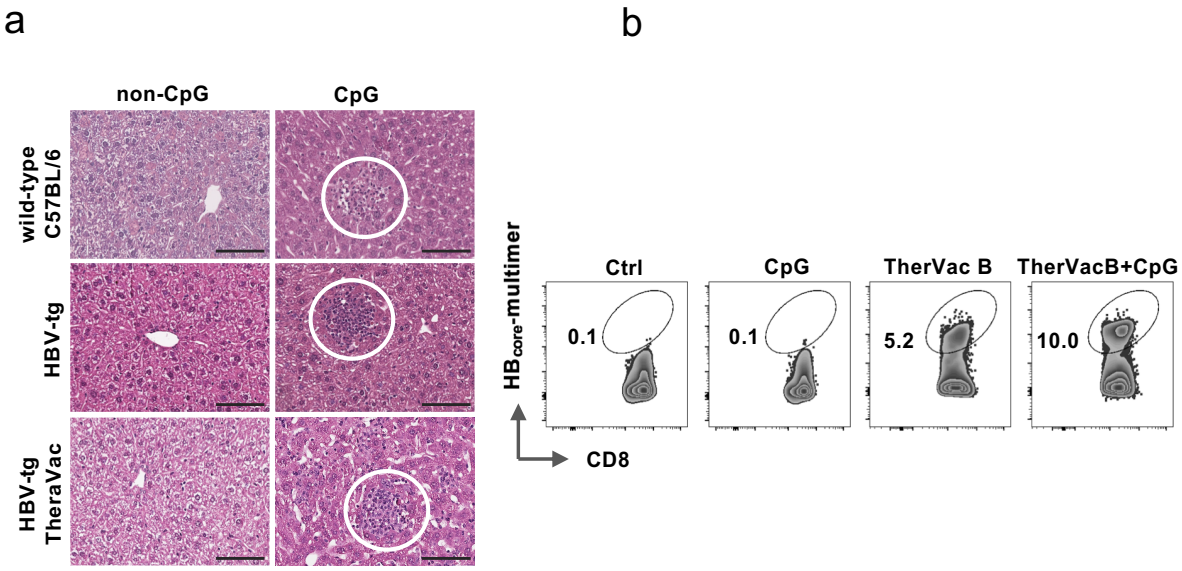

Figure 3. *iMATEs induction in liver followed by intravenous administration of CpG in immunized HBV1.3-tg mice. (a) H&E staining of liver tissue examining iMATEs at day 3 after CpG application(scale bar: 100um). (b) identification of HBc Ag-specific CD8 T cells using HBc-specific multimer staining in Liver at day 3 after CpG application. The numbers represent the percentage of liver CD8+ T cell population.*

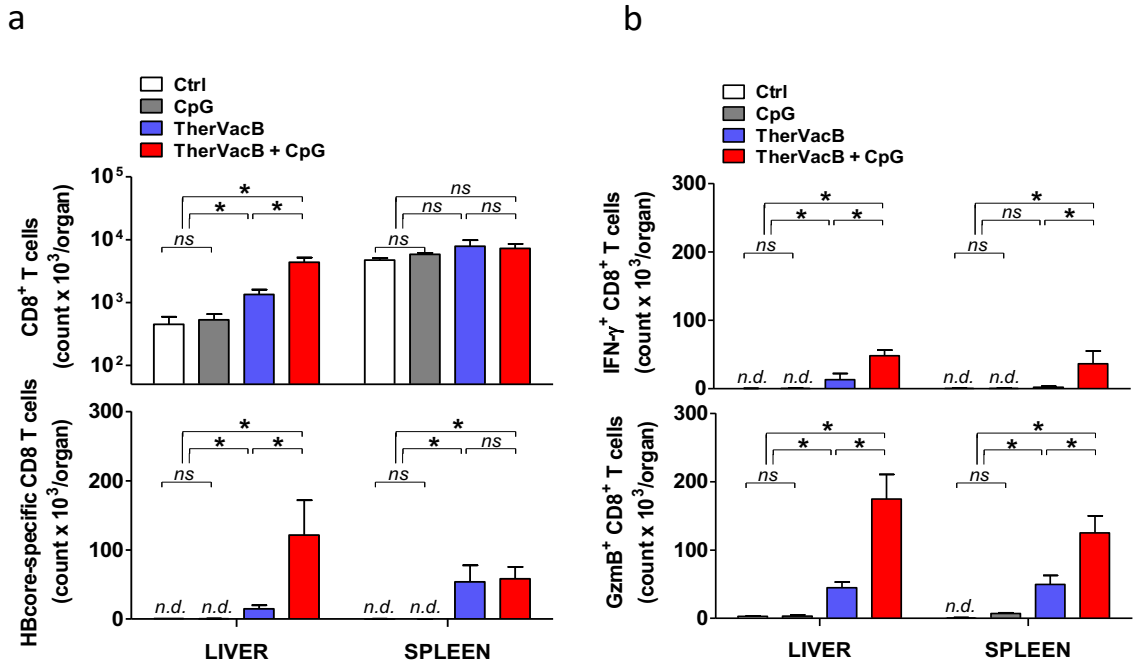

Figure 4. *Expansion of functional virus-specific CD8+ T cells in liver followed by intravenous administration of CpG in immunized HBV1.3-tg mice. (a) Quantification of HBc Ag-specific CD8+ T cells in liver and spleen at day 3 after CpG administration. (b) Estimation of IFN-γ and GzmB responses of CD8+ T cell population in liver and spleen. Bars show mean value of n ≥ 3 mice per group + SEM. Statistical analysis was performed using Kruskal Wallis test with Dunn's multiple comparison correction. Asterisks point out statistically significant differences: *p < 0.05, ns abbreviated as not significant, n.d. means not detectable.*

4a). We also determined intracellular cytokine expression of CD8+ T cells after ex vivo re-stimulation. CpG in combination with TherVacB increased IFN-γ and GzmB expressing CD8+ T cells in both liver and spleen as compare to TherVacB or CpG alone, indicating both cytolytic and noncytolytic activity (Fig. 4b). We concluded from these findings that CpG reinforced expansion of already activated HBc Ag-specific CD8+ T cells in liver which were generated by TherVacB. It also supported the notion that CpG and TherVacB operate in different anatomical compartments. Besides, heterologous prime-boost vaccination (TherVacB) along with CpG elevated serum ALT levels, signifying HBc Ag-specific CD8+ T cell mediated immunity (Fig 5a). Consequently, we detected significant decline in serum HBeAg levels as compare to vaccination or CpG treatment alone (Fig 5b). In line with serum HBeAg levels, immunohistochemistry data also showed 6-fold reduction in HBcore positive hepatocytes (Fig. 6a, b). Hence, these results indicated that CpG along with TherVacB further amplified vaccine induced HBc Ag-specific CD8+ T cell responses in liver, overcoming the immune suppression through cytolytic and noncytolytic antiviral activity in HBV-transgenic model of persistent HBV infection.

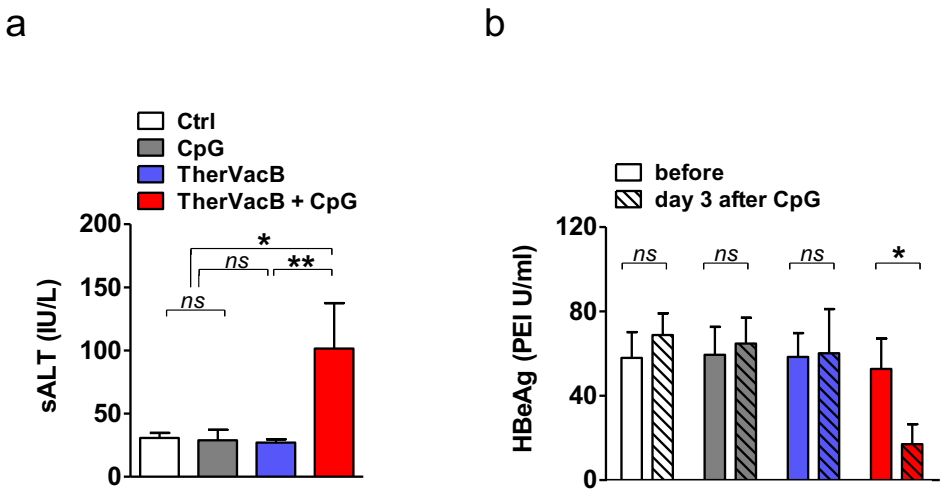

Figure 5. *Effector function of virus specific CD8+ T cells demonstrates liver damage and antiviral activity at day 3 after intravenous administration of CpG in vaccinated HBV1.3 tg mice. (a) Serum ALT levels depict liver damage before and then after 3 days of CpG application during combinatorial therapy (b) Reduction in serum HBeAg levels at day 3 at following CpG administration. Bars show mean value of n ≥ 3 mice + SEM. Statistical analysis was performed using (a) Kruskal Wallis test with Dunn's multiple comparison correction (c) paired t test. Asterisks indicate statistically significant differences: *p < 0.05, ns means not significant, n.d. abbreviated as not detectable*

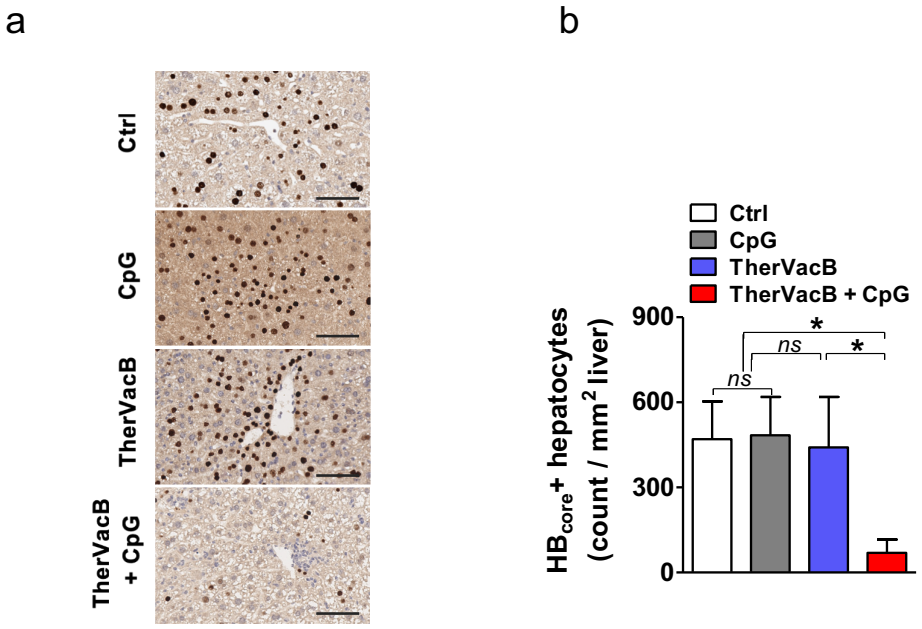

Figure 6. *Effector of antiviral activity of HBc Ag-specific CD8+ T cells on control of HBc antigen expressing hepatocytes at day 3 following therapeutic vaccination with CpG application in HBV1.3 tg mice. (a) Immunohistochemistry of liver slices depicting HBc antigen expressing hepatocytes (scale bar: 100um). (b) Quantification of HBc Antigen-positive hepatocytes. Bars in (b) show mean value of n ≥ 3 mice + SEM. Statistical analysis was performed using Kruskal Wallis test with Dunn's multiple comparison correction. Asterisks indicate statistically significant differences: *p < 0.05, ns means not significant, n.d. abbreviated as not detectable.*

3.4 Effect of combinatorial therapy on control of infection in AAV-HBV infected mice

Previously we used HBV-transgenic mice model to assess the effect of combinatorial therapy on immune suppression. Since HBV is present as transgene, therapeutic

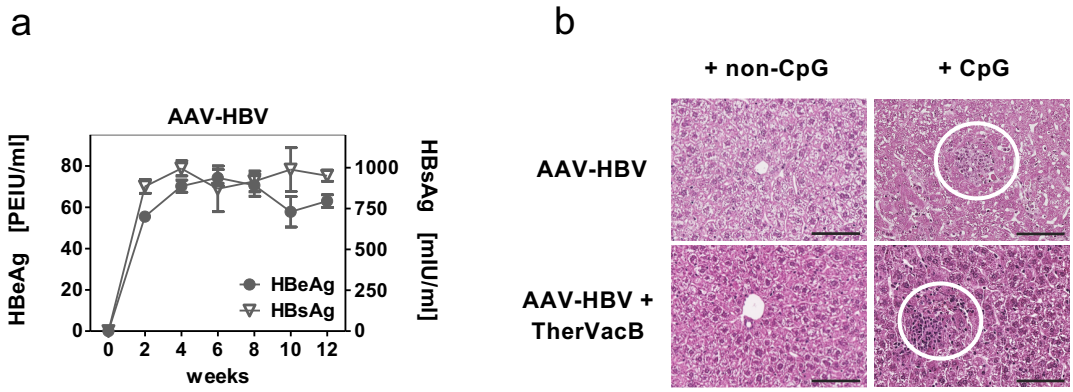

Figure 7. *Vaccine-induced iMATEs following intravenous CpG-injection in AAV-HBV mice. (a) Measurements of serum HBe antigen levels after AAV-HBV transduction demonstrating persistent infection in C57Bl/6 mice. (b) H&E staining of liver tissue slices detecting iMATEs in AAV-HBV infected mice (scale bar: 100um).*

vaccination can never succeed in controlling HBV. Therefore, here we used AAV-HBV transduced mice to observe elimination of chronic infection (see illustration 3). Viral gene transfer via adeno-associated virus (AAV) establish a persistent infection that is accompanied by a dysfunctional HBV-specific immune response. This model is ideally suited to study the relevance of increasing the numbers of HBV-specific CD8+ T cells in the clearance of HBV from infected hepatocytes in the setting of a chronic infection. In chronic AAV-HBV infection approximately 80% of hepatocytes express HBV antigens. We detected high serum HBs and HBe antigen levels after HBV gene transfer through recombinant AAV, that persisted till 12 weeks of follow-up, demonstrating persistent HBV replication (Fig. 7a). After establishing stable chronic infection, we administered heterologous therapeutic vaccination (TherVacB) followed by CpG application in AAV-HBV transduced mice. We performed end-point analysis on 3rd day after CpG application. Consistent with findings of previous experiment, we observed iMATEs induction following CpG application with or without TherVacB administration (Fig. 7b). CpG coupled with TherVacB also significantly raised HBc Ag-specific CD8+ T cell numbers in liver, however it didn't support expansion of CD8+ T cells in spleen (Fig. 8a). Besides increase in HBc Ag-specific CD8+ T cells, we also detected upsurge

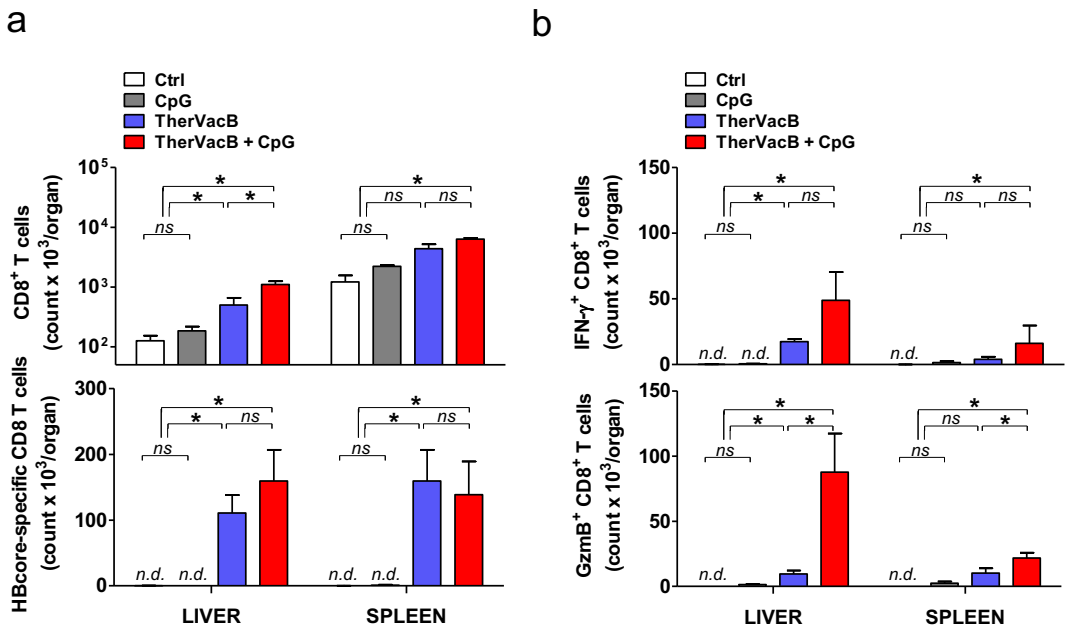

Figure 8. *Hbcore-specific CD8+ T cells were expanded further through iMATEs induction at day 3 following intravenous CpG-injection in already vaccinated AAV-HBV mice. (a) Quantification of C8+ T cells as well as HBc Ag-specific CD8+ T cells in liver and spleen. (b) Absolute count of GzmB and IFNγ expressing CD8+ T cells after ex vivo re-stimulation with HBcore peptide. Bars show mean value of n ≥ 3 mice per group + SEM. Statistical analysis was performed using Kruskal Wallis test with Dunn's multiple comparison correction. Asterisks point out statistically significant differences: *p < 0.05, ns abbreviated as not significant, n.d. means not detectable.*

in IFN-γ and GzmB expressing CD8+ T cells after ex vivo re-stimulation with HBcore peptide (Fig. 8b). Hence, we suggested that administration of TherVacB along with CpG induced more functional HBc Ag-specific CD8+ T cell responses in liver to elicit antiviral activity than TherVacB alone. Besides, CpG has no influence in priming of HBc Ag-specific CD8+ T cells in liver. Next, we determined the degree of liver damage caused by effector function of virus specific CD8+ T cells in liver through serum ALT measurements. Fluctuations in serum ALT levels depicts immunogenic or tolerogenic microenvironment of liver. TherVacB or CpG alone didn't induce considerable liver damage, but CpG together with TherVacB contributed to significant rise in serum ALT levels suggesting substantial liver damage (Fig. 9a). These elevated serum ALT levels attributed to surge in GzmB expressing HBc Ag-specific CD8+ T cells, subsequently generating effective cytolytic activity to control the infection (Fig. 9b).

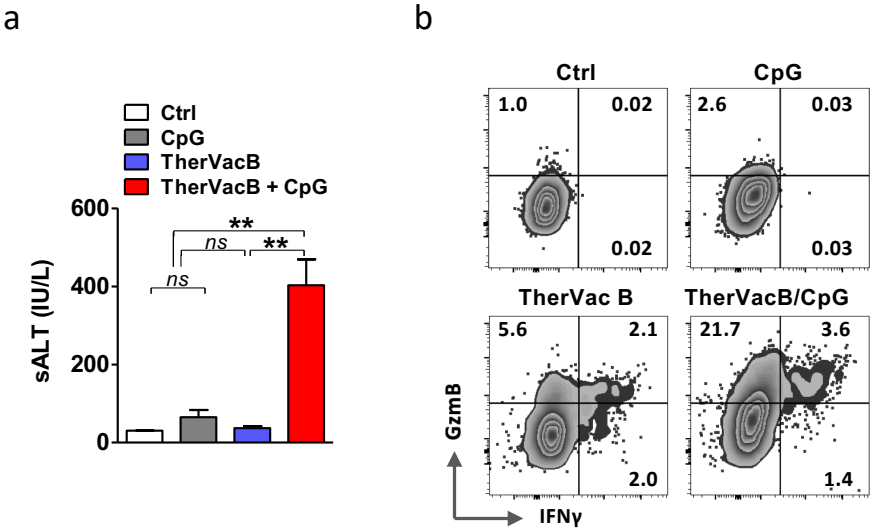

Figure 9. *Combinatorial therapy induces significant liver damage and effector function of HBc Ag-specific CD8+ T cells in AAV-HBV mice model. (a) Liver damage was assessed through serum ALT levels before and then after 3 days of CpG application during combinatorial therapy (b) GzmB and IFNγ expressing hepatic CD8+ T cells after ex vivo re-stimulation with HBcore peptide. Bars show mean value of n ≥ 3 mice + SEM. Statistical analysis was performed using Kruskal Wallis test with Dunn's multiple comparison correction. Asterisks indicate statistically significant differences: *p < 0.05, ns means not significant, n.d. abbreviated as not detectable.*

After short-term analysis of virus-specific CD8+ T cell responses in AAV-HBV infected mice, we did a follow-up for 5 weeks following sequential application of therapeutic vaccination and CpG injection. Although TherVacB alone curtailed serum HBe antigen levels, but after short period of time HBe antigen levels bounced back to the level of control group. In contrast, after CpG application together with TherVacB in, we observed substantial decline in serum HBeAg levels that remained low till 63 days of follow-up (Fig. 10). Similarly, HBs antigen levels were also decreased after CpG

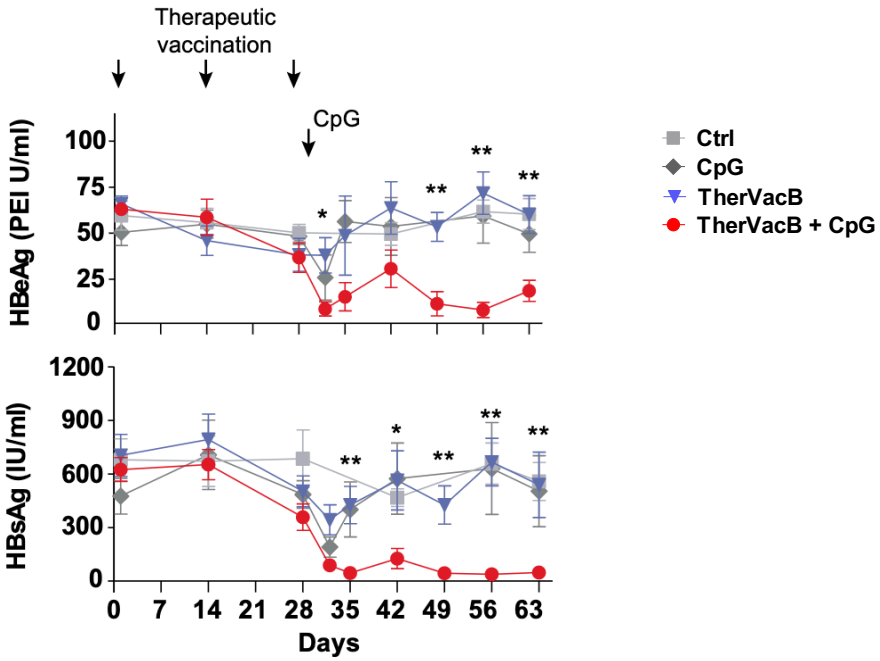

Figure 10. *Measurement of HBeAg and HBcAg in serum showing significant reduction in antigen levels following CpG application in immunized mice. Dots show mean value of n ≥ 3 mice + SEM. Statistical analysis was performed using 2-way ANOVA with Tukey's multiple comparison correction. Asterisks indicate statistically significant differences: *p < 0.05, ns means not significant, n.d. abbreviated as not detectable.*

injection in vaccinated AAV-HBV infected mice, even though we didn't detect seroconversion to anti-HBe or anti-HBs. Immunohistochemistry of liver tissues revealed that there was no difference in numbers of HBc antigen expressing hepatocytes at day 32 just after CpG injection following TherVacB as compare to TherVacB alone. However, at the end of follow-up period i.e. at day 63 after start of animal trial, there was a significant decline in HBc antigen expressing hepatocytes in mice that received CpG besides TherVacB (Fig. 11a, b). Whereas quantification of HBc-Ag expressing hepatocytes also revealed that TherVacB administration alone didn't curtail HBc Ag expressing hepatocytes as compared to combinatorial therapy. At this time point, flow cytometric analysis also revealed that only GzmB expressing HBc Ag-specific CD8+ T cells were increased upon sequential combinatorial therapy of TherVacB and CpG in AAV-HBV infected mice, pointing out the role of GzmB for prediction of long-term immune control of chronic infection (Fig. 12). Consistent with the findings in HBV-transgenic mice, we concluded that sequential administration of TherVacB and CpG also resulted in better immune control of HBV antigens in AAV-HBV infected mice model of chronic infection.

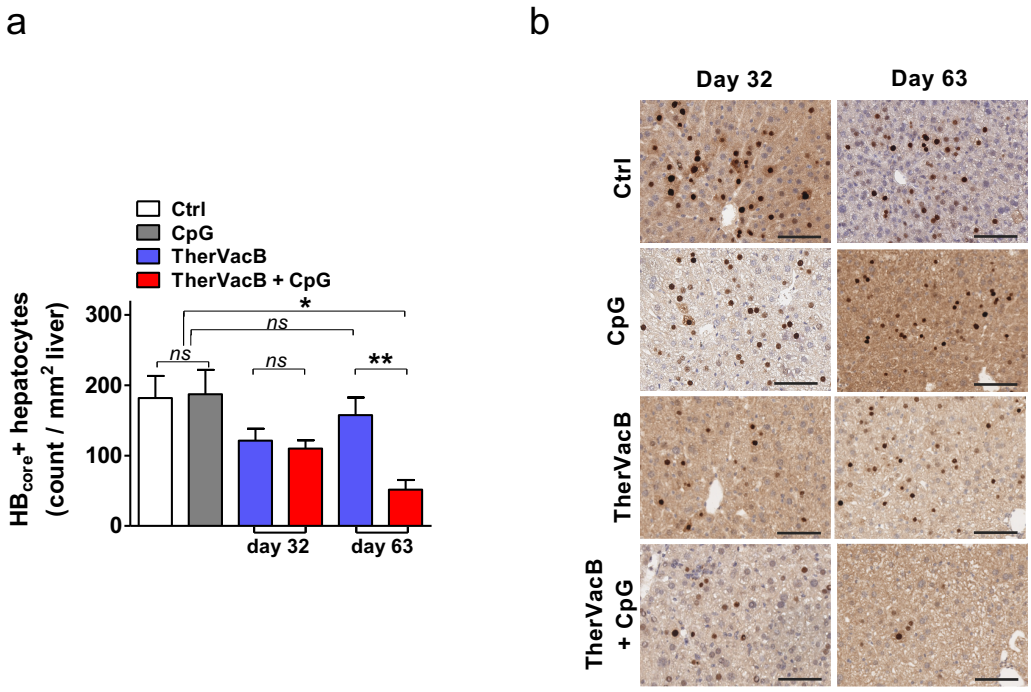

Figure 11. *Synergistic effect of therapeutic vaccination with CpG application on long-term control of HBV antigen expression in AAV-HBV chronic infection. (a) Quantification of Hbcore positive hepatocytes through immunohistochemistry. (b) Liver slices depicting HBcAg expressing hepatocytes (scale bar: 100um). Bars show mean value of n ≥ 3 mice + SEM. Statistical analysis was performed using Kruskal Wallis test with Dunn's multiple comparison correction. Asterisks indicate statistically significant differences: *p < 0.05, ns means not significant, n.d. abbreviated as not detectable.*

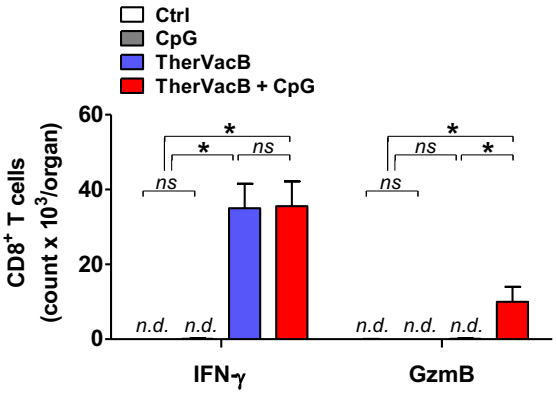

Figure 12. *Quantification of IFN-γ and GzmB expressing CD8+ T cells pointing out the role of GzmB in long-term control of infection. Bars show mean value of n ≥ 3 mice + SEM. Statistical analysis was performed using Kruskal Wallis test with Dunn's multiple comparison correction. Asterisks indicate statistically significant differences: *p < 0.05, ns means not significant, n.d. abbreviated as not detectable.*

3.5 CpG enhanced proliferation potential of hepatic immune cell populations through recruitment of CD11b+ Ly6C+ inflammatory myeloid cells

We have previously shown that CpG injection generated iMATEs in either vaccinated or non-vaccinated HBV-transgenic mice and AAV-HBV transduced mice. Here we investigated the proliferative potential of hepatic immune cells driven by sequential combinatorial therapy of TherVacB and CpG. We detected surge in mononuclear cell infiltration with higher Ki67 expression within iMATEs in liver tissues of HBV-transgenic mice and AAV-HBV transduced mice at day 3 after CpG application following TherVacB compared to TherVacB alone (Fig. 13a, b). Higher Ki67 expression predicted the pivotal role of CpG in jump expansion of hepatic immune cells after therapeutic vaccination. As CD8+ T cells play instrumental role in clearance of infected hepatocyte in infection, we analysed Ki67 expressing CD8+ T cells through flow cytometry following intravenous injection of CpG in HBV-transgenic mice and AAV-HBV transduced mice. We found that single dose of CpG is enough to significantly increase Ki67+ CD8+ T cells in liver, which implied the therapeutic relevance of CpG in combinatorial therapeutic approaches against chronic liver infections (Fig13c, d).

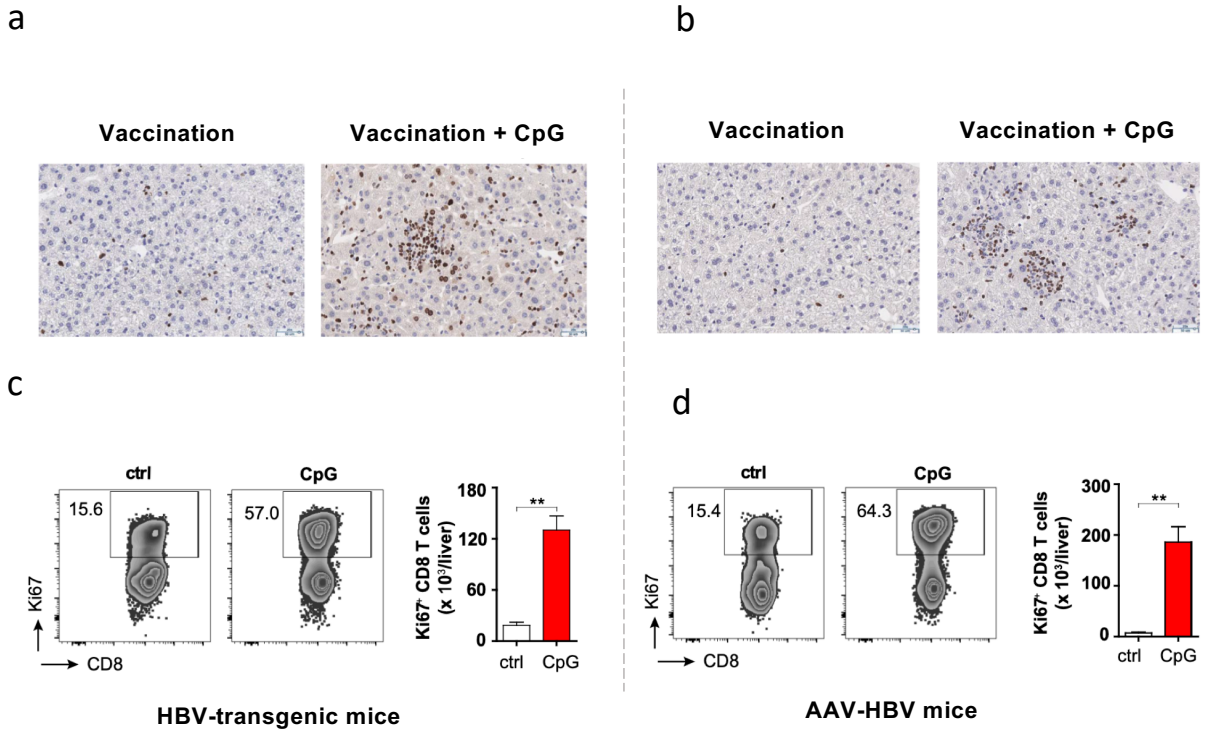

Figure 13. *CpG further increases the expression of Ki67 in immune cells of liver. (a)(b) Immunohistochemistry of liver slices manifesting Ki67 expression at day 3 following CpG administration in vaccinated mice (scale bar: 50um). (c)(d) Detection of Ki67 expressing hepatic CD8+ T cells through flow cytometry (left) and quantification (right). Bars in (c, d) show mean value of n ≥ 3 mice + SEM. Statistical analysis was performed using student 's t test. Asterisks indicate statistically significant differences: *p < 0.05.*

3. RESULTS

We proposed that proliferative potential of CD8+ T cells was enhanced through recruitment of inflammatory myeloid cell population in liver. Therefore, we further characterized hepatic myeloid cells following CpG injection and checked the relevance of increasing the numbers of CD11b+ Ly6C+ inflammatory myeloid cells with CD8+ T cell expansion in liver. After 3 days of CpG injection in HBV-transgenic mice and AAV-HBV transduced mice, we found significant rise in CD11b+ Ly6C+ monocytes with improved surface expression levels of MHCII, CD80 and CD86 as compare to the controls (Fig. 14a, b). Consistent with previous findings, we inferred that CpG generated immunogenic microenvironment in liver through infiltration of CD11b+ Ly6C+ monocytes with increased expression of CD80, CD86 and MHCII molecules, providing co-stimulatory signalling to trigger activation and proliferation of hepatic CD8+ T cells.

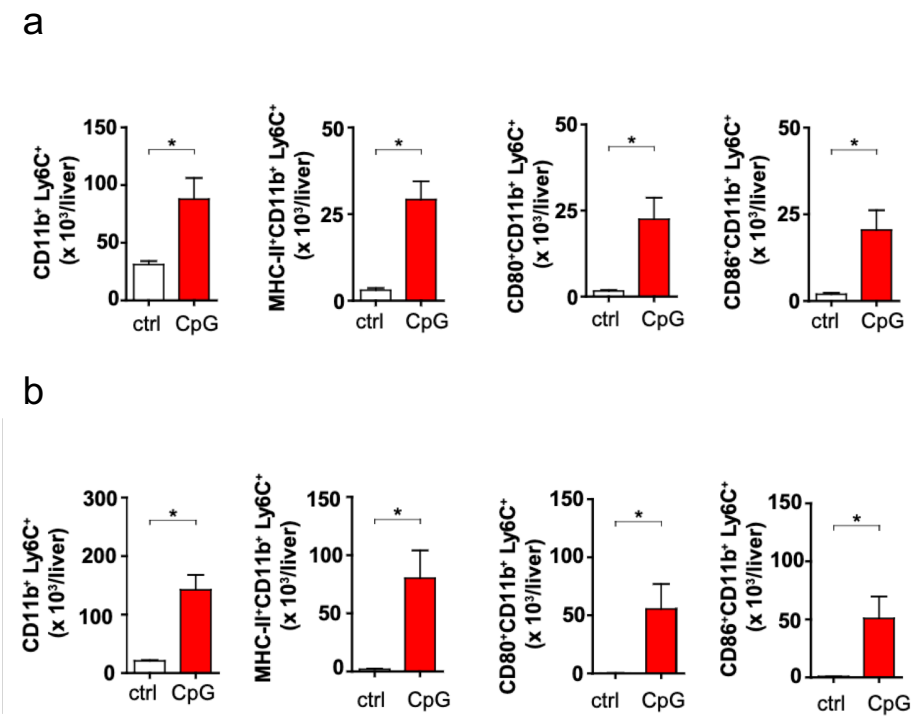

Figure 14. *CpG triggers the recruitment of inflammatory monocytes in liver through iMATEs induction in AAV-HBV and HBV transgenic mice. (a) Phenotypic characterization and quantification of CD80, CD86 and MHCII expressing hepatic myeloid cells at day 3 after CpG application in HBV transgenic mice and (b) AAV-HBV mice. Bars show mean value of n ≥ 3 mice + SEM. Statistical analysis was performed using student 's t test. Asterisks indicate statistically significant differences: *p < 0.05*

3.6 Establishment of ex vivo system of CD8+ T cell proliferation to characterize myeloid cell contribution towards CD8+ T cell expansion

After characterizing inflammatory myeloid cells in HBV-transgenic mice and AAV-HBV transduced mice, we were interested to develop an ex vivo detection system to determine the influence of myeloid cells on CD8+ T cell expansion. Besides, the phenotype and mechanisms determining the outcome of the myeloid cell-CD8+ T cell crosstalk could be studied in detail, providing the opportunity to identify the underlying mechanisms and overcome hepatic immune tolerance during chronic HBV infection. In order to optimize the ex vivo system, we first investigated the pattern of splenic CD8+ T cell proliferation after providing stimulation via anti-CD3/CD28 dynabeads CD8+ T cell activator and Interleukin-2 10^3 IU/ml in U-bottom 96-well plate starting with different CD8+ T cell numbers. As CD8+ T cells replicate exponentially after first cell division, we seeded relatively low numbers of CD8+ T cells in 96-well plate so that we could still observe the pattern of proliferation in our ex vivo system. We stimulated CD8+ T cells optimally by adding equal proportion of dynabeads with CD8+ T cells, whereas in order to mimic sub-optimal conditions of stimulation, we further diluted

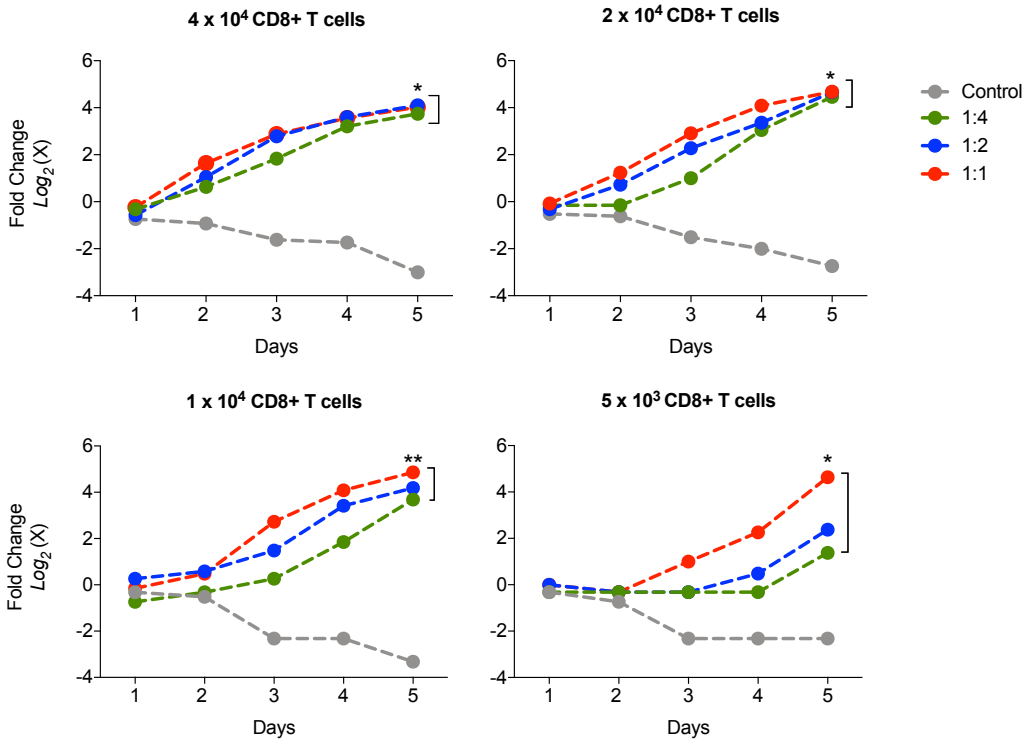

Figure 15. *Fold change of ex vivo CD8+ T cell expansion with different ratios of T-cell to Dynabeads T-activator CD3/CD28 (1:1,1:2 and 1:4). Time kinetics and pattern of CD8+ T cell proliferation starting with different cell numbers. Dots show mean value of n=2 replicates + SD. Statistical analysis was performed using 2-way ANOVA with Tukey's multiple comparison correction. Asterisks indicate statistically significant differences: *p < 0.05*

dynabeads by the factor of 2. Upon time kinetic analysis of fold change in CD8+ T cell expansion revealed that decreasing the starting CD8+ T cells numbers in 96 well plate resulted in delayed activation as compared to higher CD8+ T cell numbers at the start of replication. Similarly, decreasing the ratio of anti-CD3/CD28 dynabeads to CD8+ T cells caused sub-optimal and delayed stimulation, yielding reduced number of CD8+ T cells as compared to optimal condition of proliferation i.e. 1:1 ratio of CD8+ T cells to dynabeads (Fig. 15). Whereas it is clearly showed that we can measure the consistent rise in CD8+ T cell number ex vivo by seeding low number of CD8+ T cells at the beginning. Even after we seeded 40,000 CD8+ T cells per well at the start, we were

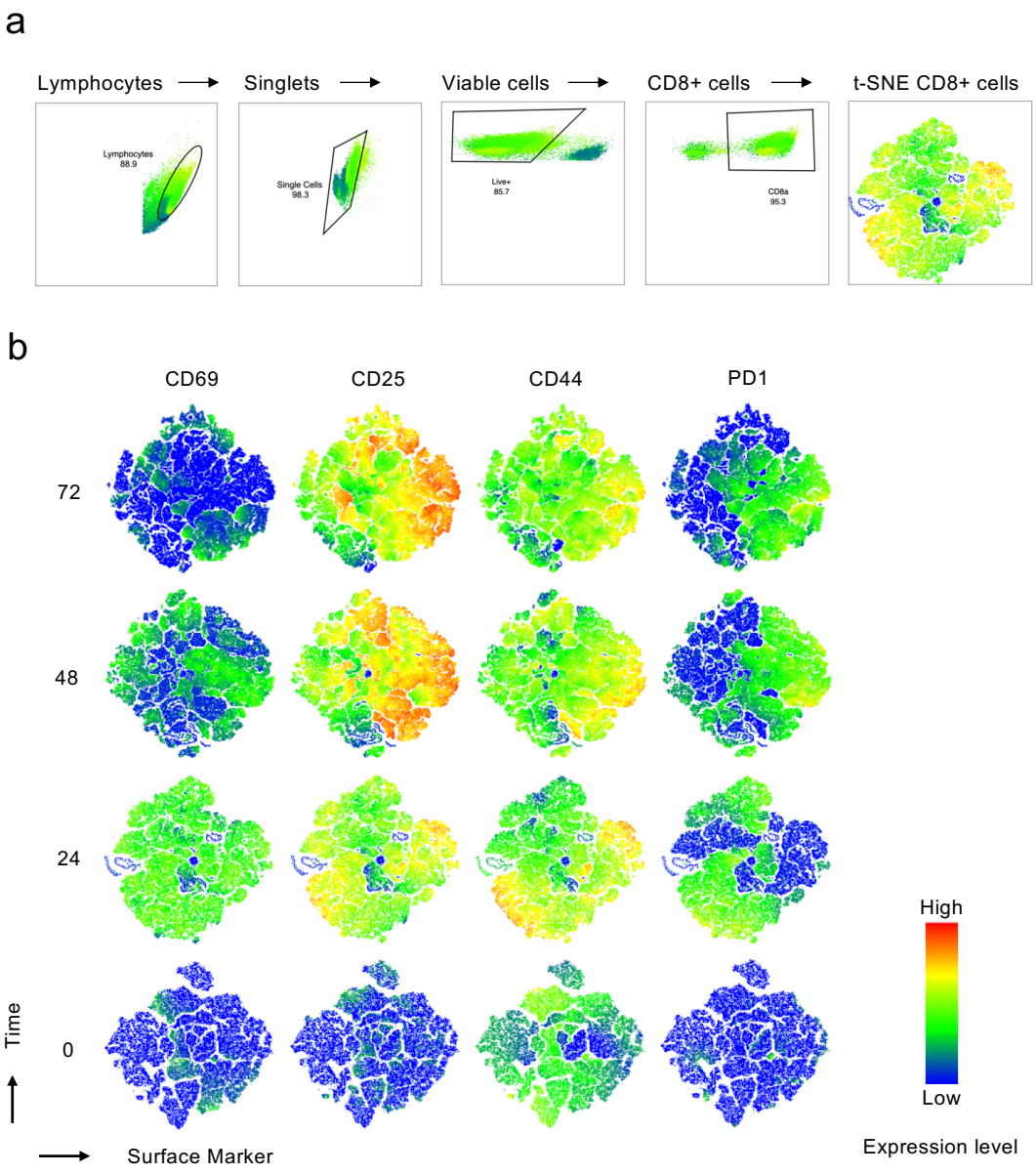

Figure 16. *Dynamics CD8+ T cell activation. (a) Gating strategy for generation of t-SNE plot of CD8+ T cells. (b) Expression of activation and exhaustion markers during CD8+ T cell activation and proliferation.*

still able to observe dynamics of CD8+ T cell proliferation ex vivo in terms of cell counts (Fig. 15). Next, we performed flow cytometric analysis to determine the dynamics of ex vivo CD8+ T cell activation. We did time kinetic analysis after stimulating CD8+ T cells with anti-CD3/CD28 dynabeads and IL-2. CD8+ T cells were activated after costimulatory signaling via CD3 and CD28 receptors (Fig. 16a). We observed upregulation of activation markers CD25, CD44 and CD69 upon activation of CD8+ T cells. Whereas we also noticed increasing expression of exhaustion marker PD1 in activated CD8+ T cells indicating certain differentiated state of proliferating CD8+ T cells. we also noted downregulation of CD69 on CD8+ T cells after 72 hours of activation, but CD44 and CD25 expression apparently remained stable (Fig 16b). Consistent with the findings of t-SNE analysis of CD8+ T cells, we observed that 80% of the total activated-CD8+ T cell population has upregulation of activation markers

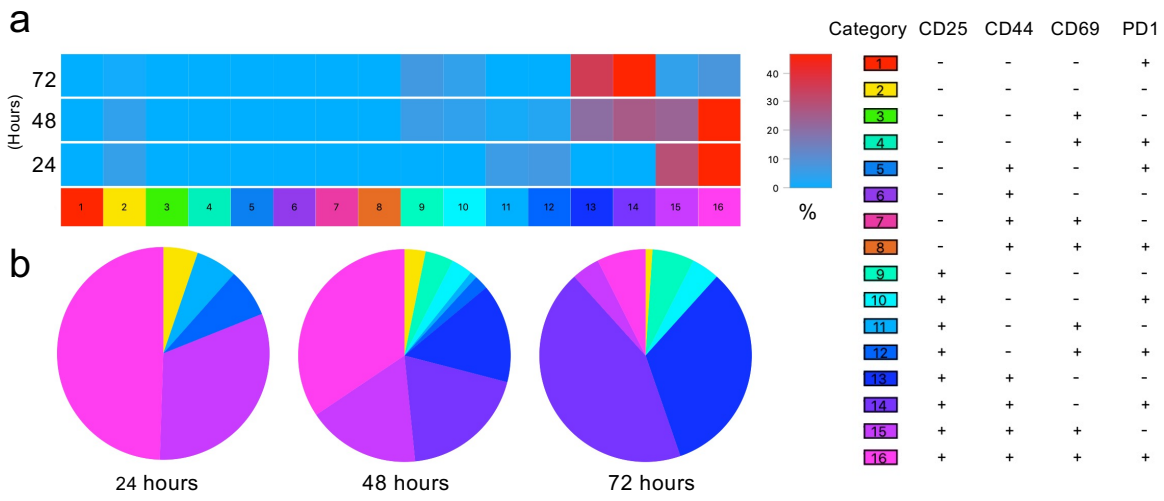

Figure 17. *Phenotypic profiling of activated-CD8+ T cells after co-stimulatory signaling via a-CD3 / a-CD28 Dynabeads and IL-2 (a) CoolPlot representation of multiple activation marker expression on CD8+ T cell population. (b) Pie chart depicting different populations of CD8+ T cells with variable activation marker expression. Each category is proportional to the percentage of whole CD8+ T cell population. Flow cytometric data was analyzed using Pestle and Spice 6.0 software. Results were sorted by permuted order.*

CD25, CD44 and CD69, while 50% of the total CD8+ T cell population also has additional PD1 expression after 24 hours of activation. Whereas, we observed downregulation of CD69 expression in almost 40% of CD25 and CD44 expressing CD8+ T cells after 48 hours of stimulation, out of which half of the cells upregulated the expression of PD1. As a consequence, proportion of CD8+ T cell population that were expressing multiple activation markers was further reduced. Interestingly, we observed further downregulation of CD69 and upregulation of PD1 in more than half of

the CD8+ T cell populations after 72 hours of CD8+ T cell activation, whereas expression of CD44 and CD25 also started to downregulate in small fraction of CD8+ T cell populations (Fig. 17). After understanding the dynamics of CD8+ T cell activation and expansion via anti-CD3/CD28 Dynabeads, we further adjusted the protocol of

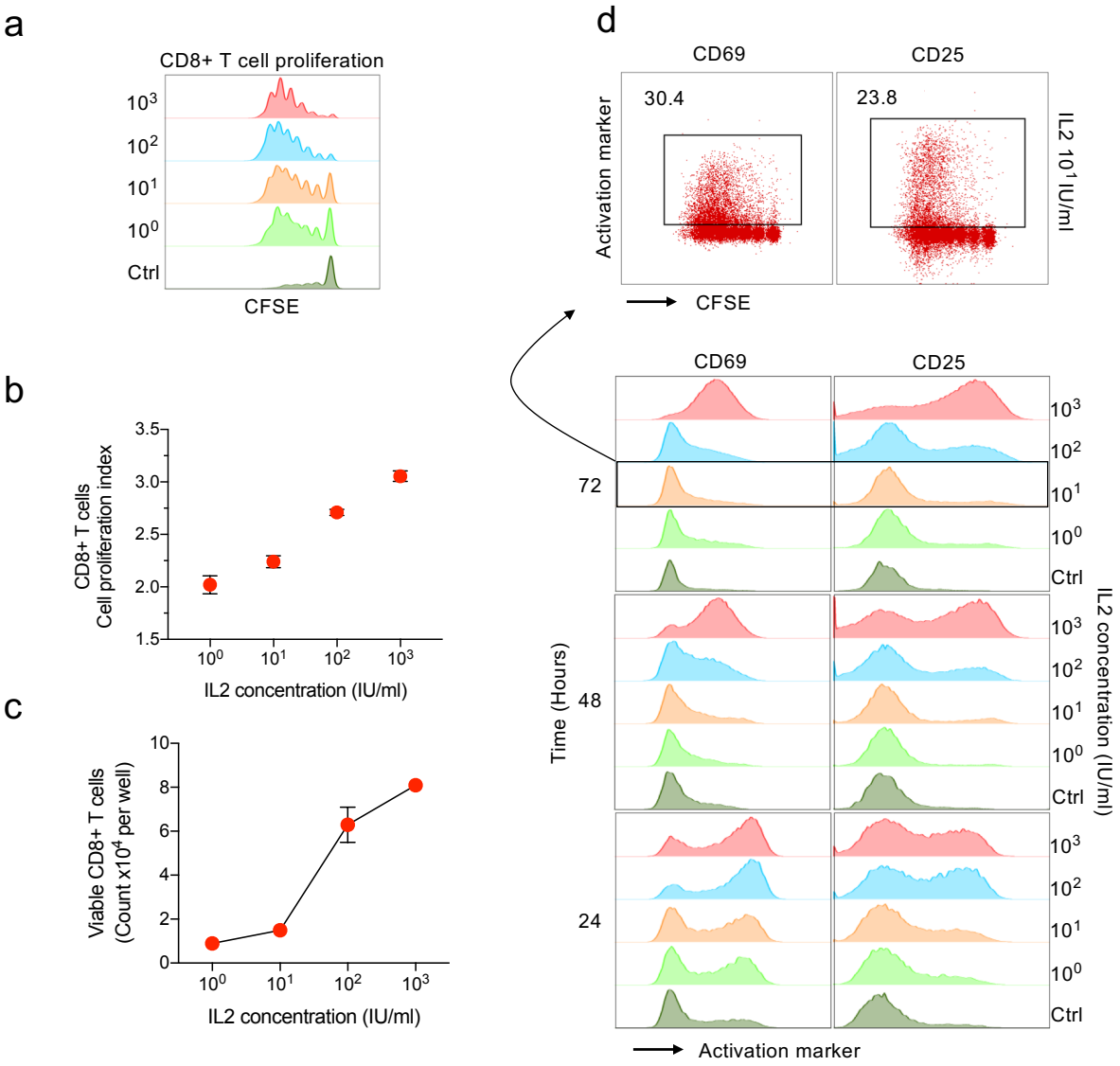

Figure 18. *CD8+ T cell activation and proliferation through Dynabeads T activator CD3/CD28 with different concentrations of IL-2. (a) CD8+ T cell proliferation pattern after 72 hours of activation. (b) Cell proliferation index of CD8+ T cells after 72 hours of activation. (c) Count of live CD8+ T cells with different concentration of IL-2 after 72 hours. (d) Histogram plots of activation markers on CD8+ T cells showing kinetics of CD8+ T cell activation. (b) CD8+ T cell viability with different concentrations of IL-2 after 72 hours of activation. Dots show mean value of n=2 replicates + SD.*

CD8+ T cell activation so that the additional influence of myeloid cells on survival and proliferation of CD8+ T cells could be detected in our ex vivo system. It is previously reported that varying concentration of IL-2 significantly changed the rate of cell death and number of T cells entering into cell division (Deenick, Gett et al. 2003). Therefore, next we incubated 40,000 CFSE-labelled CD8+ T cells with equal proportion of anti-

CD3/CD28 dynabeads and added different concentrations of IL-2. We noticed that higher concentration of IL-2 led to increasing rate of cell division and cell proliferation index of CD8+ T cells after 72 hours of incubation (Fig. 18a, b). Besides, we also observed increase in viable CD8+ T cell numbers with relatively higher concentrations of IL-2 (Fig. 18c). While there was a consistent decline in CD25 and CD69 expression on CD8+ T cells at each time point with lower concentrations of IL-2 (Fig. 18d). As a result, we detected decreasing number of dividing CD8+ cells with CD25 and CD69 downregulation and more viable undivided CD8+ T cells (Fig. 18a, b, d). Whereas Higher concentration of IL-2 triggered strong activation of CD8+ T cells, as we observed increased expression of CD69 and CD25 on proliferating CFSE-labelled

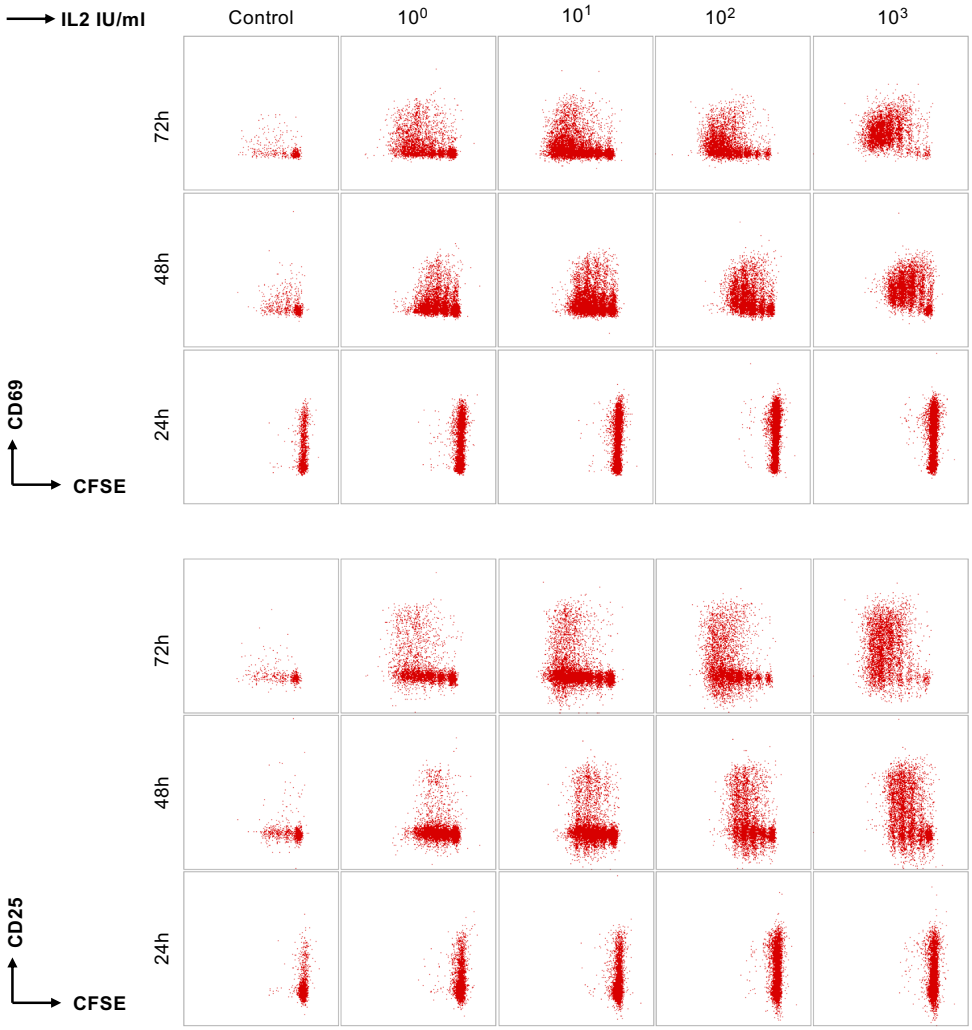

Figure 19. *Activation and proliferation potential of activated CD8+ T cells with different concentrations of IL-2. Dot plot of activated CFSE labelled CD8+ T cells versus CD69 and CD25 manifesting different proliferation pattern over the period of 3 days.*

CD8+ T cells at each time point of flow cytometric analysis compared to CD8+ T cell proliferation with lower concentration of IL-2 (Fig. 19). Consistent with these findings, higher IL-2 concentrations led to the surge in mean fluorescence intensity of CD69 and CD25 over the entire incubation period (Fig. 20). Although we observed low yield of CD8+ T cells and reduced expression of CD25 and CD69 with low concentration of IL-2 i.e. 10^1 IU, but still we detected relatively large number of CD8+ T cells that entered into their earlier cell divisions and didn't terminally differentiate as compared to CD8+ T cells that incubated with higher concentration of IL-2. Therefore, we decided to take 40,000 CD8+ T cells per well with equal proportion of anti-CD3/CD28 dynabeads CD8+ T cell activator and further fine-tune our ex vivo system by finally adjusting concentration of IL-2 to 10^1 IU. It provided us the opportunity to detect additional impact of myeloid cells on survival and proliferation of activated CFSE-labelled CD8+ T cells in our ex vivo detection system. Whereas, we can also compare the activation potential of CD8+ T cells through surface activating marker CD25 on proliferating CFSE-labelled CD8+ T cells during consecutive cell devisions.

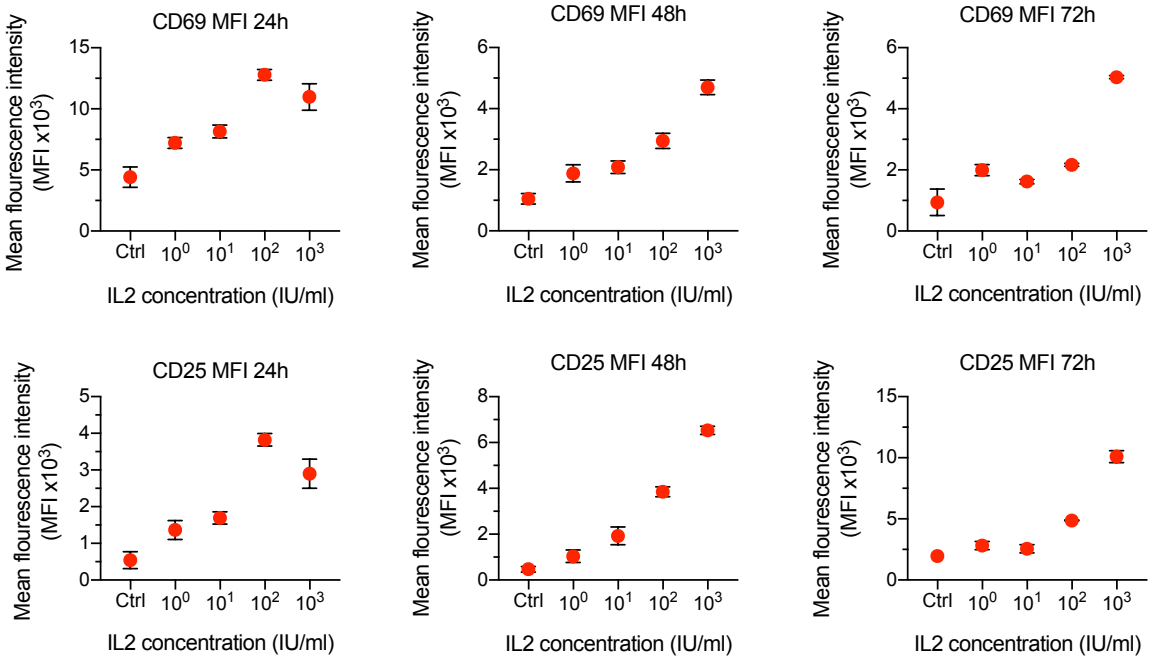

Figure 20. *Time kinetics and dynamics of CD69 and CD25 expression on proliferating CD8+ T cells under the influence of different dilutions of IL-2. Dots show mean value of n=2 replicates + SD.*

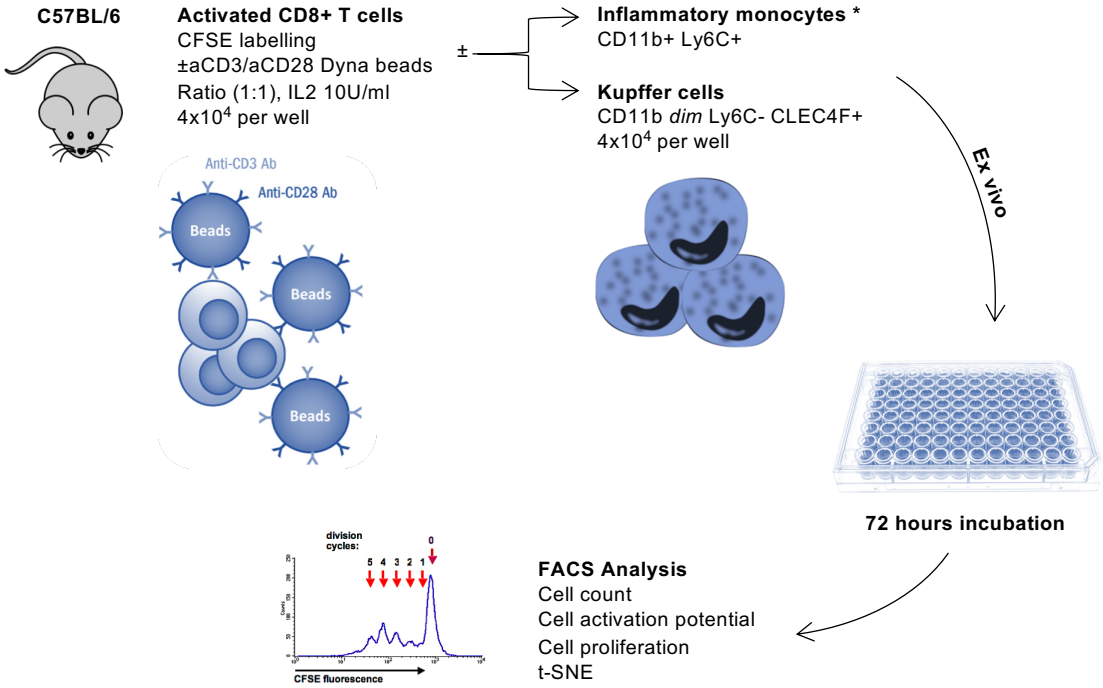

Illustration 4. *Schematic diagram of ex vivo characterization of myeloid cell contribution towards CD8+ T cell mediated immunity*

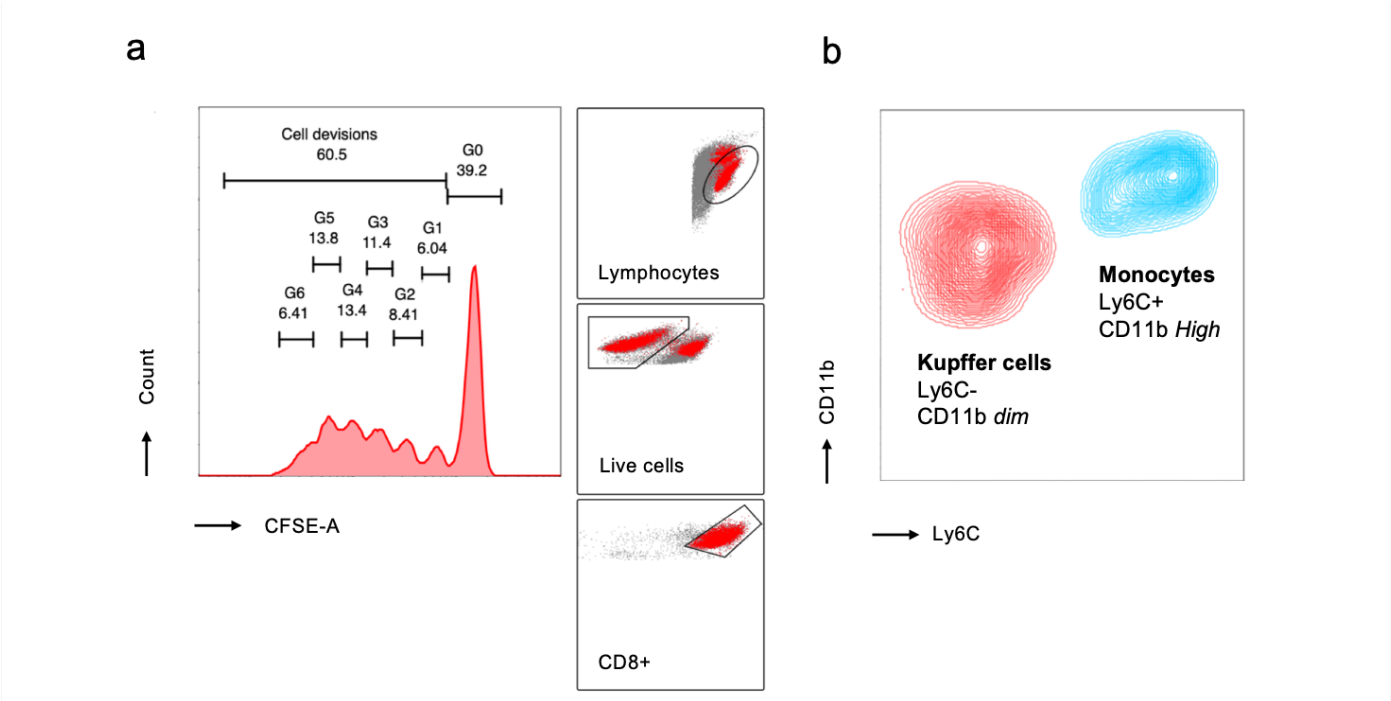

Figure 21. *Gating strategy for ex vivo characterization of myeloid cells influencing CD8+ T cell expansion. (a) Histogram of activated CFSE labelled CD8+ T cells showing consecutive cell divisions after 72 hours of activation. (b) FACS contour plot after sorting Ly6C+ CD11b+ (monocytes) and Ly6C- CD11b dim CLEC4F+ (Kupffer cells) cell populations through FACS sorter.*

3.7 Ex vivo characterization of myeloid cell contribution towards CD8+ T cell mediated immunity

After establishing ex vivo detection system, we were interested to further characterize the influence of different myeloid cell populations on CD8+ T cell proliferation. Therefore, we incubated CFSE-labelled CD8+ T cells activated via anti-CD3/CD28 dynabeads (Fig. 21a) and 10 IU/ml IL-2 with either hepatic macrophages (Kupffer cells) or hepatic inflammatory monocytes which were isolated after intravenous administration of CpG (Fig. 21b) (see illustration 4). At first, we established the role of CD11b+ Ly6C+ inflammatory monocytes that mainly constitute iMATEs following intravenous CpG-injection in wild-type mice. Therefore, we harvested CD11b+ Ly6C+ inflammatory monocytes (Fig. 21b) from freshly isolated murine liver after 48 hours of

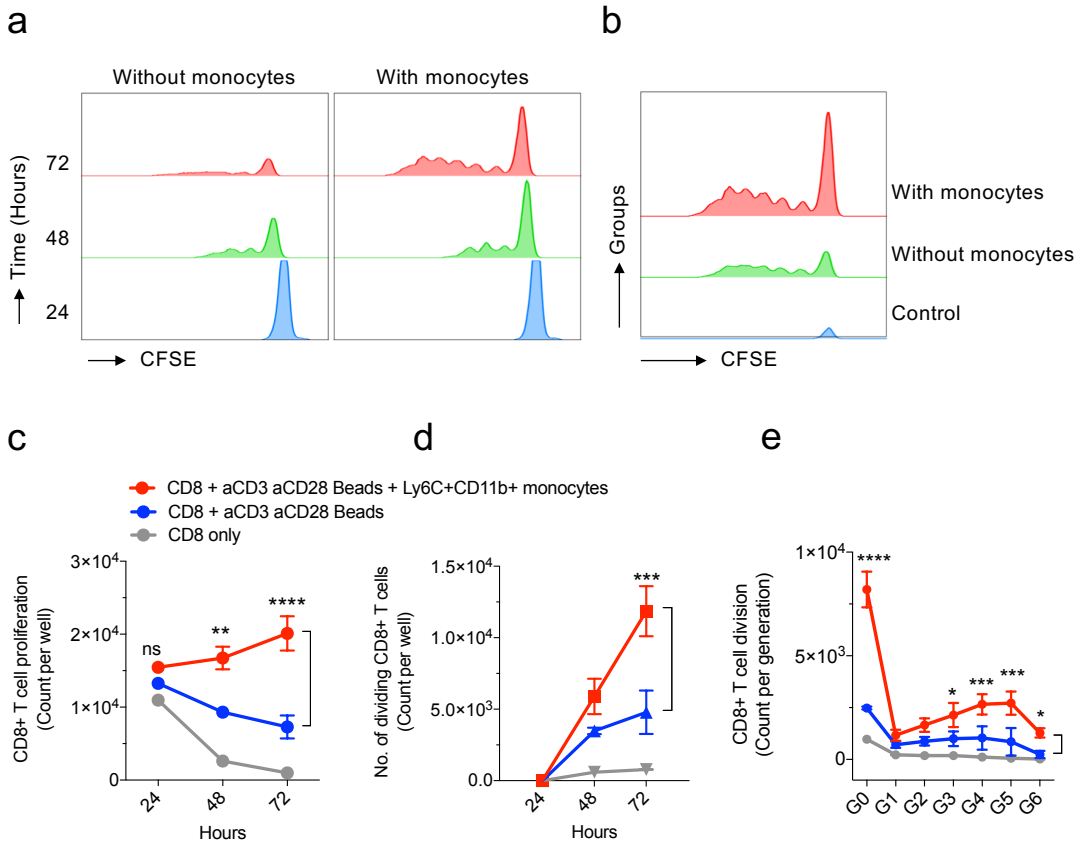

Figure 22. *Liver associated myeloid cells harvested after 48 hours of intravenous CpG-injection increase the survival and proliferation of splenic CD8+ T cells. (a) Time kinetics of CD8+ T cell proliferation incubated with monocytes. (b) Histogram of activated CFSE labelled CD8+T cells after 72 hours with monocytes. (c) Total count of CD8+ T cells co-cultured with monocytes. (d) Quantification of dividing CD8+ T cells over the period of incubation. (e) CD8+ T cell divisions after 72 hours of incubation with monocytes. Dots show mean value of n=2 replicates + SD. Statistical analysis was performed using 2-way ANOVA with Tukey's multiple comparison correction. Asterisks indicate statistically significant differences: *p < 0.05*

CpG-injection and incubated them with activated CFSE-labelled CD8+ T cells for 3 days. We performed time kinetic analysis and quantified number of C8+ T cells in successive cell divisions. We found that activated CD8+ T cells proliferated better with CD11b+ Ly6C+ monocytes (Fig. 22a, b, c). As CD8+ T cells started to divide, we observed a greater number of dividing CD8+ T cells over the entire period of incubation (Fig. 22d). We also observed increase in CD8+ T cell count in each consecutive cell

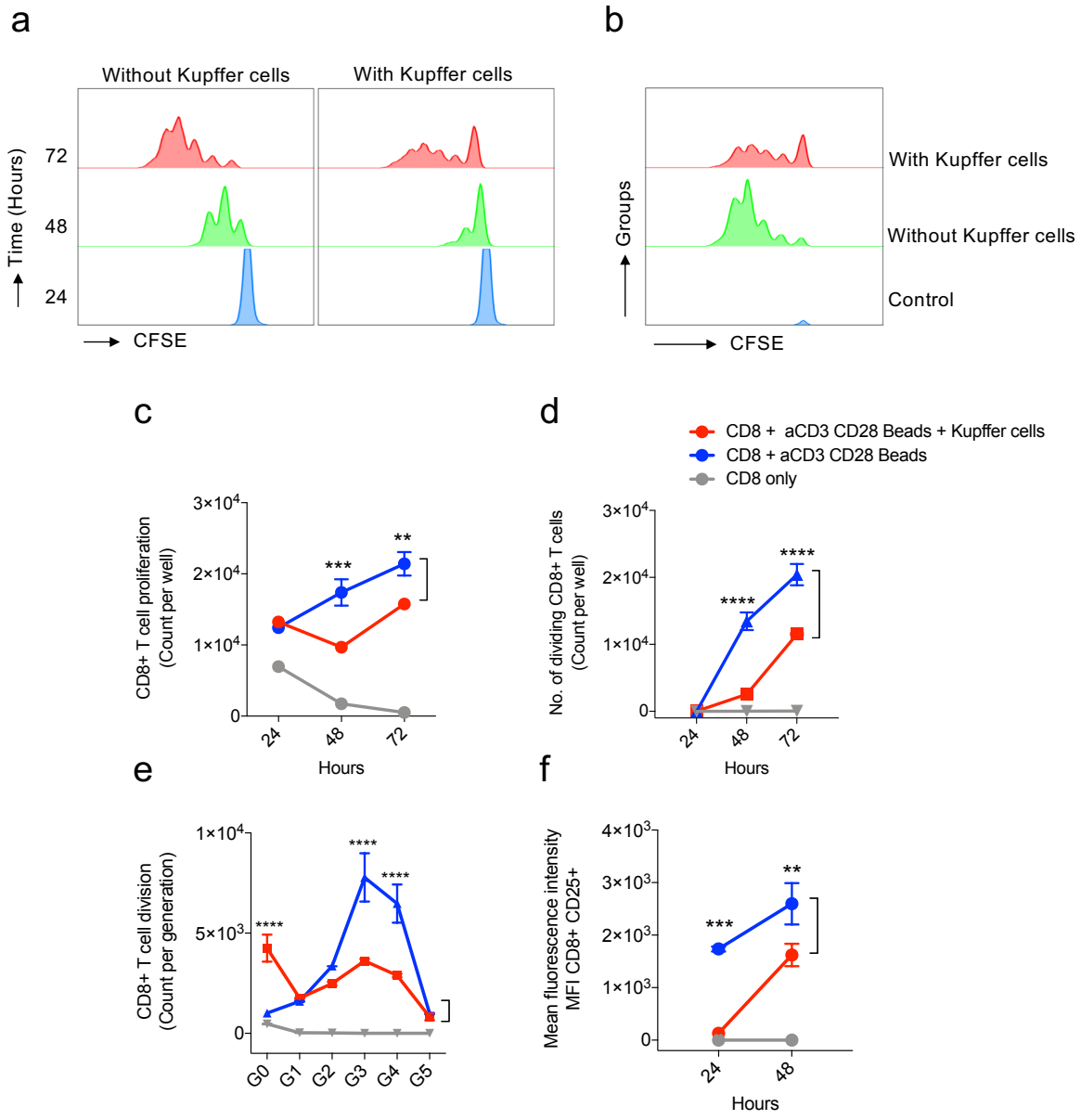

Figure 23. *Liver resident macrophages (Kupffer cells) inhibit proliferation of splenic CD8+ T cells. (a) Time kinetics of CD8+ T cell proliferation incubated with Kupffer cells. (b) CFSE labelled CD8+ T cell expansion after 72 hours. (c) Total counts of CD8+ T cells proliferated over the period of incubation. (d) Counts of dividing CD8+ T cells after activation. (d) CFSE labelled CD8+ T cell division after 72 hours of co-incubation. (f) MFI of activation marker CD25 on CD8+ T cells. Dots show mean value of n=2 replicates + SD. Statistical analysis was performed using 2-way ANOVA with Tukey's multiple comparison correction. Asterisks indicate statistically significant differences: *p < 0.05*

division after 72 hours of incubation with monocytes (Fig. 22e). Monocytes also supported the survival of CD8+ T cells, as we detected larger number of undivided viable CD8+ T cells at 72 hours of co-culture (Fig. 22a, b, e). These findings further corroborated the notion that CD11b+ Ly6C+ inflammatory myeloid cells, which are also present within iMATEs in liver after CpG application, support the ex vivo expansion of activated CD8+ T cells.

In normal physiological condition liver microenvironment promotes tolerance rather than immunity. There are several liver immune cell populations which contribute towards tolerogenic hepatic microenvironment. Liver resident macrophages also known as Kupffer cells are one of the regulatory myeloid cells that inhibit CD8+ T cell

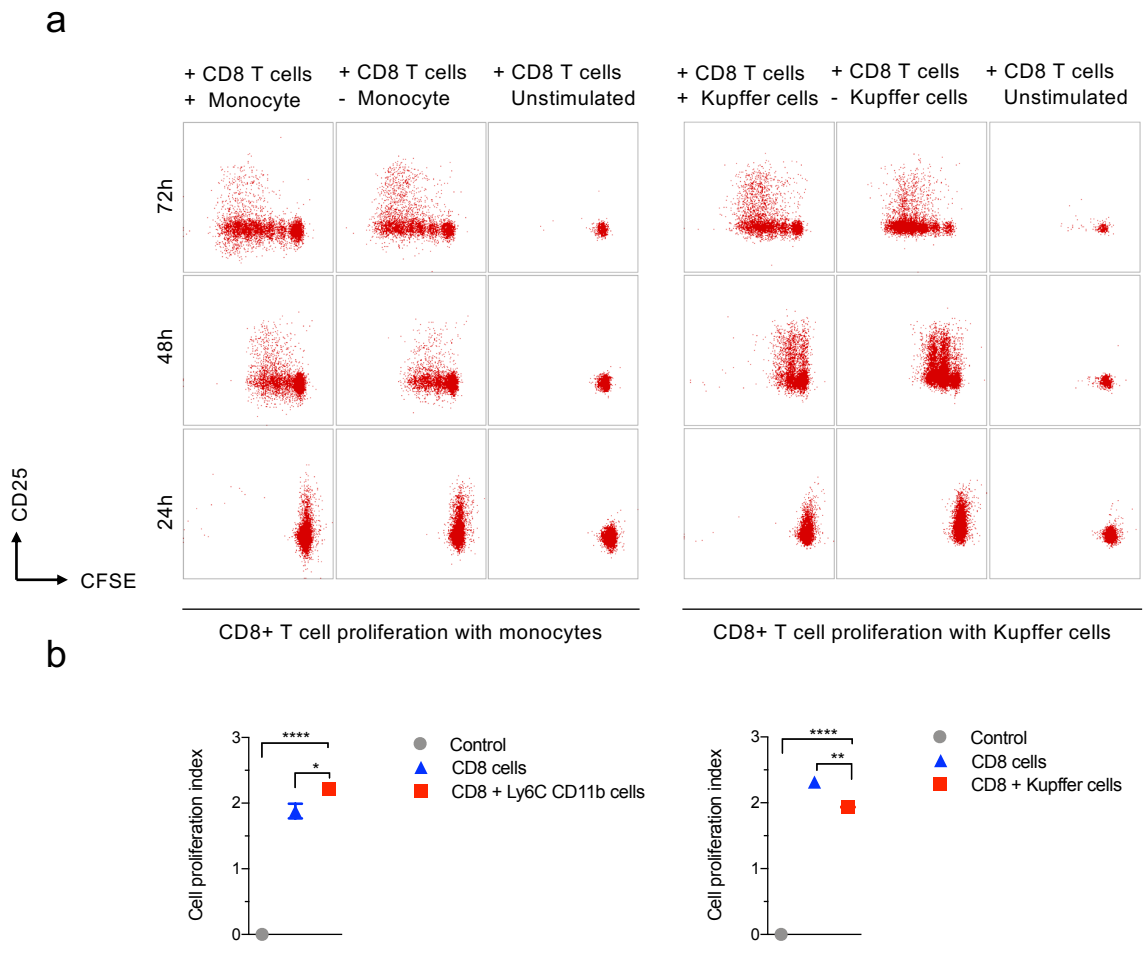

Figure 24. *Myeloid cell contribution towards CD8+ T cell activation and proliferation. (a) Dot plot of activated CFSE labelled CD8+ T cells versus CD69 and CD25, manifesting different proliferation pattern with inflammatory monocytes and Kupffer cells. (b) CD8+ T cell proliferation index after 72 hours of incubation with myeloid cells. Dots show mean value of n=2 replicates + SD. Statistical analysis was performed using 2-way ANOVA with Tukey's multiple comparison correction. Asterisks indicate statistically significant differences: *p < 0.05*

mediated immunity. Therefore, next we characterized the contribution of CD11b*dim* Ly6C- CLEC4F+ Kupffer cells (Fig. 21b) towards CD8+ T cell activation and proliferation. We incubated Kupffer cells with activated CFSE-labelled CD8+ T cells and performed time kinetic analysis. We observed that Kupffer cells triggered inhibitory effect on CD8+ T cell proliferation (Fig. 23a, b), resulting in downregulation of activation marker CD25 (Fig. 23f). As a result, relatively smaller number of CD8+ T cells proliferated under the influence of Kupffer cells during the entire period of incubation (Fig. 23c). Consequently, we detected decrease in dividing CD8+ T cells co-cultured with Kupffer cells during the entire incubation period (Fig. 23d). While we also noticed significant population of undivided CD8+ T cells even after 72 hours (Fig. 23e). Although Kupffer cells couldn't inhibit CD8+ T cell proliferation entirely, but still we detected reduction in CD8+ T cell number in consecutive cell divisions after 72 hours of co-culture (Fig. 23b, e).

Overall CD11b+ Ly6C+ monocytes that were harvested from murine liver following CpG application triggered sustained activation, proliferation and survival of already activated CD8+ T cells, whereas hepatic macrophages also known as Kupffer cells significantly reduced CD8+ T cell activation and expansion (Fig. 24a, b). We could further exploit our ex vivo system determining the intrinsic mechanisms of the myeloid cell – CD8+ T cell crosstalk to overcome hepatic immune tolerance during chronic HBV infection.

4. DISCUSSION

4.1 Immune modulation through TLR-9 signaling improved vaccine-induced HBV-specific CD8+ T cell responses

CD8+ T cell responses determine the outcome of infection during ongoing antiviral immunity against chronic HBV infection (Chisari and Ferrari 1995; Bertoletti and Ferrari 2012; Schuch, Hoh et al. 2014; Gish, Given et al. 2015). Therefore, it also signifies the importance of therapeutic vaccine as a potential therapy to induce HBV-specific T cell mediated immunity (Kosinska, Bauer et al. 2017). Several studies are already conducted on devising therapeutic vaccination strategy for the cure of chronic HBV infection, but no promising outcome is achieved so far (Lim, Agcaoili et al. 2019). It is inferred that our heterologous therapeutic vaccine is still a viable option to induce strong multi-functional HBV-specific T cell responses to overcome immune suppression in HBV-transgenic mice model (Backes, Jäger et al. 2016), which might be further synergized through different immune modulation strategies (Maini and Burton 2019). Immune modulators such as CpG/TLR-9 agonist provided us an opportunity to modulate adaptive immunity indirectly without targeting T cells or B cells (Huang, Wohlleber et al. 2013).

We conducted preclinical trials using HBV-transgenic mice and AAV-HBV mice models for chronic HBV infection (Dembek and Protzer 2015) to further synergize vaccine induced HBcAg-specific CD8+ T cell responses through immune modulation. As higher viral burden is associated with impaired HBcAg-specific CD8+ T cell responses in chronic HBV (Huang, Wu et al. 2006; Yang, Liu et al. 2014), therefore, HLA-A2 restricted responses against HBcAg epitope are vital in controlling HBV infection (Maini, Boni et al. 1999; Kefalakes, Budeus et al. 2015). We reported that CpG/TLR-9 agonist along with therapeutic vaccine enhanced the functionality of vaccine-induced HBcAg-specific CD8+ T cells as compared to vaccine alone (Yang, Liu et al. 2014). CpG is an oligodeoxynucleotide (ODN) that contains unmethylated CpG motifs. It triggers inflammatory response and improves the function of APCs through TLR-9 signaling (Krieg, Yi et al. 1995; Wagner 1999; Hemmi, Takeuchi et al. 2000). Previous clinical research also demonstrated the enhanced efficacy of HBV vaccine in combination with CpG adjuvant as compared to aluminum adjuvant (Cooper, Davis et al. 2004; Krieg 2006; Vollmer and Krieg 2009; Cooper and Mackie 2011). It was also

reported that therapeutic vaccine adjuvanted with CpG supported Th1 immune response, which plays vital role in an effective adaptive immunity towards of intracellular pathogens (Bode, Zhao et al. 2011). Consistent with these findings, our colleagues previously showed that CpG/TLR-9 agonist triggered hepatic inflammation leading to the cluster formation of inflammatory myeloid cells mostly of CD11b+ lineage within liver compartments also known as iMATEs; these structures allowed further expansion of already primed CD8+ T cells through co-stimulation dependent (CD28/OX40/IL-15R signaling) activation of CD8+ T cells. We also observed iMATEs formation regardless of therapeutic vaccine and viral load (Huang, Wohlleber et al. 2013). Hence, the combination of therapeutic vaccine is nicely complemented by subsequent iMATEs induction, as both approaches have distinct mechanism of action in different anatomical compartments. At first, therapeutic vaccine induces functional virus-specific CD8+ T cell responses through potent cross-priming, then these responses are further augmented locally in the liver by iMATEs induction. Thus, expansion of vaccine-induced T cells could be amplified further particularly in liver to increase the efficacy of existing therapeutic vaccination strategies (Maini and Pallett 2018).

Other TLR agonists such as TLR-7 ligand GS-9620 have been reported to improve proliferation of functional HBV-specific T cells following enhanced priming of DCs (Boni, Vecchi et al. 2018). However, it also stimulated the proliferation of NK cells, but surprisingly it did not delete HBV-specific T cells through NK cell-mediated apoptosis (Davidson, Maini et al. 2015). Nonetheless, this effect might be ascribed to the upregulation of interferon stimulating genes (Janssen, Brunetto et al. 2018) induced by TLR-7 signaling, as already explained in murine model of LCMV infection (Davidson, Maini et al. 2015). Similarly,TLR-8 agonist GS-9688 has also been reported to support the expansion of HBV-specific T cells through induction of IL-12 signaling (Schurich, Pallett et al. 2013; Kurktschiev, Raziorrouh et al. 2014) in chronic HBV patients. In accordance with these outcomes, we also observed a substantial increase in IFN-γ producing HBcAg-specific CD8+ T cells and recruitment of functionally active APCs of CD11b+ myeloid lineage (Ly6C+, CD80/CD86+ and MHCII+) within the liver compartments upon TLR-9 signaling. Therefore, intravenous injection of CpG/TLR-9 agonist generated iMATEs within liver compartments, which subsequently supported the local expansion of already primed HBcAg-specific CD8+ T cells, increasing the

efficacy of therapeutic vaccine against chronic HBV infection. Although, several preclinical studies gave us insight regarding mechanism of actions of different TLR-agonists, but in-depth analysis is still required to determine the role of TLR-agonists in complex hepatic microenvironment during chronic HBV.

4.2 Noncytolytic antiviral activity of HBcAg-specific CD8+ T cells augmented through iMATEs induction

Several studies demonstrated the role of inflammatory cytokines in noncytolytic control of HBV without killing the infected hepatocytes (Guidotti, Ando et al. 1994; Guidotti, Ishikawa et al. 1996; Guidotti, Rochford et al. 1999; Thimme, Wieland et al. 2003). We reported that iMATEs induction in combination with therapeutic vaccine have not only increased the population of CD8+ T cells but also enhanced the number of IFN-γ producing HBcAg-specific CD8+ T cells in the liver of HBV-transgenic mice and AAV-HBV mice models of chronic HBV infection. Consistent with our findings, increased expression of IFN-γ was detected during the antiviral activity of HBV-specific CD8+ T cells in HBV-transgenic mice and experimental HBV infection model of chimpanzee (Guidotti, Borrow et al. 1999; Guidotti and Chisari 1999; Guidotti and Chisari 2000; Guidotti and Chisari 2001). In patients with chronic HBV infection, peripheral HBV-specific CD8+ T cells manifested impaired functional response failing to proliferate and produce antiviral cytokines like IFN-γ (Boni, Fisicaro et al. 2007). The expansion of functional HBcAg-specific CD8+ T cells was also impaired due to high antigen levels during chronic HBV infection, preventing these immune cells to control the infection. HBV antigens are presented by APCs constantly on MHC molecules during the course of HBV infection, but continuous circulation of viral particles comprising of soluble HBsAg and HBeAg resulted in defective virus specific CD8+ T cell responses. Particularly, HBeAg explicitly involved in transforming the phenotypic profile of functional HBV-specific CD8+ T cells in HBV infection. As, HBV-specific CD8+ T cells could be re-stimulated and expanded in vitro secreting different cytokines like IFN-γ, but a population of HBV-specific CD8+ T cells with transformed HLA peptide tetramer binding which overlooked HBV antigen in vivo seemed to be selected by HBe antigen (Reignat, Webster et al. 2002). The underlaying mechanism of this dysfunctional HBV-specific CD8+ T cell response could be attributed to TCR downregulation and a T-cell population selection with low avidity (Welsh 2001). However, HLA peptide tetramers alone cannot estimate overall avidity of functional T-cell (Derby, Wang et al. 2001;

Rubio-Godoy, Dutoit et al. 2001; Slifka and Whitton 2001), as it is also dependent on other confounding factors such as signal transduction pathways and co-stimulatory molecules (Margulies 2001).

HBV-specific CD8+ T cells play crucial role in inducing inflammation and antiviral activity against HBV antigens (Moriyama, Guilhot et al. 1990; Maini, Boni et al. 2000; Thimme, Wieland et al. 2003). These cells are present in abundance within the hepatic compartments during HBV infection (Moriyama, Guilhot et al. 1990; Thimme, Wieland et al. 2003) and target infected hepatocytes which lead to increase in antiviral cytokines such as IFN-γ/TNF-a to further inhibit viral replication (Guidotti, Ishikawa et al. 1996; Lucifora, Xia et al. 2014; Xia, Stadler et al. 2016). Apart from CD8+ T cell mediated apoptosis, several proinflammatory non-specific immune cells were also responsible for inflammation leading to liver damage (Ando, Moriyama et al. 1993; Ando, Guidotti et al. 1994). IFN-γ producing CD8+ T cells besides triggering noncytolytic activity to clear HBV infected hepatocytes, also induced proinflammatory microenvironment leading to the recruitment of more immune cell populations in liver (Ando, Moriyama et al. 1993; Kakimi, Lane et al. 2001). This recruitment process was improved through CpG-mediated iMATEs induction along with therapeutic vaccination (Huang, Wohlleber et al. 2013), subsequently decreasing the HBeAg levels even in the presence of high viral load in HBV-transgenic mice (Backes, Jäger et al. 2016; Ochel, Cebula et al. 2016). It clearly established the vital contribution of noncytolytic mediated CD8+ T cell mediated immunity towards HBV control as demonstrated in HBV transgenic mice (Guidotti and Chisari 2001). Here, we also suggested a prominent contribution of noncytolytic effector function involving IFN-γ secretion (Guidotti, Rochford et al. 1999) along with cytolytic effector function towards immune control of infection (Ando, Guidotti et al. 1994; Thimme, Wieland et al. 2003).

4.3 Role of granzyme B as biomarker for immune control of HBV

The clearance of HBV infected hepatocytes is associated with the killing of HBV infected hepatocytes. This traditional concept is supported by several clinical studies that liver damage demonstrated by increase in ALT levels during acute HBV or interferon treatment in chronic HBV patients is attributed to cytolytic clearance of HBV by HBV-specific T cells (Hoofnagle, Peters et al. 1988; Marinos, Torre et al. 1995; Webster, Reignat et al. 2000; Nair and Perrillo 2001). CD8+ T cells could trigger

cytolytic pathway through granzyme B (GzmB) and perforin, leading to DNA fragmentation and cell death (Fukuda, Ishimura et al. 1995; Nakamoto, Guidotti et al. 1997; Shresta, Pham et al. 1998). GzmB is one of the major molecules expressing on cytotoxic T cells that is crucial in clearance of HBV infection (Tang, Kwekkeboom et al. 2003). Here, we detected significant increase in GzmB expressing HBcAg-specific CD8+ T cells along with noncytolytic immune response (Tang, Kwekkeboom et al. 2005), following sequential administration of therapeutic vaccine and CpG. As a consequence, we observed significant liver damage in the chronic HBV mice that received CpG besides vaccine. The peak of liver damage was associated with the peak of functional HBcAg-specific CD8+ T cell responses (Webster, Reignat et al. 2000). Here, We were only interested to induce HBcAg-specific CD8+ T cell responses through therapeutic vaccine, as several studies supported the notion that HBc epitope determines the course of viral persistence and should be considered as main therapeutic target concerning to the immune control of HBV (Shi, Wu et al. 2004; Xu, Chu et al. 2005; Zhang, Li et al. 2007; Lin, Huang et al. 2010).

Long-term control of HBV depends on the decline of HBV-infected hepatocytes; which is possible either through clearance of HBV-infected hepatocytes or degradation of persistent form of HBV. We showed continuous immune control of HBV manifested by significant reduction of HBcAg expressing hepatocytes after a month-long incubation period following combinatorial therapeutic vaccination in our experimental models. Of note, we could not segregate the contribution of noncytolytic and cytolytic control of HBV in our experimental design, as proinflammatory cytokines such as IFN are crucial to induce CD8+ T cell responses (Le Bon, Etchart et al. 2003; Schulz, Diebold et al. 2005) following therapeutic vaccination with iMATEs induction. While we could not directly associate clearance of HBcAg expressing hepatocytes with GzmB expressing HBcAg-specific CD8+ T cells. Whereas, persistent control of HBV infection with increase in HBcAg-specific CD8+ GzmB+ T cell population (Tang, Kwekkeboom et al. 2005) still highlighted the importance of GzmB as biomarker for immune control in prospective immune monitoring strategies after therapeutic vaccination against chronic HBV infection. Besides, GzmB has been considered as critical downstream effector molecule for T cells to achieve immune control (Mullbacher and Waring 1999). While it has also been demonstrated that strong effector function of CX_3CR1+ CD8+ T cells attributed to the high expression of GzmB molecule (Böttcher, Beyer et al. 2015;

Gerlach, Moseman et al. 2016). Consistent with previous reports, our findings concerning to the GzmB expression in vaccine-induced virus-specific CD8+ T cells followed by CpG application supports the notion that these cells can confer strong antiviral activity against chronic HBV infection.

4.4 In vivo CpG-mediated recruitment of CD11b+ inflammatory monocytes enhanced proliferation potential of hepatic CD8+ T cells

Previously, it has been shown that CpG triggered the recruitment of inflammatory myeloid cell population mostly of CD11b+ phenotype, resulting in cluster formation of these cells also known as iMATEs. These cluster of myeloid cells could prevent regulatory signals of hepatic microenvironment, supporting the expansion of already primed CD8+ T cells within the compartments of liver (Huang, Wohlleber et al. 2013). Here, we also observed significant proliferation of mononuclear immune cell population as a result of iMATEs formation after sequential administration of therapeutic vaccine and CpG in AAV-HBV and HBV-transgenic models. Besides, increase in Ki67 expressing CD8+ T cells was observed following CpG-mediated iMATEs formation in these experimental models (Huang, Wohlleber et al. 2013). As expected, we also detected significant increase in CD11b+ Ly6C+ inflammatory monocytes with increased expression of CD80, CD86 and MHCII, suggesting enhanced capacity of antigen presentation and promoted T cell expansion through TNF-signaling (Wahl, Bochtler et al. 2008; Huang, Wohlleber et al. 2013).

Recently, it has been reported that iMATEs induction evoked similar immune response with elevated levels of IFN-γ, resulting in reduction of tumor growth in murine tumor model of HCC (Jia, Zhao et al. 2016). Besides, CpG-application also resulted in attenuation of suppressive capacity of CD11b+ Ly6C- monocytes in tumor microenvironment (Lin, Hsu et al. 2018). Furthermore, it was also found that CpG treatment also altered the suppressive function of CD11b+ myeloid cells and assisted in CD8+ T cell expansion (Lin, Hsu et al. 2018). While it is already established that myeloid derived suppressor cells (MDSCs) also contribute to limit CD8+ T cell responses (Ilkovitch and Lopez 2009; Medina-Echeverz, Eggert et al. 2015). There are several strategies employed to alter the inhibitory function of MDSCs or support their differentiation. One approach is to stimulate plasmacytoid DCs and proinflammatory cytokine production using CpG, thereby promoting the maturation of MDSCs (Albeituni,

Ding et al. 2013; Najjar and Finke 2013). Maturation of DCs further stimulated proinflammatory cytokines and Th1 immune responses (Ashkar and Rosenthal 2002). Along with the outcome of previous two studies, we have demonstrated that CpG-mediated iMATEs induction could be employed to augment hepatic T cell responses in different liver-specific immunotherapies (Huang, Wohlleber et al. 2013; Lin, Hsu et al. 2018).

4.5 Dynamics of ex vivo CD8+ T cell activation and expansion with different myeloid cell populations

We established an ex vivo system to detect the contribution of myeloid cells towards CD8+ T cell expansion. Naïve T cells need co-stimulatory signaling to activate, as only TCR stimulation in the absence of additional activation signal leads to T cell anergy (Schwartz, Mueller et al. 1989). Early phase of T cell activation is tightly regulated due to limited co-stimulatory receptors on T cells, which may also enhance priming through CD3−TCR signaling. However, CD28 plays crucial role in naïve T cell priming, but in the absence of CD28, other receptors may take over the mechanism of T cell co-stimulation (Shahinian, Pfeffer et al. 1993).

We activated naïve murine CD8+ T cells ex vivo physiologically through co-stimulatory signaling using micromagnetic beads coated with antibodies against epsilon chain of CD3−TCR and CD28 surface molecules of T cells and IL-2. These antibody-coated micromagnetic beads mimic in vivo T cell activation by antigen presenting cells (APCs) (Masteller, Warner et al. 2005; Li, Theofanous et al. 2007; Huang, Wohlleber et al. 2013). In normal physiological condition, CD28 binds to CD80 and CD86 molecules expressed by APCs (Janeway Jr and Bottomly 1994), influence IL-2 release, survival, proliferation and effector function of T cells (June, Bluestone et al. 1994). As a result of co-stimulation, we detected expression of activation markers CD25, CD44 and CD69 on activated CD8+ T cells (Volpes, van den Oord et al. 1991; Veiga-Fernandes, Walter et al. 2000). Whereas, we also observed upregulation of exhaustion marker PD-1 upon activation, indicating interesting aspect of high PD-1 expression not only during persistent or strong stimulation of CD8+ T cells during chronic infection or self-antigen stimulation in the absence of co-stimulation, but also during the early stage of CD8+ T cell activation (Wherry, Ha et al. 2007; Streeck, Brumme et al. 2008; Blackburn, Shin et al. 2009; Bucks, Norton et al. 2009). Besides, PD1 expression might also be involved

in preventing CD8+ T cells from terminal differentiation, as described by murine model of chronic viral infection (Odorizzi, Pauken et al. 2015). While after 3 days of persistent stimulation of CD8+ T cells, we detected and increase in exhausted subsets of CD8+ T cells defined by upregulation of PD1 and CD44 expression and onset of CD69 downregulation (Blackburn, Shin et al. 2008; Paley, Kroy et al. 2012; Wherry and Kurachi 2015).

After developing understanding of CD8+ T cell activation through TCR/CD28 co-stimulatory signaling and IL-2, we further manipulated our ex vivo system of CD8+ T cell proliferation through adjusting concentration of IL-2. Naïve T cells grow exponentially after initial priming and achieve effector function (Veiga-Fernandes, Walter et al. 2000), therefore, adequate fine-tuning was needed to restrict the exponential growth upon activation ex vivo, so that additional contribution of myeloid cells on CD8+ T cell expansion could be detected. Hence, IL-2 concentration was eventually reduced to 10IU/ml, as reducing the level of IL-2 concentration ex vivo, resulted in low number of T cells that entered into cell division (Deenick, Gett et al. 2003). Furthermore, despite reduced surface expression of CD25 and CD69 on dividing CD8+ T cells, we detected continued proliferation of activated CFSE-labelled CD8+ T cells during the entire period of incubation ex vivo. Besides, the differential cytokine expression on proliferating T cells exclude the possibility that only IL-2 secreting precursors can differentiated into effector CD8+ T cells (Sad and Mosmann 1994; Swain, Croft et al. 1996; Veiga-Fernandes, Walter et al. 2000).

After fine-tuning and resolving discrepancies from our ex vivo system of CD8+ proliferation, we characterized the contribution of different hepatic myeloid cell populations towards CD8+ T cell expansion. Immunoregulatory mechanisms in liver microenvironment are controlled by conventional as well as unconventional APCs (Gao, Jeong et al. 2008; Thomson and Knolle 2010; Tiegs and Lohse 2010; Crispe 2014). Unconventional APCs such as Kupffer cells (KCs) have low levels of MHCI/MHCII and co-stimulatory molecules during homeostasis (Thomson and Knolle 2010). These non-migratory APCs contribute towards tolerogenic microenvironment regardless of constant invasion of bacterial antigens and food particles from gut through portal vein (Epelman, Lavine et al. 2014; Xue, Schmidt et al. 2014; Dal-Secco, Wang et al. 2015).

4. DISCUSSION

We reported that the ex vivo proliferation of activated $CD8^+$ T cells was inhibited by hepatic $CD11b^{dim}$ Ly6C- CLEC4F+ KCs (You, Cheng et al. 2008; Scott, Zheng et al. 2016). These APCs were previously characterized by surface expression of $CD11b^+$ F4/80++ CD68+ CD11c+/- CLEC4F+ TIM4+ under normal physiological conditions as well as in experimental models of hepatic lesions (Wang, Song et al. 2018). The inhibition conferred by KCs was associated with downregulation of CD25 on activated CD8+ T cells, which might be linked to IL-10/TGF-ß signaling pathways (Breous, Somanathan et al. 2009; Zhang, Xu et al. 2011). While it has also been described that besides low expression of MHCII molecule, KCs also release anti-inflammatory cytokine IL-10 (Knoll, Schlaak et al. 1995; Knolle, Uhrig et al. 1998; Heymann, Peusquens et al. 2015) and express high levels of PD-L1. These mechanisms are involved in inhibition T-cell effector function and promotion of Treg development (Heymann, Peusquens et al. 2015). It has been demonstrated that ROS-dependent induction of FOXP3+ Tregs by macrophages suppressed T cell responses (Kraaij, Savage et al. 2010). KCs also enhanced hepatic immune tolerance through upregulating indolamine 2,3-dioxygenase pathway (Yan, Wang et al. 2010) and PGE_2 secretion (You, Cheng et al. 2008). The release of PGE_2 is associated with downregulation of CD25 (IL-2 and IL-2Rα chain) on activated CD8+ T cells (Demeure, Yang et al. 1997). It is also linked with reduction of IFN-γ secretion by Th1 cells altering the cytokine profile of Th1 cells to Th2 cells (Benbernou, Esnault et al. 1997; Demeure, Yang et al. 1997). Although, several regulatory mechanisms are driven through PGE_2 pathways including T-cell differentiation, however, further insight is required to understand the rationale of these distinct discrepancies (Yao, Sakata et al. 2009).

Whereas CpG-induced hepatic CD11b+ Ly6C+ myeloid cells supported the expansion of CD8+ T cells ex vivo through OX40-receptor dependent co-stimulation (Huang, Wohlleber et al. 2013). Besides, it has also been documented that CpG while interacting with TLR9 triggered cell signaling cascade resulting in activation of MAP-kinases and transcription factors like NF-κB, IRF-7 and AP1 (Kawai and Akira 2011; Pandey, Kawai et al. 2015). CD11b+ Ly6C+ inflammatory monocytes are recruited to the site of inflammation promoting functional Th1 immune responses during viral infection (Auffray, Sieweke et al. 2009; Iijima, Mattei et al. 2011; Höchst, Mikulec et al. 2015; Song, Zhang et al. 2018). Along the line, it has been reported that Ly6C+

inflammatory monocytes through CCR2-dependent manner triggered type I interferon (IFN-I) and inflammasome activation pathways following recognition of “danger signal”, releasing crucial inflammatory cytokines such as IL-15, IL-18 and IFN-I that facilitated the vaccine-induced memory CD8+ T cells and NK cells. Subsequently, memory CD8+ T cells upregulated CD25, CD69 and CD11a with enhanced effector function manifested by increased levels of IFN-y, GzmB, perforin, T-bet and Eomes (Soudja, Ruiz et al. 2012). Although, CCR2 is not essential for Ly6C+ monocyte maturation, but it is crucial for their emergence from bone marrow and recruitment to the site of inflammation. Whereas, CpG-triggered Ly6C+ inflammatory monocytes also demonstrated strong expression of CD64 while differentiating into DCs. Interestingly, these cells secreted IL-12 that is vital for T cell survival and proliferation despite absence of CD40-signaling (De Koker, Van Hoecke et al. 2017). Thus, T cells could reactivate or re-stimulate through IL-12 and CD28 mediated signaling to exert antiviral immunity (Böttcher, Schanz et al. 2013). Also, it was also revealed that IL-12 increased mitochondrial polarization of HBV-specific CD8+ T cells, which enabled them to trigger oxidative phosphorylation to supplement glycolytic metabolism (Schurich, Pallett et al. 2016). Whereas, other inflammatory cytokines such as IL-1β, IL-6 and TNF-α were also secreted by CpG-triggered Ly6C+ inflammatory monocytes (De Koker, Van Hoecke et al. 2017). These findings further supported the notion that CD11b+ Ly6C+ inflammatory monocytes that are also present within iMATEs structure in liver following CpG application, also supported the ex vivo expansion of activated CD8+ T cells.

5. CONCLUSION

Several therapeutic approaches to cure chronic HBV infections have been adopted so far. Some therapies were tested alone, whereas some of them were evaluated in combination with therapeutic vaccination. In order to devise a combinatorial trial of HBV therapy, a comprehensive understanding is required concerning mechanism of action by therapeutic agents and underlying virologic and immunologic intricacies of chronic HBV infection. The profound knowledge of factors that contribute to T cell exhaustion or limiting the capacity of virus-specific activated-T cells, could also enable us to selectively target virus-specific T cells through direct and indirect immune modulations. While it is also imperative to build our knowledge concerning to the safety of immunotherapy during hepatic inflammation and different phases of HBV infection. The information of immunological events during different phases of chronic HBV infection, such as HBV-antigen expression on hepatocytes, HBV-peptide presentation and mechanisms of antiviral therapy, could be resourceful to assess the extent of T-mediated liver pathology. As, comprehensive insight about collateral damage of immunotherapy would allow us to minimize chronic necro-inflammatory damage and hepatic flares.

To conclude, our findings demonstrated that the combination of therapeutic vaccination followed by iMATEs induction increased functional HBcAg-specific CD8+ T cell responses, leading to the immune control of HBV in two preclinical models of chronic HBV infection. Besides, we also characterized ex vivo the contribution of different intrahepatic myeloid cell populations towards CD8+ T cell expansion. On the one hand, Kupffer cells failed to support CD8+ T cell expansion, on the other hand, CpG-triggered inflammatory myeloid cells enhanced survival and proliferation of CD8+ T cells. Furthermore, in-depth analysis is needed to study myeloid cell – CD8+ T cell crosstalk to identify the underlying mechanisms and overcome hepatic immune tolerance during chronic HBV infection. In short, a novel robust combinatorial antiviral therapy is indispensable, which is also tailored with hepatic immune modulators to boost HBV-specific immunogenicity, rendering safe and life-long immunity against chronic HBV infection.

6. LITERATURE CITED

Albeituni, S. H., et al. (2013). "Hampering the immune suppressors: therapeutic targeting of myeloid-derived suppressor cells (MDSC) in cancer." Cancer journal (Sudbury, Mass.) **19**(6): 490.

Altenburg, A. F., et al. (2014). "Modified vaccinia virus ankara (MVA) as production platform for vaccines against influenza and other viral respiratory diseases." Viruses **6**(7): 2735-2761.

Ando, K., et al. (1994). "Class I-restricted cytotoxic T lymphocytes are directly cytopathic for their target cells in vivo." The Journal of Immunology **152**(7): 3245-3253.

Ando, K., et al. (1993). "Mechanisms of class I restricted immunopathology. A transgenic mouse model of fulminant hepatitis." The Journal of experimental medicine **178**(5): 1541-1554.

Appay, V., et al. (2008). "Phenotype and function of human T lymphocyte subsets: consensus and issues." Cytometry Part A **73**(11): 975-983.

Ashkar, A. A. and K. L. Rosenthal (2002). "Toll-like receptor 9, CpG DNA and innate immunity." Current molecular medicine **2**(6): 545-556.

Auffray, C., et al. (2009). "Blood monocytes: development, heterogeneity, and relationship with dendritic cells." Annual review of immunology **27**: 669-692.

Backes, S., et al. (2016). "Protein-prime/modified vaccinia virus Ankara vector-boost vaccination overcomes tolerance in high-antigenemic HBV-transgenic mice." Vaccine **34**(7): 923-932.

Barnes, E., et al. (2012). "Novel adenovirus-based vaccines induce broad and sustained T cell responses to HCV in man." Science translational medicine **4**(115): 115ra111-115ra111.

Barnett, B. E., et al. (2016). "Cutting edge: B cell–intrinsic T-bet expression is required to control chronic viral infection." The Journal of Immunology **197**(4): 1017-1022.

Beckebaum, S., et al. (2002). "Reduction in the circulating pDC1/pDC2 ratio and impaired function of ex vivo-generated DC1 in chronic hepatitis B infection." Clinical immunology **104**(2): 138-150.

Benbernou, N., et al. (1997). "Differential regulation of IFN-γ, IL-10 and inducible nitric oxide synthase in human T cells by cyclic AMP-dependent signal transduction pathway." Immunology **91**(3): 361-368.

Bengsch, B., et al. (2016). "Bioenergetic insufficiencies due to metabolic alterations regulated by the inhibitory receptor PD-1 are an early driver of CD8+ T cell exhaustion." Immunity **45**(2): 358-373.

6. LITERATURE CITED

Bengsch, B., et al. (2018). "Epigenomic-guided mass cytometry profiling reveals disease-specific features of exhausted CD8 T cells." Immunity **48**(5): 1029-1045. e1025.

Bertoletti, A., et al. (1994). "Cytotoxic T lymphocyte response to a wild type hepatitis B virus epitope in patients chronically infected by variant viruses carrying substitutions within the epitope." The Journal of experimental medicine **180**(3): 933-943.

Bertoletti, A. and C. Ferrari (2012). "Innate and adaptive immune responses in chronic hepatitis B virus infections: towards restoration of immune control of viral infection." Gut **61**(12): 1754-1764.

Bertoletti, A. and C. Ferrari (2016). "Adaptive immunity in HBV infection." Journal of hepatology **64**(1): S71-S83.

Bertoletti, A. and L. Rivino (2014). "Hepatitis B: future curative strategies." Current opinion in infectious diseases **27**(6): 528.

Bertoletti, A., et al. (1994). "Natural variants of cytotoxic epitopes are T-cell receptor antagonists for antiviral cytotoxic T cells." Nature **369**(6479): 407-410.

Bissell, D. M., et al. (1995). "Cell-specific expression of transforming growth factor-beta in rat liver. Evidence for autocrine regulation of hepatocyte proliferation." The Journal of clinical investigation **96**(1): 447-455.

Blackburn, S. D., et al. (2008). "Selective expansion of a subset of exhausted CD8 T cells by αPD-L1 blockade." Proceedings of the National Academy of Sciences **105**(39): 15016-15021.

Blackburn, S. D., et al. (2009). "Coregulation of CD8+ T cell exhaustion by multiple inhibitory receptors during chronic viral infection." Nature immunology **10**(1): 29.

Bode, C., et al. (2011). "CpG DNA as a vaccine adjuvant." Expert review of vaccines **10**(4): 499-511.

Boni, C., et al. (2007). "Characterization of hepatitis B virus (HBV)-specific T-cell dysfunction in chronic HBV infection." Journal of virology **81**(8): 4215-4225.

Boni, C., et al. (2012). "Restored function of HBV-specific T cells after long-term effective therapy with nucleos (t) ide analogues." Gastroenterology **143**(4): 963-973. e969.

Boni, C., et al. (2015). "Natural killer cell phenotype modulation and natural killer/T-cell interplay in nucleos (t) ide analogue-treated hepatitis e antigen-negative patients with chronic hepatitis B." Hepatology **62**(6): 1697-1709.

Boni, C., et al. (2018). "TLR7 Agonist Increases Responses of Hepatitis B Virus–Specific T Cells and Natural Killer Cells in Patients With Chronic Hepatitis B Treated With Nucleos (T) Ide Analogues." Gastroenterology **154**(6): 1764-1777. e1767.

6. LITERATURE CITED

Böttcher, J. P., et al. (2015). "Functional classification of memory CD8+ T cells by CX 3 CR1 expression." Nature communications **6**(1): 1-17.

Böttcher, J. P., et al. (2013). "Liver-primed memory T cells generated under noninflammatory conditions provide anti-infectious immunity." Cell reports **3**(3): 779-795.

Bourgine, M., et al. (2012). "Optimization of immune responses induced by therapeutic vaccination with cross-reactive antigens in a humanized hepatitis B surface antigen transgenic mouse model." Virology **430**(1): 10-19.

Breous, E., et al. (2009). "Hepatic regulatory T cells and Kupffer cells are crucial mediators of systemic T cell tolerance to antigens targeting murine liver." Hepatology **50**(2): 612-621.

Brooks, D. G., et al. (2006). "Interleukin-10 determines viral clearance or persistence in vivo." Nature medicine **12**(11): 1301-1309.

Bucks, C. M., et al. (2009). "Chronic antigen stimulation alone is sufficient to drive CD8+ T cell exhaustion." The Journal of Immunology **182**(11): 6697-6708.

Burton, A. R., et al. (2018). "Circulating and intrahepatic antiviral B cells are defective in hepatitis B." The Journal of clinical investigation **128**(10): 4588-4603.

Cannon, J. P., et al. (2004). "The phylogenetic origins of the antigen-binding receptors and somatic diversification mechanisms." Immunological reviews **200**(1): 12-22.

Chen, M.-H., et al. (2017). "Hepatitis B virus reactivation in rheumatoid arthritis patients undergoing biologics treatment." The Journal of infectious diseases **215**(4): 566-573.

Chisari, F. and C. Ferrari (1995). "Immunopathogenesis of hepatitis B virus." Annu. Rev. Immunol **13**: 29-60.

Chisari, F. V. (1978). "Regulation of human lymphocyte function by a soluble extract from normal human liver." The Journal of Immunology **121**(4): 1279-1286.

Chisari, F. V. (2000). "Viruses, immunity, and cancer: lessons from hepatitis B." The American journal of pathology **156**(4): 1117.

Cooper, C., et al. (2004). "CPG 7909, an immunostimulatory TLR9 agonist oligodeoxynucleotide, as adjuvant to Engerix-B® HBV vaccine in healthy adults: A double-blind phase I/II study." Journal of clinical immunology **24**(6): 693-701.

Cooper, C. and D. Mackie (2011). "Hepatitis B surface antigen-1018 ISS adjuvant-containing vaccine: a review of HEPLISAV™ safety and efficacy." Expert review of vaccines **10**(4): 417-427.

Cooper, S., et al. (1999). "Analysis of a successful immune response against hepatitis C virus." Immunity **10**(4): 439-449.

Crispe, I. N. (2014). "Immune tolerance in liver disease." Hepatology **60**(6): 2109-2117.

Dal-Secco, D., et al. (2015). "A dynamic spectrum of monocytes arising from the in situ reprogramming of CCR2+ monocytes at a site of sterile injury." Journal of Experimental Medicine **212**(4): 447-456.

Das, A., et al. (2008). "Functional skewing of the global CD8 T cell population in chronic hepatitis B virus infection." The Journal of experimental medicine **205**(9): 2111-2124.

Davidson, S., et al. (2015). "Disease-promoting effects of type I interferons in viral, bacterial, and coinfections." Journal of Interferon & Cytokine Research **35**(4): 252-264.

De Koker, S., et al. (2017). "Inflammatory monocytes regulate Th1 oriented immunity to CpG adjuvanted protein vaccines through production of IL-12." Scientific reports **7**(1): 1-14.

Deenick, E. K., et al. (2003). "Stochastic model of T cell proliferation: a calculus revealing IL-2 regulation of precursor frequencies, cell cycle time, and survival." The Journal of Immunology **170**(10): 4963-4972.

Dembek, C. and U. Protzer (2015). "Mouse models for therapeutic vaccination against hepatitis B virus." Medical microbiology and immunology **204**(1): 95-102.

Demeure, C. E., et al. (1997). "Prostaglandin E2 primes naive T cells for the production of anti-inflammatory cytokines." European journal of immunology **27**(12): 3526-3531.

Derby, M. A., et al. (2001). "Two intermediate-avidity cytotoxic T lymphocyte clones with a disparity between functional avidity and MHC tetramer staining." International immunology **13**(6): 817-824.

Desmond, C. P., et al. (2012). "Viral adaptation to host immune responses occurs in chronic hepatitis B virus (HBV) infection, and adaptation is greatest in HBV e antigen-negative disease." Journal of virology **86**(2): 1181-1192.

Dion, S., et al. (2013). "Adeno-associated virus-mediated gene transfer leads to persistent hepatitis B virus replication in mice expressing HLA-A2 and HLA-DR1 molecules." Journal of virology **87**(10): 5554-5563.

DUAN, X. Z., et al. (2005). "Decreased numbers and impaired function of circulating dendritic cell subsets in patients with chronic hepatitis B infection (R2)." Journal of gastroenterology and hepatology **20**(2): 234-242.

Dunn, C., et al. (2007). "Cytokines induced during chronic hepatitis B virus infection promote a pathway for NK cell–mediated liver damage." The Journal of experimental medicine **204**(3): 667-680.

Dunn, C., et al. (2009). "Temporal analysis of early immune responses in patients with acute hepatitis B virus infection." Gastroenterology **137**(4): 1289-1300.

Ejrnaes, M., et al. (2006). "Resolution of a chronic viral infection after interleukin-10 receptor blockade." The Journal of experimental medicine **203**(11): 2461-2472.

6. LITERATURE CITED

El-Khoueiry, A. B., et al. (2017). "Nivolumab in patients with advanced hepatocellular carcinoma (CheckMate 040): an open-label, non-comparative, phase 1/2 dose escalation and expansion trial." The Lancet **389**(10088): 2492-2502.

Elvidge, S. (2015). Blockbuster expectations for hepatitis B therapeutic vaccine, Nature Publishing Group.

Epelman, S., et al. (2014). "Origin and functions of tissue macrophages." Immunity **41**(1): 21-35.

Ferrari, C., et al. (2017). "T cell regulation in HBV-related chronic liver disease." Journal of hepatology **66**(5): 1096-1098.

Ferrari, C., et al. (1990). "Cellular immune response to hepatitis B virus-encoded antigens in acute and chronic hepatitis B virus infection." The Journal of Immunology **145**(10): 3442-3449.

Ferri, S., et al. (2010). "A multifaceted imbalance of T cells with regulatory function characterizes type 1 autoimmune hepatitis." Hepatology **52**(3): 999-1007.

Fioravanti, J., et al. (2017). "Effector CD8+ T cell-derived interleukin-10 enhances acute liver immunopathology." Journal of hepatology **67**(3): 543-548.

Fisicaro, P., et al. (2017). "Targeting mitochondrial dysfunction can restore antiviral activity of exhausted HBV-specific CD8 T cells in chronic hepatitis B." Nature medicine **23**(3): 327.

Fisicaro, P., et al. (2010). "Antiviral intrahepatic T-cell responses can be restored by blocking programmed death-1 pathway in chronic hepatitis B." Gastroenterology **138**(2): 682-693. e684.

Foster, D. N. and L. K. Foster (1997). Immortalized cell lines for virus growth, Google Patents.

Fukuda, R., et al. (1995). "Gene Expression of Perforin and Granzyme A in the Liver in Chronic Hepatitis C." Microbiology and immunology **39**(11): 873-877.

Gane, E., et al. (2019). "Anti-PD-1 blockade with nivolumab with and without therapeutic vaccination for virally suppressed chronic hepatitis B: a pilot study." Journal of hepatology **71**(5): 900-907.

Gane, E. J., et al. (2010). "The mitochondria-targeted anti-oxidant mitoquinone decreases liver damage in a phase II study of hepatitis C patients." Liver international **30**(7): 1019-1026.

Gao, B., et al. (2008). "Liver: an organ with predominant innate immunity." Hepatology **47**(2): 729-736.

Gehring, A. J., et al. (2013). "Mobilizing monocytes to cross-present circulating viral antigen in chronic infection." The Journal of clinical investigation **123**(9): 3766-3776.

Geiger, R., et al. (2016). "L-arginine modulates T cell metabolism and enhances survival and anti-tumor activity." Cell **167**(3): 829-842. e813.

Gerlach, C., et al. (2016). "The chemokine receptor CX3CR1 defines three antigen-experienced CD8 T cell subsets with distinct roles in immune surveillance and homeostasis." Immunity **45**(6): 1270-1284.

Gish, R., et al. (2012). "Selection of chronic hepatitis B therapy with high barrier to resistance." The Lancet infectious diseases **12**(4): 341-353.

Gish, R. G., et al. (2015). "Chronic hepatitis B: virology, natural history, current management and a glimpse at future opportunities." Antiviral research **121**: 47-58.

Goel, A. and C. R. Boland (2012). "Epigenetics of colorectal cancer." Gastroenterology **143**(6): 1442-1460. e1441.

Guidotti, L. G., et al. (1994). "Cytotoxic T lymphocytes inhibit hepatitis B virus gene expression by a noncytolytic mechanism in transgenic mice." Proceedings of the National Academy of Sciences **91**(9): 3764-3768.

Guidotti, L. G., et al. (1999). "Noncytopathic clearance of lymphocytic choriomeningitis virus from the hepatocyte." The Journal of experimental medicine **189**(10): 1555-1564.

Guidotti, L. G. and F. V. Chisari (1999). "Cytokine-induced viral purging—role in viral pathogenesis." Current opinion in microbiology **2**(4): 388-391.

Guidotti, L. G. and F. V. Chisari (2000). "Cytokine-mediated control of viral infections." Virology **273**(2): 221-227.

Guidotti, L. G. and F. V. Chisari (2001). "Noncytolytic control of viral infections by the innate and adaptive immuneresponse." Annual review of immunology **19**(1): 65-91.

Guidotti, L. G., et al. (1996). "Intracellular inactivation of the hepatitis B virus by cytotoxic T lymphocytes." Immunity **4**(1): 25-36.

Guidotti, L. G., et al. (1999). "Viral clearance without destruction of infected cells during acute HBV infection." Science **284**(5415): 825-829.

Ha, S.-J., et al. (2008). "Enhancing therapeutic vaccination by blocking PD-1–mediated inhibitory signals during chronic infection." The Journal of experimental medicine **205**(3): 543-555.

Hammerich, L. and F. Tacke (2014). "Role of gamma-delta T cells in liver inflammation and fibrosis." World journal of gastrointestinal pathophysiology **5**(2): 107.

Hemmi, H., et al. (2000). "A Toll-like receptor recognizes bacterial DNA." Nature **408**(6813): 740-745.

Heymann, F., et al. (2015). "Liver inflammation abrogates immunological tolerance induced by Kupffer cells." Hepatology **62**(1): 279-291.

Heymann, F. and F. Tacke (2016). "Immunology in the liver—from homeostasis to disease." Nature reviews Gastroenterology & hepatology **13**(2): 88.

Höchst, B., et al. (2015). "Differential induction of Ly6G and Ly6C positive myeloid derived suppressor cells in chronic kidney and liver inflammation and fibrosis." PloS one **10**(3).

Hoofnagle, J. H., et al. (1988). "Randomized, controlled trial of recombinant human α-interferon in patients with chronic hepatitis B." Gastroenterology **95**(5): 1318-1325.

Hoogeveen, R. C., et al. (2019). "Phenotype and function of HBV-specific T cells is determined by the targeted epitope in addition to the stage of infection." Gut **68**(5): 893-904.

Huang, L.-R., et al. (2013). "Intrahepatic myeloid-cell aggregates enable local proliferation of CD8+ T cells and successful immunotherapy against chronic viral liver infection." Nature immunology **14**(6): 574.

Huang, L.-R., et al. (2006). "An immunocompetent mouse model for the tolerance of human chronic hepatitis B virus infection." Proceedings of the National Academy of Sciences **103**(47): 17862-17867.

Huang, W.-C., et al. (2017). "T cells infiltrating diseased liver express ligands for the NKG2D stress surveillance system." The Journal of Immunology **198**(3): 1172-1182.

Iijima, N., et al. (2011). "Recruited inflammatory monocytes stimulate antiviral Th1 immunity in infected tissue." Proceedings of the National Academy of Sciences **108**(1): 284-289.

Ilkovitch, D. and D. M. Lopez (2009). "The liver is a site for tumor-induced myeloid-derived suppressor cell accumulation and immunosuppression." Cancer research **69**(13): 5514-5521.

Iñarrairaegui, M., et al. (2018). "Immunotherapy of hepatocellular carcinoma: facts and hopes." Clinical Cancer Research **24**(7): 1518-1524.

Ishizuka, A. S., et al. (2016). "Protection against malaria at 1 year and immune correlates following PfSPZ vaccination." Nature medicine **22**(6): 614.

Isogawa, M., et al. (2005). "Oscillating CD8+ T cell effector functions after antigen recognition in the liver." Immunity **23**(1): 53-63.

Ito, H., et al. (2010). "Ability of IDO To Attenuate Liver Injury in α-Galactosylceramide–Induced Hepatitis Model." The Journal of Immunology **185**(8): 4554-4560.

Iwai, Y., et al. (2003). "PD-1 inhibits antiviral immunity at the effector phase in the liver." The Journal of experimental medicine **198**(1): 39-50.

Jacob, A. I., et al. (1977). "Endotoxin and bacteria in portal blood." Gastroenterology **72**(6): 1268-1270.

6. LITERATURE CITED

Janeway Jr, C. A. and K. Bottomly (1994). "Signals and signs for lymphocyte responses." Cell **76**(2): 275-285.

Janssen, H. L., et al. (2018). "Safety, efficacy and pharmacodynamics of vesatolimod (GS-9620) in virally suppressed patients with chronic hepatitis B." Journal of hepatology **68**(3): 431-440.

Jia, H., et al. (2016). "Therapeutic injection of a C-type CpG ODN induced an antitumor immune response in C57/BL6 mice of orthotopically transplanted hepatocellular carcinoma." Oncology Research Featuring Preclinical and Clinical Cancer Therapeutics **23**(6): 321-326.

June, C. H., et al. (1994). "The B7 and CD28 receptor families." Immunology today **15**(7): 321-331.

Kakimi, K., et al. (2001). "Blocking chemokine responsive to γ–2/Interferon (IFN)-γ inducible protein and monokine induced by IFN-γ activity in vivo reduces the pathogenetic but not the antiviral potential of Hepatitis B Virus–specific cytotoxic T lymphocytes." The Journal of experimental medicine **194**(12): 1755-1766.

Kawai, T. and S. Akira (2011). "Toll-like receptors and their crosstalk with other innate receptors in infection and immunity." Immunity **34**(5): 637-650.

Kefalakes, H., et al. (2015). "Adaptation of the hepatitis B virus core protein to CD8+ T-cell selection pressure." Hepatology **62**(1): 47-56.

Kelly, C., et al. (2016). "Chronic hepatitis C viral infection subverts vaccine-induced T-cell immunity in humans." Hepatology **63**(5): 1455-1470.

Khakpoor, A., et al. (2019). "Spatiotemporal differences in presentation of CD8 T cell epitopes during hepatitis B virus infection." Journal of virology **93**(4): e01457-01418.

Knoll, P., et al. (1995). "Human Kupffer cells secrete IL-10 in response to lipopolysaccharide (LPS) challenge." Journal of hepatology **22**(2): 226-229.

Knolle, P. A. and R. Thimme (2014). "Hepatic immune regulation and its involvement in viral hepatitis infection." Gastroenterology **146**(5): 1193-1207.

Knolle, P. A., et al. (1998). "Interleukin-10 expression is autoregulated at the transcriptional level in human and murine kupffer cells." Hepatology **27**(1): 93-99.

Knox, J. J., et al. (2017). "T-bet+ B cells are induced by human viral infections and dominate the HIV gp140 response." JCI insight **2**(8).

Kosinska, A. D., et al. (2017). "Therapeutic vaccination for chronic hepatitis B." Current opinion in virology **23**: 75-81.

Kraaij, M. D., et al. (2010). "Induction of regulatory T cells by macrophages is dependent on production of reactive oxygen species." Proceedings of the National Academy of Sciences **107**(41): 17686-17691.

6. LITERATURE CITED

Kremer, M., et al. (2012). Easy and efficient protocols for working with recombinant vaccinia virus MVA. Vaccinia Virus and Poxvirology, Springer**:** 59-92.

Krieg, A. M. (2006). "Therapeutic potential of Toll-like receptor 9 activation." Nature reviews Drug discovery **5**(6): 471-484.

Krieg, A. M., et al. (1995). "CpG motifs in bacterial DNA trigger direct B-cell activation." Nature **374**(6522): 546-549.

Kumar, B. V., et al. (2017). "Human tissue-resident memory T cells are defined by core transcriptional and functional signatures in lymphoid and mucosal sites." Cell reports **20**(12): 2921-2934.

Kurktschiev, P. D., et al. (2014). "Dysfunctional CD8+ T cells in hepatitis B and C are characterized by a lack of antigen-specific T-bet induction." Journal of Experimental Medicine **211**(10): 2047-2059.

Lang, P. A., et al. (2012). "Natural killer cell activation enhances immune pathology and promotes chronic infection by limiting CD8+ T-cell immunity." Proceedings of the National Academy of Sciences **109**(4): 1210-1215.

Le Bon, A., et al. (2003). "Cross-priming of CD8+ T cells stimulated by virus-induced type I interferon." Nature immunology **4**(10): 1009-1015.

Lechner, F., et al. (2000). "Analysis of successful immune responses in persons infected with hepatitis C virus." The Journal of experimental medicine **191**(9): 1499-1512.

Levings, M. K., et al. (2002). "The role of IL-10 and TGF-β in the differentiation and effector function of T regulatory cells." International archives of allergy and immunology **129**(4): 263-276.

Levrero, M., et al. (2016). "HBV cure: why, how, when?" Current opinion in virology **18**: 135-143.

Li, J., et al. (2007). "Transfer of in vitro expanded T lymphocytes after activation with dendritomas prolonged survival of mice challenged with EL4 tumor cells." International journal of oncology **31**(1): 193-197.

Lim, S. G., et al. (2019). "Therapeutic vaccination for chronic hepatitis B: A systematic review and meta-analysis." Journal of viral hepatitis **26**(7): 803-817.

Lin, Y.-C., et al. (2018). "Induction of liver-specific intrahepatic myeloid cells aggregation expands CD8 T cell and inhibits growth of murine hepatoma." Oncoimmunology **7**(12): e1502129.

Lin, Y.-J., et al. (2010). "Hepatitis B virus core antigen determines viral persistence in a C57BL/6 mouse model." Proceedings of the National Academy of Sciences **107**(20): 9340-9345.

Liu, J., et al. (2014). "Enhancing virus-specific immunity in vivo by combining therapeutic vaccination and PD-L1 blockade in chronic hepadnaviral infection." PLoS pathogens **10**(1).

Liu, K. H., et al. (2011). "Electroporation enhances immunogenicity of a DNA vaccine expressing woodchuck hepatitis virus surface antigen in woodchucks." Journal of virology **85**(10): 4853-4862.

Lopes, A. R., et al. (2008). "Bim-mediated deletion of antigen-specific CD8+ T cells in patients unable to control HBV infection." The Journal of clinical investigation **118**(5): 1835-1845.

Lucifora, J., et al. (2014). "Specific and nonhepatotoxic degradation of nuclear hepatitis B virus cccDNA." Science **343**(6176): 1221-1228.

Lumley, S., et al. (2016). "Hepitopes: a live interactive database of HLA class I epitopes in hepatitis B virus." Wellcome open research **1**.

Maier, H., et al. (2007). "PD-1: PD-L1 interactions contribute to the functional suppression of virus-specific CD8+ T lymphocytes in the liver." The Journal of Immunology **178**(5): 2714-2720.

Maini, M., et al. (2012). "IL-10-producing regulatory B cells in the pathogenesis of chronic hepatitis B virus infection."

Maini, M. K., et al. (2000). "The role of virus-specific CD8+ cells in liver damage and viral control during persistent hepatitis B virus infection." The Journal of experimental medicine **191**(8): 1269-1280.

Maini, M. K., et al. (1999). "Direct ex vivo analysis of hepatitis B virus-specific CD8+ T cells associated with the control of infection." Gastroenterology **117**(6): 1386-1396.

Maini, M. K. and A. R. Burton (2019). "Restoring, releasing or replacing adaptive immunity in chronic hepatitis B." Nature reviews Gastroenterology & hepatology **16**(11): 662-675.

Maini, M. K. and L. J. Pallett (2018). "Defective T-cell immunity in hepatitis B virus infection: why therapeutic vaccination needs a helping hand." The Lancet Gastroenterology & Hepatology **3**(3): 192-202.

Margulies, D. H. (2001). "TCR avidity: it's not how strong you make it, it's how you make it strong." Nature immunology **2**(8): 669-670.

Marinos, G., et al. (1995). "Induction of T-helper cell response to hepatitis B core antigen in chronic hepatitis B: a major factor in activation of the host immune response to the hepatitis B virus." Hepatology **22**(4): 1040-1049.

Martin, P., et al. (2015). "TG1050, an immunotherapeutic to treat chronic hepatitis B, induces robust T cells and exerts an antiviral effect in HBV-persistent mice." Gut **64**(12): 1961-1971.

6. LITERATURE CITED

Masteller, E. L., et al. (2005). "Expansion of functional endogenous antigen-specific CD4+ CD25+ regulatory T cells from nonobese diabetic mice." The Journal of Immunology **175**(5): 3053-3059.

Medina-Echeverz, J., et al. (2015). "Hepatic myeloid-derived suppressor cells in cancer." Cancer Immunology, Immunotherapy **64**(8): 931-940.

Moriyama, T., et al. (1990). "Immunobiology and pathogenesis of hepatocellular injury in hepatitis B virus transgenic mice." Science **248**(4953): 361-364.

Mueller, S. N. and R. Ahmed (2009). "High antigen levels are the cause of T cell exhaustion during chronic viral infection." Proceedings of the National Academy of Sciences **106**(21): 8623-8628.

Mühlbauer, M., et al. (2006). "PD-L1 is induced in hepatocytes by viral infection and by interferon-α and-γ and mediates T cell apoptosis." Journal of hepatology **45**(4): 520-528.

Mullbacher, A. and P. Waring (1999). "Tha Hla R, Tran T, Chin S, Stehle T, Museteanu C, Simon MM. Granzymes are the essential downstream effector molecules for the control of primary virus infections by cytolytic leukocytes." Proc Natl Acad Sci USA **96**(24): 13950-13955.

Nair, S. and R. P. Perrillo (2001). "Serum alanine aminotransferase flares during interferon treatment of chronic hepatitis B: is sustained clearance of HBV DNA dependent on levels of pretreatment viremia?" Hepatology **34**(5): 1021-1026.

Najjar, Y. G. and J. H. Finke (2013). "Clinical perspectives on targeting of myeloid derived suppressor cells in the treatment of cancer." Frontiers in oncology **3**: 49.

Nakamoto, Y., et al. (1997). "Differential target cell sensitivity to CTL-activated death pathways in hepatitis B virus transgenic mice." The Journal of Immunology **158**(12): 5692-5697.

Nebbia, G., et al. (2012). "Upregulation of the Tim-3/galectin-9 pathway of T cell exhaustion in chronic hepatitis B virus infection." PloS one **7**(10).

Ochel, A., et al. (2016). "Effective intrahepatic CD8+ T-cell immune responses are induced by low but not high numbers of antigen-expressing hepatocytes." Cellular & molecular immunology **13**(6): 805-815.

Odorizzi, P. M., et al. (2015). "Genetic absence of PD-1 promotes accumulation of terminally differentiated exhausted CD8+ T cells." Journal of Experimental Medicine **212**(7): 1125-1137.

Otano, I., et al. (2018). "Molecular recalibration of PD-1+ antigen-specific T cells from blood and liver." Molecular Therapy **26**(11): 2553-2566.

Paley, M. A., et al. (2012). "Progenitor and terminal subsets of CD8+ T cells cooperate to contain chronic viral infection." Science **338**(6111): 1220-1225.

Pallett, L. J., et al. (2017). "IL-2high tissue-resident T cells in the human liver: Sentinels for hepatotropic infection." Journal of Experimental Medicine **214**(6): 1567-1580.

Pallett, L. J., et al. (2015). "Metabolic regulation of hepatitis B immunopathology by myeloid-derived suppressor cells." Nature medicine **21**(6): 591.

Pandey, S., et al. (2015). "Microbial sensing by Toll-like receptors and intracellular nucleic acid sensors." Cold Spring Harbor perspectives in biology **7**(1): a016246.

Park, J.-J., et al. (2016). "Hepatitis B virus–specific and global T-cell dysfunction in chronic hepatitis B." Gastroenterology **150**(3): 684-695. e685.

Pauken, K. E., et al. (2016). "Epigenetic stability of exhausted T cells limits durability of reinvigoration by PD-1 blockade." Science **354**(6316): 1160-1165.

Paul, S., et al. (2017). "Role of surface antibody in hepatitis B reactivation in patients with resolved infection and hematologic malignancy: a meta-analysis." Hepatology **66**(2): 379-388.

Penna, A., et al. (2007). "Dysfunction and functional restoration of HCV-specific CD8 responses in chronic hepatitis C virus infection." Hepatology **45**(3): 588-601.

Peppa, D., et al. (2013). "Up-regulation of a death receptor renders antiviral T cells susceptible to NK cell–mediated deletion." Journal of Experimental Medicine **210**(1): 99-114.

Peppa, D., et al. (2010). "Blockade of immunosuppressive cytokines restores NK cell antiviral function in chronic hepatitis B virus infection." PLoS pathogens **6**(12).

Racanelli, V. and B. Rehermann (2006). "The liver as an immunological organ." Hepatology **43**(S1): S54-S62.

Raziorrouh, B., et al. (2010). "The immunoregulatory role of CD244 in chronic hepatitis B infection and its inhibitory potential on virus-specific CD8+ T-cell function." Hepatology **52**(6): 1934-1947.

Rehermann, B., et al. (1996). "The hepatitis B virus persists for decades after patients' recovery from acute viral hepatitis despite active maintenance of a cytotoxic T–lymphocyte response." Nature medicine **2**(10): 1104-1108.

Rehermann, B., et al. (1995). "Hepatitis B virus (HBV) sequence variation of cytotoxic T lymphocyte epitopes is not common in patients with chronic HBV infection." The Journal of clinical investigation **96**(3): 1527-1534.

Rehermann, B. and R. Thimme (2019). "Insights from antiviral therapy into immune responses to hepatitis B and C virus infection." Gastroenterology **156**(2): 369-383.

Reignat, S., et al. (2002). "Escaping high viral load exhaustion: CD8 cells with altered tetramer binding in chronic hepatitis B virus infection." The Journal of experimental medicine **195**(9): 1089-1101.

Rubio-Godoy, V., et al. (2001). "Discrepancy between ELISPOT IFN-γ secretion and binding of A2/peptide multimers to TCR reveals interclonal dissociation of CTL effector function from TCR-peptide/MHC complexes half-life." Proceedings of the National Academy of Sciences **98**(18): 10302-10307.

Rubtsova, K., et al. (2013). "T-box transcription factor T-bet, a key player in a unique type of B-cell activation essential for effective viral clearance." Proceedings of the National Academy of Sciences **110**(34): E3216-E3224.

Sad, S. and T. R. Mosmann (1994). "Single IL-2-secreting precursor CD4 T cell can develop into either Th1 or Th2 cytokine secretion phenotype." The Journal of Immunology **153**(8): 3514-3522.

Salimzadeh, L., et al. (2018). "PD-1 blockade partially recovers dysfunctional virus–specific B cells in chronic hepatitis B infection." The Journal of clinical investigation **128**(10): 4573-4587.

Sandalova, E., et al. (2012). "Increased levels of arginase in patients with acute hepatitis B suppress antiviral T cells." Gastroenterology **143**(1): 78-87. e73.

Scharping, N. E., et al. (2016). "The tumor microenvironment represses T cell mitochondrial biogenesis to drive intratumoral T cell metabolic insufficiency and dysfunction." Immunity **45**(2): 374-388.

Schuch, A., et al. (2019). "Phenotypic and functional differences of HBV core-specific versus HBV polymerase-specific CD8+ T cells in chronically HBV-infected patients with low viral load." Gut **68**(5): 905-915.

Schuch, A., et al. (2014). "The role of natural killer cells and CD8+ T cells in hepatitis B virus infection." Frontiers in immunology **5**: 258.

Schulz, O., et al. (2005). "Toll-like receptor 3 promotes cross-priming to virus-infected cells." Nature **433**(7028): 887-892.

Schurich, A., et al. (2011). "Role of the coinhibitory receptor cytotoxic T lymphocyte antigen-4 on apoptosis-Prone CD8 T cells in persistent hepatitis B virus infection." Hepatology **53**(5): 1494-1503.

Schurich, A., et al. (2016). "Distinct metabolic requirements of exhausted and functional virus-specific CD8 T cells in the same host." Cell reports **16**(5): 1243-1252.

Schurich, A., et al. (2013). "The third signal cytokine IL-12 rescues the anti-viral function of exhausted HBV-specific CD8 T cells." PLoS pathogens **9**(3).

Schwartz, R., et al. (1989). T-cell clonal anergy. Cold Spring Harbor Symposia on Quantitative Biology, Cold Spring Harbor Laboratory Press.

Scott, C. L., et al. (2016). "Bone marrow-derived monocytes give rise to self-renewing and fully differentiated Kupffer cells." Nature communications **7**: 10321.

Sen, D. R., et al. (2016). "The epigenetic landscape of T cell exhaustion." Science **354**(6316): 1165-1169.

Shahinian, A., et al. (1993). "Differential T cell costimulatory requirements in CD28-deficient mice." Science **261**(5121): 609-612.

Shi, T.-D., et al. (2004). "Therapeutic polypeptides based on HBV core 18-27 epitope can induce CD8+ CTL-mediated cytotoxicity in HLA-A2+ human PBMCs." World journal of gastroenterology: WJG **10**(13): 1902.

Shresta, S., et al. (1998). "How do cytotoxic lymphocytes kill their targets?" Current opinion in immunology **10**(5): 581-587.

Singh, H. D., et al. (2017). "TRAIL regulatory receptors constrain human hepatic stellate cell apoptosis." Scientific reports **7**(1): 1-11.

Slifka, M. K. and J. L. Whitton (2001). "Functional avidity maturation of CD8+ T cells without selection of higher affinity TCR." Nature immunology **2**(8): 711-717.

Song, P., et al. (2018). "Hepatic recruitment of CD11b+ Ly6C+ inflammatory monocytes promotes hepatic ischemia/reperfusion injury." International journal of molecular medicine **41**(2): 935-945.

Soudja, S. M. H., et al. (2012). "Inflammatory monocytes activate memory CD8+ T and innate NK lymphocytes independent of cognate antigen during microbial pathogen invasion." Immunity **37**(3): 549-562.

Stanaway, J. D., et al. (2016). "The global burden of viral hepatitis from 1990 to 2013: findings from the Global Burden of Disease Study 2013." The Lancet **388**(10049): 1081-1088.

Stegmann, K. A., et al. (2016). "CXCR6 marks a novel subset of T-bet lo Eomes hi natural killer cells residing in human liver." Scientific reports **6**(1): 1-10.

Stoop, J. N., et al. (2005). "Regulatory T cells contribute to the impaired immune response in patients with chronic hepatitis B virus infection." Hepatology **41**(4): 771-778.

Streeck, H., et al. (2008). "Antigen load and viral sequence diversification determine the functional profile of HIV-1–specific CD8+ T cells." PLoS medicine **5**(5).

Stross, L., et al. (2012). "Foxp3+ regulatory T cells protect the liver from immune damage and compromise virus control during acute experimental hepatitis B virus infection in mice." Hepatology **56**(3): 873-883.

Sun, J., et al. (2009). "Effector T cells control lung inflammation during acute influenza virus infection by producing IL-10." Nature medicine **15**(3): 277.

Swadling, L., et al. (2014). "A human vaccine strategy based on chimpanzee adenoviral and MVA vectors that primes, boosts, and sustains functional HCV-specific T cell memory." Science translational medicine **6**(261): 261ra153-261ra153.

Swadling, L., et al. (2016). "Highly-immunogenic virally-vectored T-cell vaccines cannot overcome subversion of the T-cell response by HCV during chronic infection." Vaccines **4**(3): 27.

Swain, S. L., et al. (1996). "From naive to memory T cells." Immunological reviews **150**(1): 143-167.

Tang, T. J., et al. (2003). "The role of intrahepatic immune effector cells in inflammatory liver injury and viral control during chronic hepatitis B infection." Journal of viral hepatitis **10**(3): 159-167.

Tang, T. J., et al. (2005). "Intrahepatic CD8+ T-lymphocyte response is important for therapy-induced viral clearance in chronic hepatitis B infection." Journal of hepatology **43**(1): 45-52.

Taubert, R., et al. (2014). "Intrahepatic regulatory T cells in autoimmune hepatitis are associated with treatment response and depleted with current therapies." Journal of hepatology **61**(5): 1106-1114.

Thimme, R., et al. (2002). "Viral and immunological determinants of hepatitis C virus clearance, persistence, and disease." Proceedings of the National Academy of Sciences **99**(24): 15661-15668.

Thimme, R., et al. (2001). "Determinants of viral clearance and persistence during acute hepatitis C virus infection." The Journal of experimental medicine **194**(10): 1395-1406.

Thimme, R., et al. (2003). "CD8+ T cells mediate viral clearance and disease pathogenesis during acute hepatitis B virus infection." Journal of virology **77**(1): 68-76.

Thomson, A. W. and P. A. Knolle (2010). "Antigen-presenting cell function in the tolerogenic liver environment." Nature Reviews Immunology **10**(11): 753.

Tiegs, G. and A. W. Lohse (2010). "Immune tolerance: what is unique about the liver." Journal of autoimmunity **34**(1): 1-6.

Titanji, K., et al. (2010). "Acute depletion of activated memory B cells involves the PD-1 pathway in rapidly progressing SIV-infected macaques." The Journal of clinical investigation **120**(11): 3878-3890.

Utzschneider, D. T., et al. (2016). "High antigen levels induce an exhausted phenotype in a chronic infection without impairing T cell expansion and survival." Journal of Experimental Medicine **213**(9): 1819-1834.

Utzschneider, D. T., et al. (2018). "Active maintenance of T cell memory in acute and chronic viral infection depends on continuous expression of FOXO1." Cell reports **22**(13): 3454-3467.

Utzschneider, D. T., et al. (2013). "T cells maintain an exhausted phenotype after antigen withdrawal and population reexpansion." Nature immunology **14**(6): 603.

van der Molen, R. G., et al. (2004). "Functional impairment of myeloid and plasmacytoid dendritic cells of patients with chronic hepatitis B." Hepatology **40**(3): 738-746.

Veiga-Fernandes, H., et al. (2000). "Response of naive and memory CD8+ T cells to antigen stimulation in vivo." Nature immunology **1**(1): 47-53.

Vollmer, J. and A. M. Krieg (2009). "Immunotherapeutic applications of CpG oligodeoxynucleotide TLR9 agonists." Advanced drug delivery reviews **61**(3): 195-204.

Volpes, R., et al. (1991). "Memory T cells represent the predominant lymphocyte subset in acute and chronic liver inflammation." Hepatology **13**(5): 826-829.

von Buttlar, H., et al. (2014). "Identification of toll-like receptor 9 as parapoxvirus ovis-sensing receptor in plasmacytoid dendritic cells." PloS one **9**(8).

Waggoner, S. N., et al. (2012). "Natural killer cells act as rheostats modulating antiviral T cells." Nature **481**(7381): 394-398.

Wagner, H. (1999). Bacterial CpG DNA activates immune cells to signal infectious danger. Advances in immunology, Elsevier. **73:** 329-368.

Wahl, C., et al. (2008). "B7-H1 on hepatocytes facilitates priming of specific CD8 T cells but limits the specific recall of primed responses." Gastroenterology **135**(3): 980-988.

Wang, F.-S., et al. (2001). "Dysfunction of peripheral blood dendritic cells from patients with chronic hepatitis B virus infection." World journal of gastroenterology **7**(4): 537.

Wang, Y., et al. (2018). "A proteomics landscape of circadian clock in mouse liver." Nature communications **9**(1): 1-16.

Webster, G. J., et al. (2004). "Longitudinal analysis of CD8+ T cells specific for structural and nonstructural hepatitis B virus proteins in patients with chronic hepatitis B: implications for immunotherapy." Journal of virology **78**(11): 5707-5719.

Webster, G. J., et al. (2000). "Incubation phase of acute hepatitis B in man: dynamic of cellular immune mechanisms." Hepatology **32**(5): 1117-1124.

Wedemeyer, H., et al. (2002). "Impaired effector function of hepatitis C virus-specific CD8+ T cells in chronic hepatitis C virus infection." The Journal of Immunology **169**(6): 3447-3458.

Welsh, R. M. (2001). "Assessing CD8 T cell number and dysfunction in the presence of antigen." The Journal of experimental medicine **193**(5): F19-F22.

Wherry, E. J., et al. (2007). "Molecular signature of CD8+ T cell exhaustion during chronic viral infection." Immunity **27**(4): 670-684.

Wherry, E. J. and M. Kurachi (2015). "Molecular and cellular insights into T cell exhaustion." Nature Reviews Immunology **15**(8): 486-499.

Wieland, D., et al. (2017). "TCF1+ hepatitis C virus-specific CD8+ T cells are maintained after cessation of chronic antigen stimulation." Nature communications **8**(1): 1-13.

Wu, W., et al. (2012). "Blockade of T im-3 signaling restores the virus-specific CD 8+ T-cell response in patients with chronic hepatitis B." European journal of immunology **42**(5): 1180-1191.

Xia, Y., et al. (2016). "Interferon-γ and tumor necrosis factor-α produced by T cells reduce the HBV persistence form, cccDNA, without cytolysis." Gastroenterology **150**(1): 194-205.

Xu, D., et al. (2006). "Circulating and liver resident CD4+ CD25+ regulatory T cells actively influence the antiviral immune response and disease progression in patients with hepatitis B." The Journal of Immunology **177**(1): 739-747.

Xu, W., et al. (2005). "Endoplasmic reticulum targeting sequence enhances HBV-specific cytotoxic T lymphocytes induced by a CTL epitope-based DNA vaccine." Virology **334**(2): 255-263.

Xue, J., et al. (2014). "Transcriptome-based network analysis reveals a spectrum model of human macrophage activation." Immunity **40**(2): 274-288.

Yan, M.-L., et al. (2010). "Inhibition of allogeneic T-cell response by Kupffer cells expressing indoleamine 2, 3-dioxygenase." World journal of gastroenterology: WJG **16**(5): 636.

Yang, D., et al. (2014). "A mouse model for HBV immunotolerance and immunotherapy." Cellular & molecular immunology **11**(1): 71-78.

Yang, G., et al. (2007). "Association of CD4+ CD25+ Foxp3+ regulatory T cells with chronic activity and viral clearance in patients with hepatitis B." International immunology **19**(2): 133-140.

Yang, P. L., et al. (2010). "Immune effectors required for hepatitis B virus clearance." Proceedings of the National Academy of Sciences **107**(2): 798-802.

Yao, C., et al. (2009). "Prostaglandin E 2–EP4 signaling promotes immune inflammation through T H 1 cell differentiation and T H 17 cell expansion." Nature medicine **15**(6): 633.

You, Q., et al. (2008). "Mechanism of T cell tolerance induction by murine hepatic Kupffer cells." Hepatology **48**(3): 978-990.

Zeisel, M. B., et al. (2015). "Towards an HBV cure: state-of-the-art and unresolved questions—report of the ANRS workshop on HBV cure." Gut **64**(8): 1314-1326.

Zhang, M., et al. (2011). "Apoptotic cells attenuate fulminant hepatitis by priming Kupffer cells to produce interleukin-10 through membrane-bound TGF-β." Hepatology **53**(1): 306-316.

Zhang, Y., et al. (2007). "Hepatitis B virus core antigen epitopes presented by HLA-A2 single-chain trimers induce functional epitope-specific CD8+ T-cell responses in HLA-A2· 1/Kb transgenic mice." Immunology **121**(1): 105-112.

Zhou, W., et al. (2009). "FoxO4 inhibits NF-κB and protects mice against colonic injury and inflammation." Gastroenterology **137**(4): 1403-1414.

7. PUBLICATION AND POSTER PRESENTATION

7.1 Publication

Kosinska AD, **Moeed A**, Kallin N, Festag J, Su J, Steiger K, Michel ML, Protzer U, Knolle PA. Synergy of therapeutic heterologous prime-boost hepatitis B vaccination with CpG-application to improve immune control of persistent HBV infection. *Scientific reports*. 2019 Jul 25;9(1):1-0.

7.2 Poster presentation

Moeed A, Kosinska AD, Kallin N, Yassin AA, Baumann T, Knolle PA, Protzer U. Characterization of hepatic myeloid cell contribution to increase CD8 T cell immunity and boost vaccination efficiency against experimental chronic HBV infection. *Intl. HBV Meeting Melbourne*. 2019 Oct 1-5.

8. LIST OF ILLUSTRATIONS AND FIGURES

8.1 Illustrations

8.2 Figures

8. LIST OF ILLUSTRATIONS AND FIGURES

9. LIST OF ABBREVIATIONS

(s)ALT	(Serum) Alaninaminotransferase
2B4	Natural Killer cell receptor
AAV	Adeno-associated virus
AAV-HBV	Adeno-associated viral vector carrying HBV antigens
ACK	Ammonium-Chloride-Potassium
Ag	Antigen
ANOVA	Analysis of variance
anti- / a-	Antibodies
APCs	Antigen presenting cells
AST	Aspartate aminotransferase
Bcl-2	B-cell lymphoma 2
Bim	Bcl-2-interacting mediator of cell death
BSA	Bovine serum albumin
BSL	Biosafety level
c-di-AMP	Bis-(3'-5')-cyclic dimeric adenosine monophosphate
CAR-T	Chimeric antigen receptor (CAR) T cells
Caspase	Cysteinyl aspartic acid protease
cccDNA	Covalently closed circular DNA
CD	Cluster of differentiation
CFSE	(5(6)-Carboxyfluorescein diacetate N-hydroxysuccinimidyl ester)
CHB	Chronic Hepatitis B
cm	Centi-meter
CPE	Cytopathic effect
CpG ODN	Cytosine triphosphate deoxynucleotide (C) followed by a guanine triphosphate deoxynucleotide (G) oligodeoxynucleotides
CTLA-4	Cytotoxic T lymphocyte antigen 4
CTLs	Cytotoxic T lymphocytes
DCs	Dendritic cells
DMEM	Dublecco´s Modified Eagle Medium
DMSO	Dimethyl Sulfoxide
DNA	Deoxyribonucleic acid
ELISPOT	Enzyme linked immune absorbent spot

9. LIST OF ABBREVIATIONS

Eomes	Eomesodermin
ETC	Electron transport chain
FACS	Fetal calf serum
FACS	Fluorescence-activated cell sorting
FAS	Fas-Membrane protein of the death receptor family
FASL	CD95L or CD178 - Type-II transmembrane protein of tumor necrosis factor (TNF) family
FELASA	Federation of European Laboratory Animal Science Associations
Fig	Figure
FMO	Fluorescence minus one control
g	Gravitational force / Gram
geq	Genome equivalents
GOT	Glutamic oxaloacetic transaminase
GzmB	Granzyme B
HBc	Hepatitis B core antigen
HBcAg	Hepatitis B core antigen
HBe	Hepatitis B envelope antigen
HBeAg	Hepatitis B envelope antigen
HBs	Hepatitis B surface antigen
HBsAg	Hepatitis B surface antigen
HBV	Hepatitis B virus
HBV-tg	HBV transgenic mice
HCC	Hepatocellular carcinoma
HCV	Hepatitis C virus
HIV	Human immunodeficiency viruses
HLA	Human leukocyte antigen
i.m.	Intramuscular
i.v.	Intravenous
IFN-y	Interferon – Gemma
IFN-α	Interferon – Alpha
IL	Interleukin
iMATEs	intrahepatic myeloid cell aggregates support local T cell expansion
inj.	Injection

9. LIST OF ABBREVIATIONS

IU	International unit
KCs	Kupffer cells
Kg	Kilogram
L	Liter
LCMV	Lymphocytic choriomeningitis virus
LSEC	liver sinusoidal endothelial cell
MACS	Magnetic-activated cell sorting
MDSCs	Myeloid derived suppressor cells
MFI	Mean flourescence intensity
mg	Milli-gram
MHC	Membrane histocompatibility complex
min	Minute
MitoTEMPO	Mitochondria-targeted antioxidant
ml	Milli-liter
MOI	Multiplicity of infection
MVA	Modified Vaccinia Ankara virus
MVA-c	Modified Vaccinia Ankara viral vector encoded by HBc antigen
n	Group size/Number
NK	Natural Killer cells
NKG2D	C-type lectin-like receptor expressed on CD8+ T and NK cells
ns	Not significant
Ova	Ovalbumin
OX40	CD134 - TNF receptor superfamily member 4
P-value	Probability value
PAMPs	Pathogen-associated molecular patterns
PBS	Phosphate buffered saline
PD-L1	Program death ligand 1
PD1	Program death 1
PFU	Plaque forming units
PRR	Pattern recognition receptor
RNA	Ribonucleic acid
ROS	Reactive oxygen species
rpm	Rounds per minute
RT	Room temperature

9. LIST OF ABBREVIATIONS

RT	Reverse transcriptase
s / sec	Second
SD	Standard deviation
SEM	Standards error mean
T-bet	T-box transcription factor
$TCID_{50}$	50% tissue culture infective dose
TCR	T-cell receptor
TGF-β	Transforming growth factor - Beta
TherVacB	Therapeutic vaccine against Hepatitis B
TIM-3	T-cell immunoglobulin mucin 3
TLR9-L	Toll-like receptor 9 Ligand
TLRs	Toll-like receptors
TNF	Tumor necrosis factor
TNFR	TNF receptor
TRAIL	Tumor necrosis factor related apoptosis-inducing ligand
Treg	Regulatory T cells
U	Units
UC	Ultracentrifuge
vp	Viral particles
w / o	Without
WHO	World health organization
wt / WT	Wild type
γT	Gemma T lymphocytes
δT	Delta T lymphocytes
ζ-chain	Zeta chain
µg	Micro-gram
µl	Micro-liter
µm	Micro-meter
µM	Micro-Molar